

Daniela Prinz, BSc

# **Novel alkaloid-like compounds effectively target breast and lung cancer stem cells**

## **Master's Thesis**

To achieve the university degree of

Master of Science

Master's degree program: Biochemistry and Molecular Biomedical Sciences

Submitted to

**Graz University of Technology**

Supervisor:

Assoz. Prof.<sup>in</sup> Priv.-Doz.<sup>in</sup> Mag.<sup>a</sup> Dr.<sup>in</sup> rer. nat. Nadia Dandachi

Medical University of Graz

Department of Internal Medicine, Division of Oncology

Graz, March 2016

Daniela Prinz, BSc

# **Wirkung neuer Alkaloid-ähnlicher Verbindungen auf Brust- und Lungenkrebsstammzellen**

## **Masterarbeit**

Zur Erlangung des akademischen Grades

Master of Science

Masterstudium Biochemie und molekulare Biomedizin

Eingereicht an der

**Technischen Universität Graz**

Betreuerin

Assoz. Prof.<sup>in</sup> Priv.-Doz.<sup>in</sup> Mag.<sup>a</sup> Dr.<sup>in</sup> rer. nat. Nadia Dandachi

Medizinische Universität Graz

Institut für Innere Medizin, Abteilung für Onkologie

Graz, März 2016

## **Eidesstaatliche Erklärung - Affidavit**

Ich erkläre an Eides statt, dass ich die vorliegende Arbeit selbstständig verfasst, andere als die angegebenen Quellen/Hilfsmittel nicht benutzt, und die den benutzten Quellen wörtlich und inhaltlich entnommenen Stellen als solche kenntlich gemacht habe. Das in TUGRAZonline hochgeladene Textdokument ist mit der vorliegenden Masterarbeit identisch.

I declare that I have authored this thesis independently, that I have not used other than the declared sources, and that I have explicitly indicated all material which have been quoted either literally or by content from the sources used. The text document uploaded to TUGRAZonline is identical to the present's master's thesis dissertation.

---

Date

---

Signature

## **Acknowledgement**

First of all I want to thank Mag. Dr. Nadia Dandachi for giving me the great opportunity to work on this project and in her lab group. The friendly and welcoming work environment was always motivating to me and within the last year I learned very much. I also want to thank Verena for making the beginning of my practical work with cell culture methods really easy thanks to her patience and useful tips. Theresa and Nina were always helpful in finding up lab equipment and they kindly helped me out in the cell culture lab during holidays.

A diploma thesis that consists of extensive practical work requires much time and therefore support and sympathy from family and friends is essential. I therefore want to thank first of all my mother for always being thoughtful towards me and for supporting me through motivating and comforting talks in the evenings after long work days. My brother used to always cheer me up with some funny quotes and jokes even in times of frustration. A very important and big thank you also belongs to my wonderful boyfriend Jürgen, who has always been understanding when I was under stress and hence not always easy to handle I suppose. He also always managed to calm me down and helped me relax on weekends to find strength and motivation for the following week. My friend Judith has played an important role in my life since we met during the first semester of our bachelor studies. She not only supported me in everyday-life situations but also understood the frustrations scientific work brings along from time to time.

## **Abstract**

Breast and lung cancer are the most common types of cancer worldwide. Treatment of these diseases is still a major challenge, especially if the tumor has already spread to distant sites. In the last years of cancer research, scientists have formulated, based on experimental findings, the theory of cancer stem cells (CSCs). According to this hypothesis CSCs are held responsible for therapy resistance, tumor recurrence and metastasis. The development of new drugs, targeting this subpopulation of the tumor, is therefore thought to significantly improve treatment of this disease.

In this work the effect of clathroidin derivatives, an alkaloid naturally found in sponges, on this rare yet important subpopulation of cancer cells is examined. 19 compounds were screened for their effect on the viability of breast and lung cancer cell lines. Lead compounds were chosen and dose response experiments were performed to calculate IC50 values for all cell lines growing as monolayer and tumorspheres. Sphere formation assays showed that the ability to generate spheres was significantly inhibited following treatment with the lead compounds. To further investigate the action of the most promising compound, C19, gene expression analysis using qRT-PCR was performed.

The results of this project provide evidence that alkaloid derivatives breast and lung cancer cells and CSCs. Specifically, treatment with C19 lead to a decrease in tumorsphere formation accompanied by downregulation of CSC associated marker genes including Sox2, Vimentin or ALDH1.

Further experiments to uncover pathways through which the compounds interfere with CSCs are needed to better understand the mechanism of action of these compounds in order to specifically target CSCs. This work has shown that alkaloids may be a promising group of compounds in the fight against cancer.

## Zusammenfassung

Brust- und Lungenkrebserkrankungen sind die häufigsten Krebserkrankungen weltweit. Die Behandlung dieser Erkrankungen stellt Ärzte und Wissenschaftler noch immer vor eine große Herausforderung, besonders wenn die Tumoren bereits Metastasen gebildet haben. In den letzten Jahren wurde, basierend auf Forschungsergebnissen, in der Krebsforschung die Hypothese der Krebsstammzellen entwickelt. Laut dieser Theorie werden diese Krebsstammzellen für Therapieresistenz, Tumorrückbildungen sowie für Metastasierung verantwortlich gemacht. Die Entwicklung von neuen Medikamenten, die gezielt diese Subpopulation der Krebszellen angreift, würde deshalb zu einer deutlichen Verbesserung in der Behandlung dieser Gruppe von Krankheiten führen.

In dieser Arbeit wurde der Effekt von Clathrocin Derivaten, ein in marinen Schwämmen natürlich vorkommendes Alkaloid, auf Krebsstammzellen untersucht. Nach erstem Screening von 19 Derivaten auf deren Effekt auf die Lebensfähigkeit von Brust- und Lungenkrebszellen fokussierten wir uns auf die drei vielversprechendsten Verbindungen. Auf Basis von Dose-Response Kurven wurde der IC50 für alle verwendeten Zelllinien unter Monolayer- und Tumorsphären-Wachstumsbedingungen berechnet. Sphere formation assays belegten, dass die Fähigkeit der Zellen, Tumorsphären zu bilden signifikant durch die Behandlung dieser Verbindungen gehindert wurde. Um die Art der Wirkung des vielversprechendsten Derivats, C19, genauer zu untersuchen wurden Gen-Expressions Analysen mittels qRT-PCR durchgeführt.

Als Ergebnis dieses Projekts konnte bestätigt werden, dass Alkaloid Derivate Brust- und Lungenzellen sowie Eigenschaften und Gene, die mit Krebsstammzellen assoziiert werden beeinflussen. Vor allem die Behandlung mit C19 führte zu einer Verminderung der Tumorsphärenbildung und zu einer niedrigeren Expression von Krebsstammzell-Markergenen wie Sox2, Vimentin oder ALDH1. Somit konnte mit dieser Arbeit gezeigt werden, dass Alkaloide eine vielversprechende Gruppe von Molekülen im Kampf gegen Krebs darstellt.

## Index

1. Introduction .....	1
1.1 Cancer .....	1
1.1.1 Lung Cancer .....	1
1.1.2 Breast Cancer.....	3
1.2 Tumor Heterogeneity .....	5
1.3 Evolution of Cancer and the Cancer Stem Cell theory .....	7
1.3.1 Identification of CSCs .....	11
1.3.2 Clinical relevance of CSCs .....	14
1.4 Alkaloids in Medicine.....	17
2. Thesis objective .....	19
3. Materials and Methods.....	20
3.1 Chemical compounds.....	20
3.2 Cancer cell lines and patient-derived cancer cells .....	22
3.2.1 Culture of adherently growing cells.....	24
3.2.2 Culture of tumorspheres .....	25
3.3 Screening of the compounds .....	27
3.4 Dose Response Curves and IC50 calculations .....	29
3.5 Sphere Formation Assay.....	30
3.6 Reverse Transcription Quantitative Real-Time PCR.....	31

4. Results.....	34
4.1 Sphere generation .....	34
4.2 Screening of the Compounds.....	38
4.3 Dose Response Experiments with lead compounds .....	44
4.3.1 Compound 1 .....	44
4.3.2 Compound 19.....	47
4.3.3 Compound 2.....	50
4.3.4 Primary breast and lung cancer cells.....	52
4.4 Sphere Formation Assay.....	56
4.5 q-PCR .....	62
5. Discussion.....	70
5.1 Generation of spheres.....	70
5.2 Screening and dose response experiments .....	72
5.3 Sphere formation experiments .....	74
5.4 <i>Reverse transcription quantitative real-time PCR</i> .....	76
6. Conclusion and Outlook.....	81
Appendix .....	i
Abbreviations.....	i
List of Tables .....	iv
Bibliography.....	x
Supplementary Data .....	xvii



# 1. Introduction

## 1.1 Cancer

In 2012, 14.1 million new cancer cases and 8.2 million cancer deaths occurred worldwide.<sup>1</sup> Lung and breast cancer are worldwide the most frequently diagnosed cancers and the leading cause of cancer death in men and women respectively.<sup>2</sup> The World Health Organisation (WHO) estimated in 2011 that cancer is expected to cause more deaths than coronary heart diseases or strokes in the next years and by 2025 there are expected to be 20 million new cancer cases annually.

Despite advances in diagnosis and treatment, cancer remains a major public health problem. Treatment of the primary lesion not always prevents the development of distant metastases and at the time of diagnosis most tumors have already spread and formed metastases, which are the major cause of death in cancer patients.<sup>3</sup>

### 1.1.1 Lung Cancer

Lung cancer is the most common type of cancer and the leading cause of cancer death worldwide, accounting for 13% of the total cancer cases and 19% of cancer-related deaths.<sup>1</sup> In Austria, lung cancer is the second most common type of cancer in men and the third most common in women accounting for 11% of all new cancer cases in 2011.<sup>4</sup>

The leading risk factor for developing lung cancer remains tobacco smoke, being responsible for 80-90% of all lung cancer cases (relative risk factor = 10 to 30 compared to nonsmokers).<sup>5</sup> However, 10-15% of patients diagnosed with this disease have never smoked.<sup>6</sup> Other risk factors are for example, exposure to radon, radiation, asbestos, second-hand cigarette smoke or chemical compounds such as arsenic. About 8% of all lung cancers are associated with inherited germline mutations.<sup>7</sup>

Histologically lung tumors are classified into two major groups: non-small-cell lung cancer (NSCLS) and small-cell lung cancer (SCLC).

**NSCLCs** are with 80% the majority of lung cancer cases and can be further classified into adenocarcinoma, squamous cell carcinoma and large cell carcinoma with adenocarcinomas (40%) being the most common type of lung cancer. Among smokers the most common type of lung cancer is squamous cell carcinoma, whereas adenocarcinomas are more common in never-smokers.<sup>8,9</sup> Although most NSCLCs initially respond well to chemotherapy, these tumors have a poor prognosis because they frequently relapse. More recently, NSCLC subsets have been identified with specific genetic alterations.<sup>10</sup> For example, 15% of Caucasian patients and 40-50% of Asian patients with lung adenocarcinomas harbour mutations in the EGFR gene.<sup>11</sup> Another 3-7% of patients with NSCLS have an activated anaplastic lymphoma kinase (ALK) gene, usually formed by rearrangement of ALK with the echinoderm microtubule-associated protein-like 4 (EML4) gene.<sup>11</sup> Mutations in the proto-oncogene Kirsten rat sarcoma viral oncogene homolog (Kras) have been associated with 10-30% of lung adenocarcinomas.<sup>12</sup> Importantly, it has been shown in recent years that molecular-targeted therapies using specific inhibitors that target activated EGFR or ALK – are very successful in treating patients with NSCLC.<sup>13</sup>

**SCLCs** are representing 10-15% of lung cancer cases and are highly aggressive and form metastases earlier during disease progression compared to NSCLC, which results in an overall survival of less than four months if left untreated. This type of lung carcinoma is almost exclusively found in current smokers or former smokers.<sup>14</sup> Two-third of SCLC patients present with metastatic disease and have a 5-year survival rate of less than 1%.<sup>15</sup>

As with all cancers, prognosis depends on the stage of diagnosis. Many lung cancers are only discovered by incidence due to unspecific symptoms at early stages of the disease. At the time of diagnosis lung cancer has most of the time already spread to secondary sites and formed metastasis, predominantly in the brain, bone or liver.<sup>9</sup> Compared to other types of cancer, lung cancer has a relatively poor prognosis. In Austria, the five year survival rate for lung cancer is only 18% compared to 85% for breast or 93% for prostate cancer.<sup>4</sup>

### 1.1.2 Breast Cancer

Breast cancer is the second most common type of cancer worldwide and the most common cancer in women. In 2012, 12% of all new cancer cases were tumors of the breast.<sup>16</sup> In Austria breast cancer accounts for 30% of all new cancer cases in women and has a 5-year survival rate of 85% (breast cancers diagnosed between 2004 and 2008).<sup>17</sup> Risk factors that contribute to the development of breast cancer include gender, family history, obesity, aging, drinking alcohol, lack of physical exercise and having fewer children or not having children.<sup>18</sup> 5-10% of breast cancer cases are due to inherited genetic alterations including mutations in BRCA1 and/or BRCA2 genes among others.<sup>19</sup>

Breast cancer is a highly heterogeneous disease that consists of several subtypes, differing considerably in terms of histopathological and biological features and clinical outcome and therapy response.<sup>20</sup> One common way to differentiate distinct subtypes is based on the expression of receptors on the cell surface. Examples are estrogen receptor (ER), progesterone receptor (PR) and the human epidermal growth factor receptor 2 (HER2).<sup>20</sup> Based on the receptor status and gene expression profiles breast cancer can be classified into five major subtypes.<sup>21,22,23</sup>

**Luminal A** breast cancer is the most common subtype (about 40%) and patients diagnosed with this type have the best prognosis. These tumors originate from luminal cells lining the inner of the ducts. They tend to be ER positive and/or PR positive, but HER2 negative.<sup>24</sup>

**Luminal B** subtype of breast cancer accounts for about 10 - 20% of all breast cancer cases and has also a good prognosis although not as good as luminal A type breast cancer. These tumors tend to be ER positive and/or PR positive. Luminal B breast cancer can be further divided into HER2 positive and HER2 negative. In comparison to luminal A breast cancer this subtype tends to be larger in size and lymph node positive.<sup>24</sup>

**Triple negative/basal like** breast cancers are defined by absence of the hormonal receptors ER and PR and no amplification of HER2. They occur at a rate of 15-20% and it is the most aggressive and invasive subtype of breast cancer.

Most triple negative cancers show expression of basal-like associated proteins and most basal-like lesions are triple negative. These tumors share many molecular and clinical features also in regard to prognosis and therapy response and are therefore often classified together into one subtype.<sup>24</sup>

**HER2 enriched** breast cancers are missing the ER and PR expression, but instead are overexpressing HER2. This subtype is rather infrequent, accounting for only 10% of all breast cancers.<sup>25</sup> Although this subtype of breast cancer is called HER2 enriched about 30% of these cancers are HER2 negative.<sup>24</sup> This is because classification is based on genome profiles, clustering genes into groups. Tumors that are negative for HER2 and nevertheless express gene clusters of the HER2 enriched subtype hence also fall in this subgroup of breast cancer. Tumors belonging to this category have a poor prognosis and are prone to early metastasis and recurrence.

**Claudin-low** breast cancer has only recently been discovered as an intrinsic subtype of this heterogeneous disease.<sup>26</sup> Whereas the receptor status of such tumors closely resemble those of triple negative/basal-like breast cancers (yet 15-25% of claudin-low breast cancer express HER2) the claudin-low subtype also reveals low expression of cell-cell adhesion molecules like claudins or E-cadherin and is the most undifferentiated subtype of breast cancer with poor prognosis and limiting treatment options.<sup>27</sup>

Treatment options for breast cancer depend on the stage of the disease at the time of diagnosis and on histological and biological characteristics of the tumor. Most patients undergo surgery combined with additional therapy approaches. Radiation therapy is used as an adjuvant therapy to breast surgery. Hormonal therapy (for example tamoxifen) is the preferred treatment for tumors expressing ER such as luminal A or B subtypes. For patients with HER2 positive tumors a targeted therapy against this molecule is beneficial in combination with conventional chemotherapy. For example, monoclonal antibodies targeting HER2 are trastuzumab and pertuzumab are approved by the food and drug administration (FDA). Patients with triple negative/basal-like tumors face the worst prognosis since they cannot be treated with hormone therapy or drugs that target HER2.<sup>28,29</sup>

## 1.2 Tumor Heterogeneity

Tumor heterogeneity describes the existence of subpopulations of cells with distinct differences at the cellular and molecular level. For many decades, tumor heterogeneity has been recognized by pathologists and has translated into the classification of different histological and molecular tumor subtypes with varied clinical outcome among patients.<sup>30–33</sup> During the last decade, technological advances have facilitated in-depth analyses of cancer genomes and this knowledge has further defined the remarkable heterogeneity of this disease.<sup>34,35</sup> Based on these new techniques many tumors were divided into subtypes based on genetic aberrations and/or molecular patterns. Examples mirroring this classification of tumors are the previously described subtypes of breast and lung cancers. Similarly to these types of tumors, many other cancers can also be divided into subgroups, each showing specific histological, phenotypical and molecular characteristics.<sup>20,36–38</sup>

**Inter-tumor heterogeneity** is a term used to describe molecular and pathological differences between tumor types. There are now more than 100 different types of tumors known, each deriving from distinct tissues, showing individual histological and molecular characteristics.<sup>39</sup> But not only is there a difference between distinct tumor entities. Great diversity also exists among pathologically equal tumors from different patients.<sup>39</sup> This heterogeneity leads to significant differences in disease outcome, discrepancies in treatment response and poses a major difficulty in optimizing treatment strategies.

Tumor cells can also vary significantly within individual tumors with distinct phenotypical and morphological properties. Cells within tumors can differ in the expression of proteins, but also at genetic and epigenetic level.<sup>40</sup> One cause for this **intra-tumor heterogeneity** is genetic variation. Due to changes in the tumor microenvironment (TME) during tumor progression, and metastasis, clones with favourable somatic mutations grow selectively.<sup>41</sup> Over time, different clones evolve in parallel and several clones, bearing different somatic mutations and physiological properties coexist within one tumor.<sup>42</sup> Also chemo- or radiotherapy can influence the TME and consequently effect clonal evolution of the tumor. In this context somatic mutations occur spontaneously and pose an advantage for the cell, also called acquired resistance, or an existing mutation proves favour-

able for survival which leads to clonal expansion of this cell (intrinsic resistance).<sup>43-45</sup> But phenotypic heterogeneity is not always due to genetic variations between clones. There are also stochastic events in gene expression, epigenetic divergence and protein stability that add to the factors responsible for intra-tumor heterogeneity.<sup>40</sup>

Consequently, these observations of genetic diversity among tumor cells within one tumor lead to the conclusion that different clones evolve and coexist in parallel. Theories also suggest, that specific clones and hence subtypes of a tumor may be responsible for different programs and functions of the tumor. Invasion and metastasis for example may be attributed to cells from clonal origin A whereas a different subset of tumor cells, subset B, is responsible for therapy resistance.<sup>42</sup>



An alternative model is the cancer stem cell hypothesis which states that only a small subset of cells within a tumor has the ability to initiate and maintain tumor growth. The unique function of these so called CSCs is maintained through the properties of self-renewal and differentiation.<sup>47</sup> Self-renewing ability means that cells can undergo several cell divisions and maintain their undifferentiated state through the mechanism of asymmetric cell division, giving rise to one identical stem cell and one more differentiated daughter cell (Figure 2). This model suggests that tumors are, similar to tissue organization, highly hierarchical with CSCs at the top of the hierarchy.<sup>47</sup> This approach emphasizes the concept of functional heterogeneity rather than intracellular genetic heterogeneity.<sup>48</sup> Based on this model, recurrence of tumors after therapy would hence result from a therapy resistant, slowly dividing CSC fraction, surviving therapy and re-initiating tumor growth.<sup>49</sup> Metastasis would also rely on the subpopulation of CSCs as only these cells are able to re-initiate tumor growth through asymmetric cell division.<sup>49</sup>

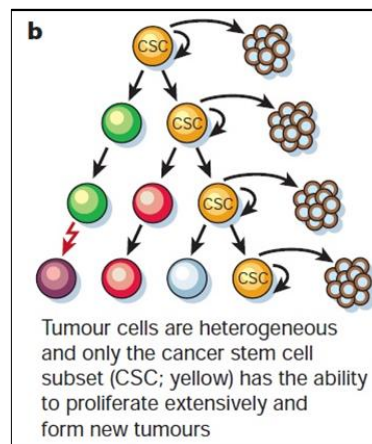


**Figure 2:** Hierarchical organisation of tumors.<sup>47</sup> The CSC model posits that only a subset of cells (shown in yellow) are able to generate a new tumor.

First evidence for CSCs was found 1997 by John Dick's laboratory who identified leukemia-initiating stem cells. They showed that only a small subpopulation of primary leukemia cells was capable of initiating and maintaining leukemia when transplanted into mice. Moreover, the transplanted cells differentiated *in vivo* and acquired the same phenotype as seen in the patient. Regarding the



finding, that the phenotype of these leukemia inducing stem cells (LI-SC) was the same, independent of the leukemia patient sample, it is suggested that LI-SCs arise from primitive normal stem cells rather than committed progenitors. Supporting this hypothesis, all leukemia inducing cells carried the same cell surface markers as normal haematopoietic stem cells. Injection of as little as 5.000 cells carrying these surface markers (CD34<sup>+</sup>/CD38<sup>-</sup>) were able to induce leukemia in NOD/SCID mice whereas 500.000 cells, lacking these markers, failed to do so.<sup>50</sup> Soon afterwards CSCs have been also described in breast,<sup>51</sup> brain,<sup>52</sup> prostate,<sup>53</sup> ovarian,<sup>54</sup> colon,<sup>55-57</sup> liver,<sup>58</sup> lung<sup>59</sup> and pancreatic tumors.<sup>60</sup> In addition to the capacity to engraft in animal models, solid tumor stem cells from many tumors are able to grow under non-adherent cell culture conditions and give rise to so-called tumorspheres.<sup>61-63</sup>

Breast cancer was the first solid cancer in which CSCs were identified.<sup>51</sup> A subpopulation of cells with a CD44<sup>+</sup>/CD24<sup>-</sup> phenotype has been shown to possess tumor-initiating capacities upon injection into immunocompromised NOD/SCID mice.<sup>51,64</sup> This phenotype of breast cancer cells also expresses high levels of ALDH1<sup>65</sup> and seems to play a role in breast cancer metastasis.<sup>66</sup>

In lung cancer, several putative surface markers associated with a Lung CSC phenotype have been identified. It has been reported, that a subpopulation of NSCLC express CD44,<sup>67</sup> a marker, which has previously been identified as putative CSC marker in breast cancer.<sup>51</sup> Recently CD133 has also been used as potential cancer stem cell marker in NSCLC.<sup>68</sup> Cells with this phenotype have been shown to resist conventional chemotherapy, a property that is frequently addressed to CSCs.<sup>69</sup> Additionally, intracellular CSC markers like ALDH1, which has important functions in cancer metabolism, has also been shown to be expressed in lung cancer cells.<sup>70</sup>

Recent studies, however, indicate that both the stochastic model and the cancer stem cell model are not mutually exclusive but moreover both hypotheses may be closely related. The broader hypothesis rather is, that genetic diversity and the tumor microenvironment as well as epigenetic mechanisms and rearrangements direct tumor evolution in concert.<sup>46</sup> Hence it may be necessary to connect both models, the stochastic as well as the CSCs (hierarchical) model, to fully explain phenomena like metastasis, therapy resistance and relapse.<sup>46</sup> Accord-

ing to the CSC model, a tumor arises from one transformed (stem) cell, which has undergone clonal expansion. Therefore subpopulations of the tumor have different tumor-initiating potential as CSC give rise to more differentiated, less-tumorigenic cells. This model would also explain tumor recurrence, as CSCs are a slowly dividing, self-renewing subpopulation of the tumor, which cannot be addressed by conventional drugs, targeting rapidly dividing cells. On the other hand the stochastic model, in which all cells can be transformed into proliferating cancer cells, giving rise to new tumors, mainly focus on genetic heterogeneity as a result of stochastic intrinsic and extrinsic factors and stimuli rather than a hierarchical evolution.<sup>40,46,42</sup> According to this model, therapy resistance or metastasis are due to the spontaneous acquirement of favourable mutations supporting these events. The truth, eventually, lies between the two models and both hypothesis may rather contribute to the understanding of tumor biology and development.

### 1.3.1 Identification of CSCs

CSCs have been first identified in myeloid leukaemia<sup>71</sup> and soon afterwards in solid tumors including the breast,<sup>51</sup> the brain,<sup>72</sup> lung,<sup>73</sup> colon<sup>56</sup> and pancreas<sup>74</sup> using combinations of CSC associated markers. In the past years, methods and experimental setups have been developed to enrich this rare population of cancer cells.

The most established in vitro method to identify CSCs is based on the expression of **CSC-associated surface markers** using fluorescence activated cell sorting (FACS). Antibodies designed to specifically bind to these marker proteins on the cell surface are conjugated to a fluorophore. Scanning the tumor cell sample cell by cell hence makes it possible, based on the fluorescence signal generated upon binding of the antibody to its target marker molecule, to characterize and determine the fraction of CSCs in the sample. For example, the first isolation of breast CSCs was based on the expression of the cell surface marker CD44 and the absence or low expression of CD24.<sup>51</sup> CD44 is a cell surface molecule involved in cell-cell interactions, proliferation, migration and angiogenesis<sup>75</sup> and has been used for identification of CSCs in breast (Al-Hajj), colorectal, pancreatic and prostate cancer to mention only mention a few.<sup>76</sup> CD24 is a heat stable protein normally expressed on the cell surface of B-lymphocytes and granulocytes and is involved in cell-cell and cell-matrix interactions.<sup>77</sup> It is highly expressed in ovarian, bladder, prostate, renal and non-small-cell carcinomas among others.<sup>78</sup> In addition to cell-surface markers, the intracellular protein Aldehyde dehydrogenase 1 (ALDH1) has been used to mark CSCs in breast, lung, colon, pancreatic and prostate cancer.<sup>49</sup> ALDH1 is an enzyme functioning in the oxidation of intracellular aldehydes<sup>79</sup> and sorting cells with high ALDH1 activity has been shown to yield in cells displaying CSC properties.<sup>70</sup> Another frequently used CSC marker molecule is CD133, which has been used to identify CSCs in a variety of tumors including brain, colorectal cancers, pancreatic cancers, breast and prostate cancers, ovarian cancers and some lung cancers.<sup>76</sup> CD133, also referred to as prominin-1, and although it is a widely used marker for CSC identification, little is known about its function in normal and malignant tissue.<sup>80</sup>

The identification of cells that effectively efflux the Hoechst dye 33342 is another possibility to study CSCs. CSCs possess multidrug-resistance genes (ABC transporters) which not only shuttle cytotoxins but also Hoechst dye out of the cell. This so called **side-population (SP)** was firstly described for stem cells of the bone marrow and muscle<sup>81</sup> and has then been applied for ovarian,<sup>82</sup> thyroid,<sup>83</sup> brain,<sup>84</sup> and gastrointestinal cancers.<sup>85</sup> This SP has also shown CSC features like increased expression of stem cell markers.<sup>86</sup>

The gold standard to study CSCs is to assess the tumorigenic or tumor initiating potential of a putative CSC subpopulation by implanting the cells into **immune compromised host mice**.<sup>87</sup> To identify CSCs in human tumors, cells isolated from the primary tumor are implanted into immune compromised mice. The tumors are then isolated from the mice and cells derived from the xenograft need to be re-implanted into other host mice. This procedure is called serial transplantation and is needed to show self-renewal and tumor initiating capacities.<sup>88</sup> Several reports have shown that CSCs characterized by CSC associated markers can initiate tumor growth in host mice at significantly lower cell numbers than tumor cells not expressing these markers. For example, only as few as 200 CD44<sup>+</sup>/CD24<sup>-</sup> breast cancer cells were able to generate mammary tumors, whereas breast cancer cells without these markers failed to do so at the same cell numbers. In fact, a total 100.000 cells without these markers were needed to initiate tumor growth in this experimental setup.<sup>51</sup> Moreover, tumors from CSCs, highly resemble the original tumors from which they were derived, recapitulating the full tumor heterogeneity of the parental tumor.<sup>51</sup> Similar results could also be obtained in other tumor types, including the lung<sup>89,59</sup> and colon<sup>56</sup>. CSCs are for this reason also often termed tumor-initiating cells.

Another possibility to enrich cells with CSC characteristics is to culture the cancer cells under specific culture conditions. It has been shown that CSCs grow under non-adherent serum-free culture conditions supplemented with bFGF and EGF.<sup>90</sup> Under these conditions, cells form spherical three-dimensional structures also called tumorspheres or spheres. This technique has been successfully used to enrich CSCs from breast,<sup>91</sup> colon,<sup>92</sup> lung,<sup>59</sup> ovarian<sup>93</sup> and brain<sup>52</sup> cancer. Tumorspheres can be serially passaged and are enriched for CSC marker genes and possess also higher tumor initiating properties.<sup>59,94,95</sup> Tumorspheres

possess clonal origin provided that cells are seeded at a clonal density of 0.2 to 20 cells per  $\mu\text{l}$ <sup>96</sup>, and they can vary in size from <50  $\mu\text{m}$  to about 250  $\mu\text{m}$  in diameter.<sup>97,98</sup>

Despite the successful use of CSC markers, it has been reported that several of these markers are not consistently sufficient to identify CSCs.<sup>49</sup> Most of the currently used CSC markers are not expressed exclusively by CSCs but also by tissue stem cells.<sup>88</sup> Thus CSC marker expression needs to be combined with functional *in vitro* and/or *in vivo* assays. However, functional assays themselves also have many limitations. Sphere formation assays for example, suffer from the drawback, that it is difficult to really approve clonal proliferation and to exclude accumulation of cells. Additionally, culture media conditions most probably exert a selection pressure on the cells which leads to the survival and proliferation of the clone, best adapted to these conditions. Additionally, suspension culture conditions largely differ from the *in vivo* situation.<sup>76,88</sup> Furthermore, *in vitro* assays only measure *ex-vivo* proliferation rather than self-renewal which is why confirmation is needed from *in vivo* experiments. But also the currently appointed gold-standard, the serial transplantation assay, is not fully perfect to study self-renewal properties of human CSC. Host animals may offer a completely different set of signals from the tumor microenvironment which probably lacks signals needed to maintain the true CSC population.<sup>88</sup>

Moreover, additionally to these technical hurdles that need to be overcome, it has lately been proposed that there may be several subpopulations of CSCs, harbouring different CSC properties.<sup>60,99,100,101</sup> This would mean that there are different CSC population responsible for tumor maintenance, metastasis, drug resistance or tumor recurrence and that these subpopulations of CSCs differ in their pheno- or probably also in their genotype.

### 1.3.2 Clinical relevance of CSCs

A major challenge of a treatment is the fact that many tumors develop drug resistance. Most currently approved anti-cancer drugs target rapidly proliferating cells. However, the subpopulation of CSCs is described as being quiescent or dormant. As a result, CSCs are not as efficiently or not at all affected conventional chemotherapeutics or radiation therapy (Figure 3). Hence an initial shrinking of the tumor is often observed, before, after some time, the tumor relapse. The time that lies between the therapy and the re-initiation of tumor growth varies and can last up to several months or years.<sup>102</sup>

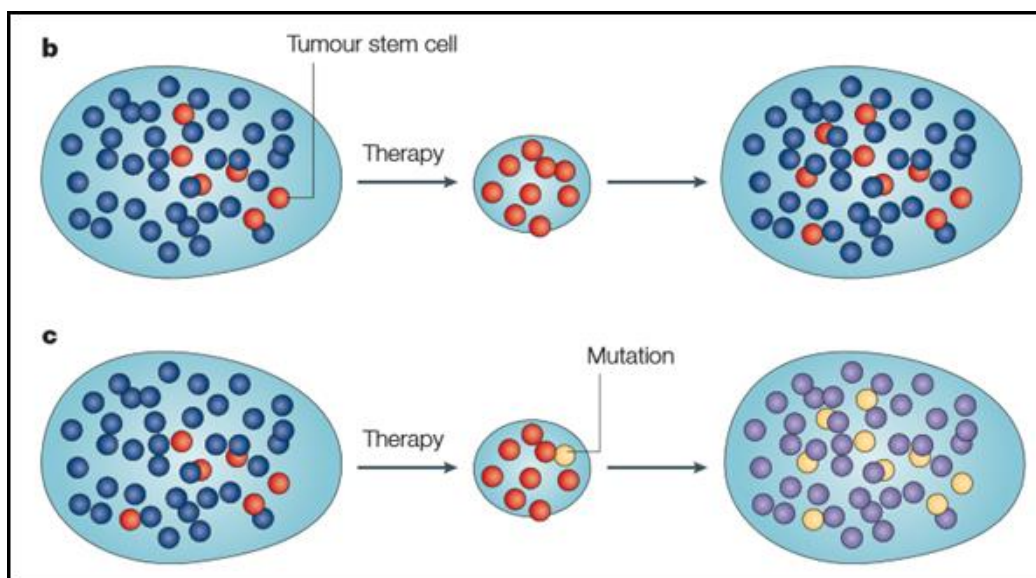


**Figure 3:** Cancer stem cells and tumor recurrence after therapy. In a) CSCs with intrinsic therapy resistance survive chemo- or radiotherapy and lead to a relapse and a de-novo re-initiation of tumor growth. In b) CSCs acquire mutations that lead to therapy resistance. All cells of the recurring tumor are thus resistant to therapy as they arose through clonal expansion of the mutated CSC-clone.

Additionally, CSCs have also been shown to possess certain mechanisms that lead to resistance to chemotherapeutics. One such mechanism would be the drug efflux by special drug transporter proteins, also called ATP-binding cassette (ABC) transporter. Three of these ABC transporter genes (ABCB1, ABCC1 and ABCG2) are also called “principal multidrug-resistance genes” and have recently been shown to be expressed in CSCs.<sup>103,69</sup> These enzymes actively transport cytotoxic compounds out of the cell by using the energy from ATP hydrolysis.<sup>103</sup> This mechanism usually is used by healthy cells for example in the epithelia of the intestinal tract and cells of the blood-brain barrier to protect them from cytotoxic agents.<sup>104</sup>

But not only do CSCs possess intrinsic properties of drug resistance. Through evolutionary selection pressure, clones, that acquired resistance to chemotherapeutics may succeed, giving rise to a recurrent, multi-resistant tumor. There may be mutations in ABC transporter genes leading to permanent overexpression of these proteins or mutations in proteins involved in apoptotic pathways, leading to an impaired or dysfunctional apoptosis machinery.<sup>105</sup>

A second major problem in long time survival of cancer patients is the occurrence of metastasis. In order to metastasize and spread to other sites in the body, a tumor cell has to leave the primary tumor, invade the blood or lymph stream and seed at distinct body sites. Hence in epithelial cancers, epithelial-to-mesenchymal transition (EMT) is considered to play an important role in the metastatic process. Under the influence of certain environmental factors, cells with epithelial character undergo a transition to more mesenchymal like cells. The process of EMT is tightly regulated under normal healthy conditions as this program plays a major role in embryonic development, wound healing or tissue regeneration.<sup>106</sup> Yet in cancer, EMT is often switched on as many cellular processes get deregulated. This represents a first step towards invasion and metastasis which is generally linked to poor survival of the patient.<sup>107</sup> An association between CSCs and EMT has recently been made by Mani et al 2008. The authors have shown, that through induction of EMT, differentiated cancer cells can be forced to establish CSC-like properties.<sup>108</sup> This links the concept of CSCs and EMT and provides a reasonable mechanism for metastasis. Transcription factors (TFs) involved in the cellular reprogramming of EMT like Twist,

Zeb1/2 or SNAI1 have been shown to be highly expressed in CSCs further proving a possible link between CSCs and metastasis.<sup>109,110</sup>

Furthermore, the proposed mechanism of CSCs being responsible for metastasis also makes sense when considering, that patients suffering from metastatic lesions often do not respond well to chemotherapy. Accordingly to the previously discussed properties of CSCs, cancer cells from metastatic lesions enriched in CSCs would have intrinsic or acquired mechanisms of resistance to anti-cancer treatment strategies.

Overall one can summarize, that cancer stem cells are of major clinical relevance. Considering the proposed mechanisms of drug-resistance and metastasis, conventional anti-cancer therapies mostly target the bulk of the tumor and leave CSCs almost or totally unaffected.<sup>69,111</sup> Improved knowledge of biological properties and pathways involved in regulating, maintaining and governing CSC-ness therefore would improve our understanding of this complex and highly heterogeneous disease and help us overcome current problems in treatment.



## 1.4 Alkaloids in Medicine

Alkaloids are one of the most diverse groups of secondary metabolites and they are produced in many biosynthetic pathways. Alkaloids are structurally highly diverse and can be found in plants, insects and marine invertebrates as well as in microorganisms.<sup>112</sup> The chemical characteristics of alkaloids are broad and therefore many different classification systems exist. However alkaloids share some main characteristics. They contain at least one nitrogen atom, usually present as part of the heterocyclic system of the molecule.<sup>113</sup> However, exceptions exist when the nitrogen is part of the aliphatic side chain. A variety of these molecules also contain an oxygen atom and most of the alkaloids are basic.<sup>114</sup> These molecules do not only exist as monomers but tend to form dimeric or even trimeric and tetrameric structures.<sup>113</sup>

Additionally to the vast diversity in structural and chemical features of alkaloids, this class of molecules is also known to possess a broad variety of diverse pharmacological properties e. g. analgesic,<sup>115</sup> antibacterial<sup>116</sup> or anticancer<sup>117</sup> properties. Therefore, alkaloids have been used for over 4000 years in medicine. The South American Indians, for example, used coca leaves since ancient times and opium poppies are described in Chinese books from the 1<sup>st</sup> – 3<sup>rd</sup> century BC.<sup>112</sup> Also, extracts from plants containing toxic alkaloids like aconitine have been used since antiquity for poisoning arrows by indigenous peoples in South America, Africa and Asia.<sup>113</sup> First extensive studies of alkaloids began in the early 19<sup>th</sup> century. Researchers were able to isolate many alkaloids in the first half of the 19<sup>th</sup> century and the first complete synthesis of an alkaloid was achieved in 1886 by a German chemist.<sup>112</sup> The development of spectroscopic and chromatographic techniques enormously facilitated the isolation and characterization of these molecules and by 2008 over 12,000 alkaloids had been identified.<sup>118</sup>

Most Alkaloids have a bitter taste or are even poisonous when ingested.<sup>119</sup> Alkaloids in plants seem to have evolved to protect them from herbivores, however some animals have developed detoxifying mechanisms for alkaloids.<sup>120</sup> These secondary metabolites seem to have protective roles and contribute to the survival of the organism.<sup>121</sup> However, the role of alkaloids for living organisms that produce them is still partially unclear.<sup>113</sup> It is also believed that their

metabolites play a role in plant interaction with animals and other plants or may serve as attractants for insects to contribute to pollination.<sup>112,121</sup>

Some alkaloids have also been described for their anti-tumoral properties and are currently used as chemotherapeutics.<sup>117</sup> For example, vinca alkaloids are the second-most-used class of chemotherapeutics. They originally derive from the periwinkle plant *Catharanthus roseus* and are now produced synthetically.<sup>122</sup> Vinca alkaloids act cell-cycle specific and prevent the formation of microtubules that form the spindle apparatus which is necessary during cell division.<sup>123</sup> Thus, these alkaloids target only proliferating cells, while quiescent tumor remain unaffected.

Currently, four vinca alkaloids are clinically used to treat cancer – vinblastine (Velbe), vincristine (Oncovin), vindesine (Eldisine) and vinorelbine (Navelbine). Vinca-alkaloids are used to treat breast, lung and uterine cancer, osteosarcoma, neuroblastoma, germ cell tumors, acute leukemia, Hodgekin's lymphoma and other lymphomas.<sup>122</sup>

## 2. Thesis objective

As discussed in the introduction, cancer stem cells are of major clinical relevance. Current therapeutic strategies often don't meet the expectations and phenomena like therapy resistance, tumor recurrence and metastasis remain a major hurdle to improve treatment of this rather complex and heterogeneous disease. Being able to specifically target CSCs, would therefore be a major improvement in the combat against cancer. The aim of this study thus is to investigate the anti-tumoral effect of novel alkaloid-like compounds on cancer stem cells.

This work focuses on breast and lung cancer as these types of cancer are the most common ones.

Specific aims of this work were

- to generate spheres from breast and lung cancer cell lines to enrich for CSCs,
- to screen the effect of 19 alkaloid derivatives on cell viability of breast and lung cancer (stem) cells,
- to assess the IC50 values of the selected lead-compounds,
- to assess the effect of the lead compounds on sphere formation in breast cancer cell lines
- to assess whether treatment with lead compounds affects expression of CSC-associated markers.

### 3. Materials and Methods

#### 3.1 Chemical compounds

The compounds used in this study are derivatives of the alkaloid clathrocin (Figure 4) and were developed and provided by Danijel Kikelj from the Faculty of Pharmacy at the University of Ljubljana within the COST action CM1106 “Chemical approaches to target drug resistance in cancer stem cells”. A total of 19 compounds were subjected to an initial screening (Table 1). Compounds were dissolved as 10mM aliquots in DMSO and stored as aliquots at -80°C until use.

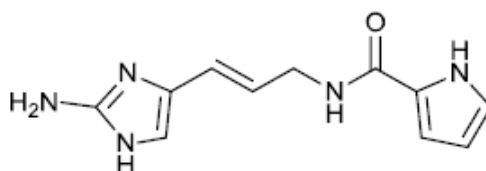
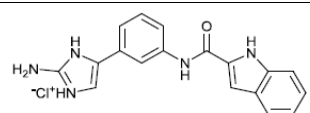
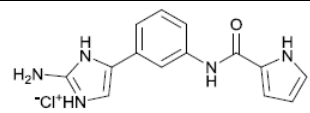
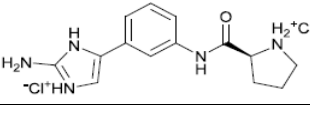
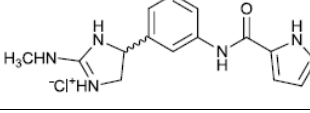
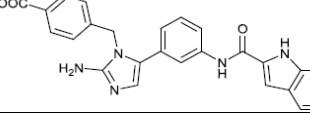
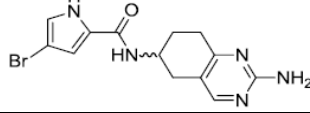


Figure 4: Structure of Clathrocin

Table 1: List of compounds received from the University of Ljubljana.

ID	compound	MW (g/mol)	Structure
1	UL-NZ-10_2	353,81	
2	UL-NZ-13	303,75	
3	UL-NZ-15	344,24	
4	UL-NZ-41	319,79	
5	UL-NHM-18	451,49	
6	UL-KLS-4	415,08	

7	UL-KZH-71	355,25	
8	UL-KZH-127	343,42	
9	UL-KZH-137	255,27	
10	UL-AFS-114-2	342,33	
11	UL-AFS-92-1	442,45	
12	UL-AFS-50-2	193,23	
13	UL-AFS-102-1	293,34	
14	UL-THT-02	330,38	
15	UL-THT-13	412,46	
16	UL-TTM-14	339,28	
17	UL-KSK-02	520,2	
18	UL-KSK-06	331,22	
19	UL-NZ-63-2	371,8	

### **3.2 Cancer cell lines and patient-derived cancer cells**

To account for the heterogeneity of breast cancer we used four different established breast cancer cell lines (MCF7, BT474, MDA-MB231 and SUM159) representing the various molecular breast cancer subtypes. In addition, two non-transformed and non-tumorigenic human breast cells (MCF10A and MCF12A) were used for initial screening experiments. For modelling lung cancer, two lung adenocarcinoma cell lines (A549 and H1299) were used representing the most common type of lung cancer. Finally, two established in-house patient-derived cancer cell lines were used for selected experiments. LT22 is derived from a primary lung adenocarcinoma and PL24 from a pleural effusion of a breast cancer patient. All cell lines and patient-derived cells have been authenticated using short tandem repeat profiling by the Core Facility Molecular Biology at the Centre for Medical Research. Table 3 gives an overview of all cell lines used in this study.

**Table 2:** List of cell lines used for experiments

<b>Cell line</b>	<b>Cell Type</b>	<b>Subtype</b>
<b>MCF7</b>	Breast carcinoma, IDC <sup>1</sup>	Luminal A (ER <sup>2</sup> and PR <sup>3</sup> positive, HER2 <sup>4</sup> negative)
<b>BT474</b>	Breast carcinoma, IDC <sup>1</sup>	Luminal B (ER <sup>2</sup> negative, PR <sup>3</sup> positive, HER2 <sup>4</sup> positive)
<b>SUM159</b>	Breast carcinoma, IDC <sup>1</sup>	Triple negative/basal
<b>MDA-MB231</b>	Breast carcinoma	Claudin-low (ER <sup>2</sup> and PR <sup>3</sup> negative, HER2 <sup>4</sup> positive)
<b>MCF10A</b>	Mammary cell	Luminal
<b>MCF12A</b>	Mammary cell	Basal
<b>NCI-H1299</b>	Lung adenocarcinoma	
<b>A549</b>	Lung adenocarcinoma	
<b>PL24</b>	Breast carcinoma, IDC <sup>1</sup>	ER <sup>2</sup> and PR <sup>3</sup> negative, HER2 <sup>4</sup> positive
<b>LT22</b>	Lung adenocarcinoma	

<sup>1</sup> IDC: Invasive ductal carcinoma

<sup>2</sup> ER: Estrogen receptor

<sup>3</sup> PR: Progesteron receptor

<sup>4</sup> HER2: Human epithelial receptor 2

### 3.2.1 *Culture of adherently growing cells*

Adherently growing breast cancer cell lines were cultured in DMEM/F12 (1:1) media supplemented with 10% FBS superior, 0.2% Normocin and 0.2% Kanamycin at 37°C with 5% CO<sub>2</sub>.

Adherently growing lung cancer cell lines were cultured in RPMI 1640 media supplemented with 10% FBS superior, 0.2% Normocin and 0.2% Kanamycin.

Human non-transformed mammary cells (MCF10A and MCF12A) were grown in DMEM/F12 (1:1) media supplemented with 5% FBS superior, 1% antibiotics and antimycotics, 20 ng/ml EGF, 10 µg/ml insulin and 0.5 µg/ml hydrocortisone.

Adherent cells were grown at 37°C with 5% CO<sub>2</sub> up to 80% confluence. For splitting, the media supernatant was discarded and the monolayer was incubated with TrypLE (Gibco) for 5 minutes at 37°C. After the cells detached from the flask, the reaction was stopped with the addition of PBS. The cell suspension was centrifuged at 1200 rpm for 5 minutes. Cells were counted with a “Cellometer Auto 1000” (Nexcelon Biosciences) and seeded at appropriate density into new cell culture flasks.



### 3.2.2 *Culture of tumorspheres*

Tumorspheres of breast and lung cancer cell lines, as well as primary lung adenocarcinoma cells were grown in DMEM/F12 (1:1) media supplemented with 2% B27 supplement, 10 ng/ml human basic fibroblast growth factor (bFGF), 20 ng/ml human epidermal growth factor (EGF), and 300 IU Heparin. Breast and lung cancer tumorsphere media was supplemented with 0.2% Normocin and 0.2% Kanamycin. Primary lung adenocarcinoma media was supplemented with 0.2% Gentamycin and 0.5% Primocin instead. Tumorspheres were grown in ultra-low attachment culture flasks.

Primary breast cancer cells were grown in MEBM media supplemented with 2% B27 supplement, 10 ng/ml bFGF, 20 ng/ml EGF, 6000 IU Heparin, 0.5% Primocin and 0.2% Gentamycin. Primary breast cancer cells were also grown in ultra-low attachment culture flasks.

Tumorspheres were grown at 37°C with 5% CO<sub>2</sub>. Spheres were splitted to a single cell solution when they were at least about 50 µm in diameter and before they develop a dark necrotic center. Spheres were centrifuged at 1200 rpm for 5 minutes, the supernatant was discarded and the cell pellet was incubated with TrypLE for 5 minute at 37°C. After 2 min of incubation time, the cell suspension was mixed through pipetting to enhance splitting of the spheres. The reaction was stopped upon the addition of PBS and the single cell suspension was centrifuged again. The cell pellet was resuspended in 1 ml PBS, and cells were counted with the Cellometer Auto 1000 (Nexcelon Biosciences) and seeded at a clonal density of  $2 \times 10^5$  cells per 75 cm<sup>2</sup> ultra-low attachment flask. Seeding at clonal density is necessary in order to minimize formation of cell aggregates.<sup>96</sup>

Primary patient-derived lung adenocarcinoma tumorspheres and the breast cancer tumorspheres were handled equally.

Table 4 lists all cell culture supplements used. All flasks and plates used were produced by Corning (New York, USA).

**Table 3:** List of cell culture media and supplements

<b>Reagent</b>	<b>Additional information</b>	<b>Company</b>
<b>DMEM/F12</b>	1:1 Without L-glutamine	Gibco, life technologies
<b>RMPI 1640</b>	With L-glutamine	Gibco, life technologies
<b>MEBM</b>		Lonza
<b>B27 supplement</b>	Serum free supplement, 50x	Gibco, life technologies
<b>EGF</b>		Prepotech
<b>bFGF</b>		Prepotech
<b>Heparin</b>	5000 I.E./ml	Gilvasan
<b>Normocin</b>		InvivoGen
<b>Kanamycin</b>	50 mg/ml in 0.9% NaCl	Sigma-Aldrich
<b>Primocin</b>		InvivoGen
<b>Gentamicin</b>	10 mg/ml in H <sub>2</sub> O	Sigma
<b>Hydrocortison</b>		Sigma-Aldrich
<b>ABAM</b>	Antibiotics, Antimycotics	Sigma
<b>FBS Superior</b>		Biochrome AG
<b>TrypLE</b>		ThermoFisher Scientific

### 3.3 Screening of the compounds

Cell viability was assessed in a primary screen of all 19 compounds at a concentration of 50  $\mu\text{M}$ . Cell viability was measured according to the PrestoBlue Cell Viability Reagent Protocol (Invitrogen) after 72 hours of compound treatment.

PrestoBlue is a resazurin-based fluorescent indicator of cell metabolism. In viable cells, resazurin is reduced to the highly fluorescent dye resofurin, which can be quantitatively measured to determine viability.

Viability assays were performed with both adherent and sphere culture conditions (except for MCF10A and MCF12A as these cell lines do not grow as spheres). Experiments were done in two independent biological replicates (different passages were used) and five technical replicates.

In preparation for the cell viability assay, cells were seeded on day 1 at different cell numbers (Table 4) into wells of a 96-well plate. The outer wells were left unfilled in order to reduce unspecific effects due to media evaporation. A blank consisting of media without cells was also included on all plates in order to subtract background fluorescence.

On day 2, compounds were added at a final concentration of 50  $\mu\text{M}$  and cells were incubated at 37°C with 5%  $\text{CO}_2$ . A vehicle control consisting of 0.5% DMSO (Sigma Life Science) was also included on all plates.

After 72 hours of treatment, 20  $\mu\text{l}$  of the PrestoBlue reagent were added to each well. The cells were incubated for 1h at 37°C before fluorescence was measured with a FLUOstar Omega plate reader (BMG Labtech) at the emission wavelength of 615 nm.

**Table 4:** Seeding densities of cell lines used for viability assays

Cell line	Adherent conditions	Sphere conditions
	#cells/well	#cells/well
<b>MCF7</b>	1500	2500
<b>BT474</b>	2500	2500
<b>SUM159</b>	750	2500
<b>MDA-MB231</b>	750	2500
<b>NCI-H1299</b>	750	2500
<b>A549</b>	750	2500
<b>MCF10A</b>	750	ND <sup>5</sup>
<b>MCF12A</b>	750	ND <sup>5</sup>

<sup>5</sup> ND: not done

### **3.4 Dose Response Curves and IC50 calculations**

Three compounds (C1, C19 and C2) that significantly inhibited viability in the primary screen were selected for follow-up experiments. The potency of these lead compounds was quantified by generating dose-response curves with nine different concentrations for each cell line and culture condition. Again, all experiments were done in two independent biological replicates (different passages were used) and five technical replicates.

Cells were seeded on day 1 at cell densities according to table 4 into the wells of a 96-well plate. A blank was included consisting of media without cells in order to subtract background fluorescence.

On day 2, the cells were treated with nine different compound concentrations in a range from 0.05 to 50  $\mu\text{M}$  [0.05 – 0.1 – 0.5 – 1 – 5 – 10 – 25 – 50  $\mu\text{M}$ ] or with 0.5% DMSO.

After 72 hours of treatment, 20  $\mu\text{l}$  PrestoBlue reagent were added and after 1h of incubation the fluorescence signal was measured in a plate reader.

The 50% inhibitory concentrations (IC50) and statistical analysis were calculated with GraphPad Prism6 (Graphpad Software, La Jolla, CA, USA) non-linear regression analysis (variable Hill slope). A four parameter fit was chosen to calculate the curves and the IC50 values.

### 3.5 Sphere Formation Assay

Sphere formation assays are widely used as a method to estimate the clonogenic stem cell frequency and correlate directly with self-renewal capacity. In preparation for sphere formation assays, cells are seeded at low density to avoid formation of aggregates.

The sphere formation assay (SFA) was performed according to the protocol as described by Lombardo et al.<sup>124</sup>

Adherently growing cells were splitted according to the protocol described in section 3.2.1 and the single cell suspension was counted in the cellometer. Cells were seeded in 750 µl sphere media (see chapter 3.2.2) at a density of 500 cells per cm<sup>2</sup> into a 24-well ULA plate (950 cells/well).

Cells were treated with 5 different compound concentrations ranging from 0.5 to 25 µM end concentration [0.5 – 1 – 5 – 10 – 25 µM].

The plate was then incubated at 37°C with 5% CO<sub>2</sub> for 5 days. The plate was not moved during this time to prevent formation of aggregates. After the incubation period, the wells were investigated under microscope and spheres > 40 µm in diameter were counted.

The sphere forming efficiency (SFE) was then calculated using the following formula:

$$SFE = \frac{\# \text{ spheres per well}}{\# \text{ seeded cells per well}} * 100$$

### 3.6 Reverse Transcription Quantitative Real-Time PCR

To test whether treatment with compound 19 (C19) affects expression of CSC-associated genes, single cells derived from sphere culture were seeded into a 6-well ULA-plate. Cells were left to grow for 3 days and cells were treated on day 4 with 5 and 10  $\mu$ M compound and 0.07% DMSO as vehicle control. After 24 hours of treatment, the cell suspension was removed from the plate, centrifuged and the cell pellet was resuspended in 300  $\mu$ l RLT buffer (Qiagen). The cell lysate was either frozen for storage at  $-20^{\circ}\text{C}$  or RNA was isolated immediately according to the RNeasy Mini Kit (Qiagen).

RNA concentration and 260/280 values were assessed for all samples using the Nanodrop 2000 instrument (Thermo Scientific). For each sample 2000 ng RNA were processed with the Quantitect reverse transcription Kit (Qiagen) on a Bio-rad cycler. RNA samples were incubated in genomic wipeout buffer for removal of genomic DNA (gDNA). After elimination of gDNA, samples were directly used for reverse transcription. As a “no amplification control (NAC)” three samples were pooled together and processed simultaneously in order to ensure that the gDNA elimination step was successful and the sample contained no remaining gDNA. The NAC contained all components except the reverse transcriptase. The generated cDNA was then stored at  $-20^{\circ}\text{C}$  or q-PCR was performed immediately.

qPCR was performed in 96-well plates using the LightCycler 480 instrument (Roche). Reactions were performed in a total volume of 20  $\mu$ l, comprising 1x SYBR Green I Master Mix (Roche), 20 ng cDNA and 25  $\mu$ M of each primer (final concentration). All qPCR reactions were performed in duplicate and quantification cycle values were averaged. Each run also included a no template control using water instead of cDNA. The PCR cycling conditions are listed in table 5. Calculation of expression values was done using the qBase<sup>plus</sup> software (Biogazelle).<sup>125</sup> TATA-binding protein (TBP, designed), glyceraldehyde-3-phosphate dehydrogenase (GAPDH, designed) and lactate dehydrogenase A (LDHA, designed) were determined as appropriate reference genes using the geNorm module in qBase<sup>plus</sup> and were used to normalize gene expression levels.

Following primers were used for qCPR: ALDH1 (designed), CD44 (RTPrimerDB ID88) and E-Cadherin (E-Cad, RTPrimerDB, ID1685), Sex-determining region Y-box 2 (Sox2), octamer-binding transcription factor 4 (Oct4), Nanog, N-Cadherin (N-Cad), Vimentin (Vim), Fibronectin (FN), Slug, Snail2 and Twist.<sup>126</sup> All primer sequences are listed in table 6.

**Table 5: Light Cycler Conditions**

<b>Program</b>	<b>Cycles</b>	<b>Temp (°C)</b>	<b>Acquisition Mode</b>	<b>Time</b>	<b>Ramp Rate (°C/s)</b>	<b>Acquisition (per °C)</b>
<b>Pre-Incubation</b>	1	95	None	10 min	4.4	
<b>Amplification</b>	45	95	None	10 sec	4.4	
		60	None	20 sec	2.2	
		72	Single	15 sec	4.4	
<b>Melting curve</b>	1	95	None	5 sec	4.4	
		40	None	1 min	2.2	
		90	Continuous			10
<b>Cooling</b>	1	40		10 sec	2.	



**Table 6:** Primer sequences used for qRT-PCR

<b>Gene</b>	<b>Forward primer Sequence [5' → 3']</b>	<b>Reverse primer Sequence [5' → 3']</b>	<b>Amplicon Size (bp)</b>
LDHA	TGTAGCAGATTTGGCAGAGAG	CATCATCCTTTATTCCG- TAAAGAC	95
GAPDH	CCACTCCTCCACCTTTGAC	ACCCTGTTGCTGTAGCC	102
TBP	CGGTTTGCTGCGGTAATC	TCTGGACTGTTCTTCAC- TCTTG	108
CD44	TGCCGCTTTGCAGGTGTAT	GGCCTCCGTCCGAGAGA	66
Sox2	GCACATGAACGGCTGGAG- CAACG	TGCTGCGAGTAG- GACATGCTGTAGG	207
Oct4	GACAACAATGAAAATCTTCAG- GAG	CTGGCGCCGGTTACAGAAC- CA	216
ALDH1	AGAAGGAGATAAGGAGGAT	AATCAGCCAACCTGTATAA- TAG	125
Slug	GCGATGCCAGTCTAGAAAA	GCAGTGAGGGCAAGAAAAAG	203
Snail2	GCTGCAG- GACTCTAATCCAGAGTT	GACAGAGTCCCAGATGAG- CATTG	130
Twist	GGAGTCCGCAGTCTTACGAG	TCTGGAGGACCTGGTAGAGG	201
E-Cad	TGAGTGTCCCCCGGTATCTTC	CAG- TATCAGCCGCTTTCAGATTTT	87
N-Cad	GACGGTTCGCCATCCAGAC	TCGATTGGTTTGACCACGG	67
Vim	CAACCTGGCCGAGGACAT	ACGCATT- GTCAACATCCTGTCT	113
FN	CCGCCGAATGTAGGACAAGA	TGCCAACAG- GATGACATGAAA	100

## 4. Results

### 4.1 Sphere generation

In this project we used the ability of CSCs to form tumorspheres under non-adherent serum-free conditions as an *in vitro* model to identify compounds that inhibit CSC viability. This *in vitro* tumorsphere model represents a widely used and ideal preclinical tool for studying the biology of CSCs.<sup>127,128,129</sup>

We successfully generated tumorspheres from lung and breast cancer cell lines as depicted in Figures 5 and 6 (right panel). Figures 5 and 6 (left panel) also show the corresponding cell line grown under adherent condition. All cell lines were able to form tumorspheres after 4-7 days with different morphologies under suspension culture conditions. All cell lines maintained spheres over multiple passages.

Using this growth condition, MCF7, SUM159 and BT474 formed smooth, tightly packed and round spheres (Figure 5A, B and C, right panel) while MDA-MB231 cells formed loosely packed grapelike spheres (Figure 5D, right panel). Tumorspheres also differed in size. While tumorspheres from MCF7, BT474 and MDA-MB231 cells reached up to 250  $\mu\text{m}$  in diameter (Figures 5A,B and D right panel), SUM159 tumorspheres only reached about 100  $\mu\text{m}$  in diameter (Figure 5C, right panel) before the culture was splitted into a single cell suspension.

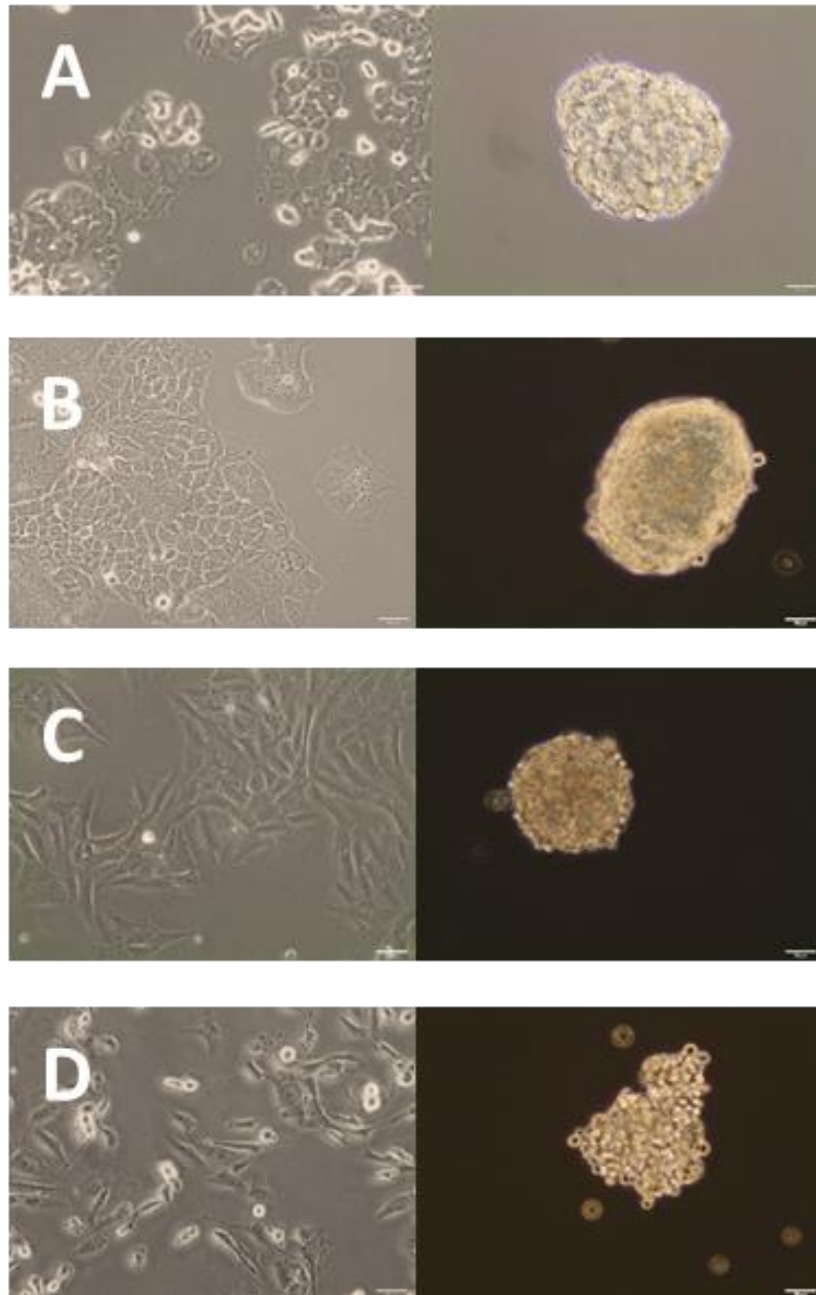


**Figure 5:** Morphology of breast cancer cells grown under adherent (left panel) and suspension (right panel) culture conditions. Tumorspheres were generated after 4-7 days of culture in serum-free suspension culture conditions. **A)** MCF7 **B)** BT474 **C)** SUM159 **D)** MDA-MB231. Scale bars represent 50  $\mu\text{m}$ .

A549 and H1299 lung adenocarcinoma cells generated less tightly organized spheres (Figure 6A and B, right panel). A549 tumorspheres reached a maximum diameter of about 100  $\mu\text{m}$ , whereas spheres derived from H1299 reached up to 250  $\mu\text{m}$  diameter.

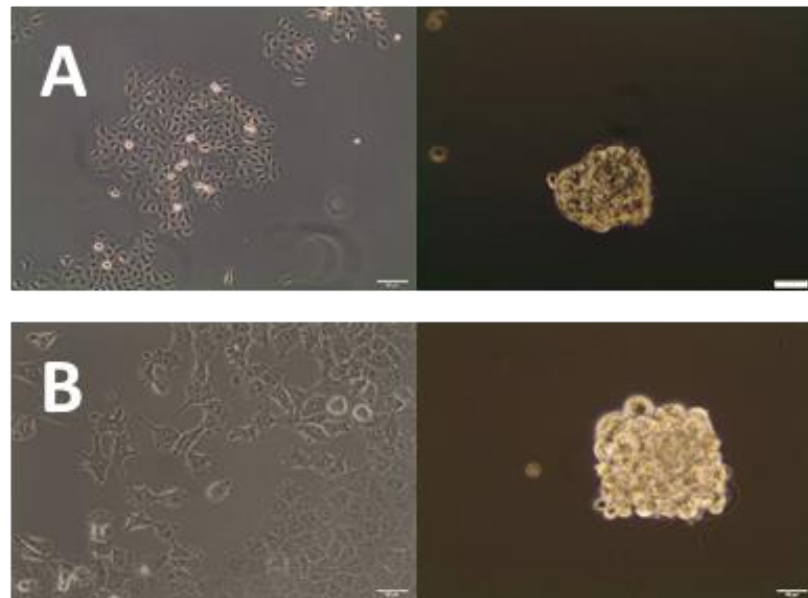


**Figure 6:** Morphology of lung adenocarcinoma cells grown under adherent (left panel) and suspension (right panel) culture conditions. Tumorspheres were generated after 5 -7 days of culture in serum-free suspension culture conditions. **A)** A549 **B)** NCI-H1299. Scale bars represent 50  $\mu\text{m}$ .

Additionally, we used two established in-house patient-derived cancer cell lines. PL24 cells originated from a breast cancer patient and LT22 cells originated from a lung adenocarcinoma patient. Under suspension culture conditions both cell lines generated huge (up to 250  $\mu\text{m}$  in diameter), tightly packed spheres as shown in Figure 7.

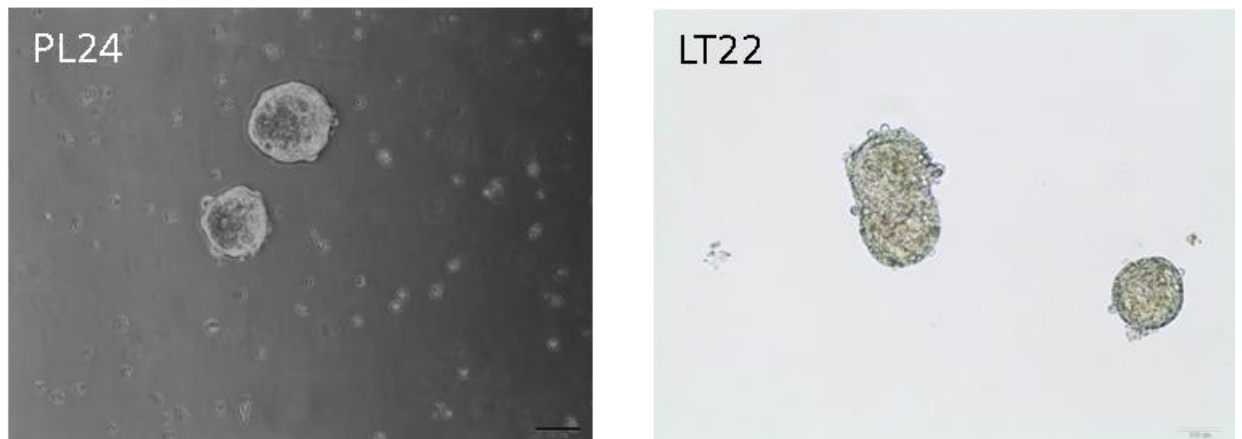


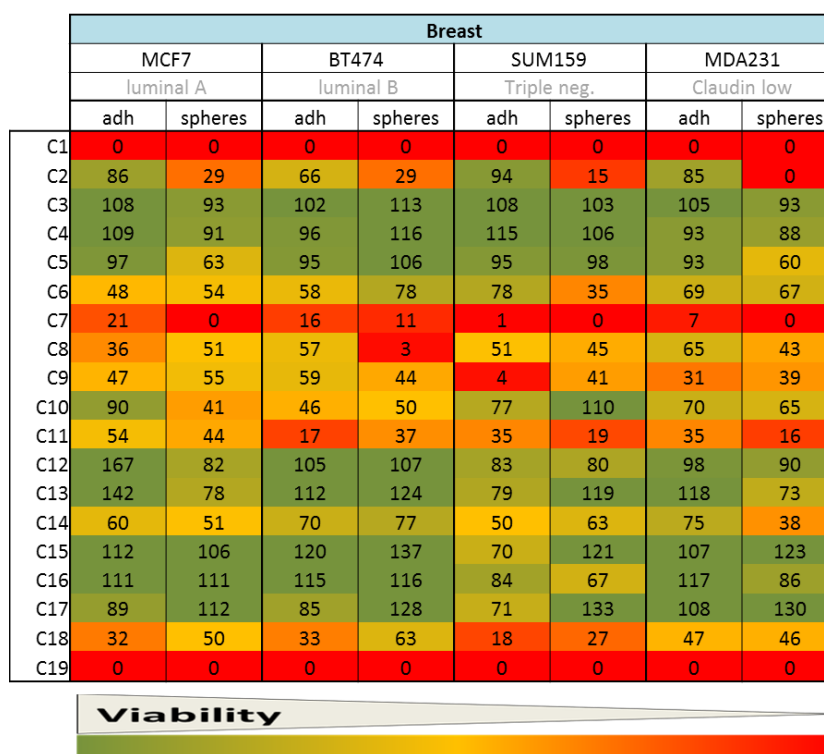
**Figure 7:** Morphology of in-house patient-derived cancer cell lines grown under suspension culture conditions. PL24 originated from a pleural effusion of a breast cancer patient (left side) and LT22 originated from a lung adenocarcinoma patient (right side). Scale bars represent 50  $\mu\text{m}$ .

## 4.2 Screening of the Compounds

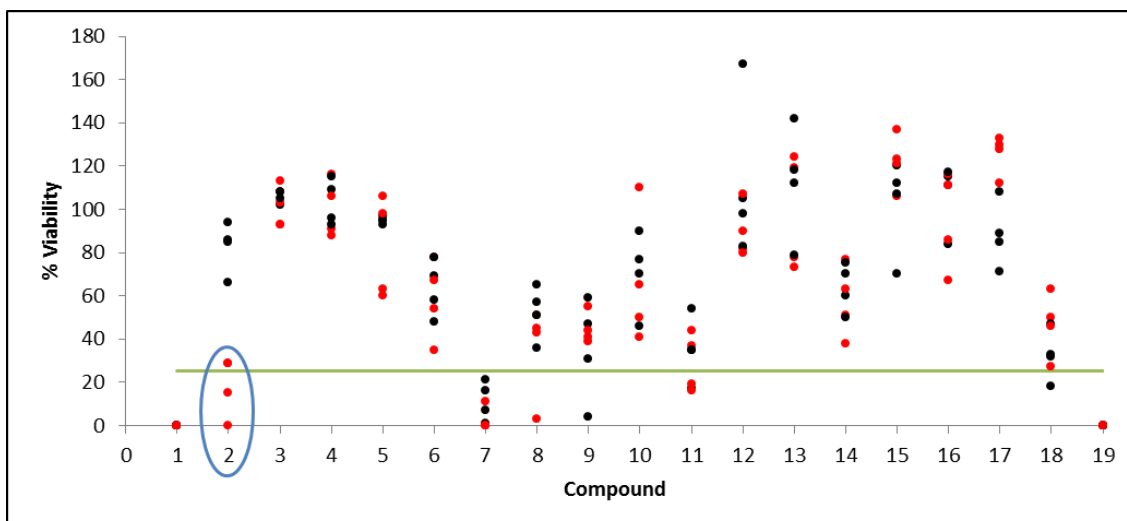
Our first object was to identify candidate compounds that inhibit viability of breast and lung cancer cell lines. We performed a primary screen of 19 compounds using Prestoblue as viability assay in both adherent and suspension culture conditions. The results of the primary screening experiments of breast cancer cell lines are summarized in Figure 8. To better visualize the results, values were coloured according to the calculated viability in percent, normalized to the vehicle control. Red cells mirror low viability whereas green cells show high viability.

In these primary screening experiments several compounds showed varying effects in biologically different breast cancer cell lines or in the two culture conditions. Compound 10, for example, reduced viability of BT474 by greater than 50% and of MDA-MB231 cells by greater than 70%. Viability was also reduced in MCF7 cells grown as spheres to below 50%, while C10 had merely no effect on adherently grown MCF7 cells (90%). When cells were treated with compound 18, viability of cells growing as monolayer was reduced more effectively than in tumorspheres (except for MDA-MB231). Treatment with compound 8 had a strong inhibition on viability of BT474 tumorspheres (3%) whereas viability of all other cell lines and culture conditions was only reduced by about 40-50%. Treatment with compound 9 inhibited viability of SUM159 monolayer cells (4%), whereas viability of all other cell lines and culture conditions was only reduced by 50%. C11 treatment leads to a decrease of viability by about 80% in BT44 monolayer and SUM159 and MDA-MB231 tumorspheres. Other breast cancer cell lines and were, independently from the growth conditions, not affected to such a large extent.

Three of the 19 compounds (C1, C7 and C19) decreased viability dramatically with a reduction by greater than 80%. Of these compounds, C1 and C19 completely inhibited cell viability in all breast cancer cell lines in both monolayer and tumorspheres. C7 treatment also significantly inhibited viability of all breast cancer cell lines under both culture conditions. However, viability was not decreased to a minimum in all breast cancer cell lines, with values ranging from 0% (SUM159 tumorspheres) to 21% (MCF7 monolayers) viability. Therefore, compounds 1 and 19 were chosen as lead compounds for follow-up experiments. In addition to C1 and C19, compound 2 showed an interesting effect on viability. Specifically, this compound seemed to selectively decrease the viability of tumorspheres by about 70% and more, while adherently growing cells remained unaffected. Hence, we decided to include C2 in follow-up experiments.



**Figure 8:** Results of the primary screening experiments in breast cancer cell lines depicted as a heat map with green representing high and red low viability. Values are given in percent normalized to the vehicle control. Only C1 and C19 completely inhibited viability in all breast cancer cell lines and both culture conditions analysed. Interestingly, C2 decreases viability selectively in breast cancer cells cultured as tumorspheres.



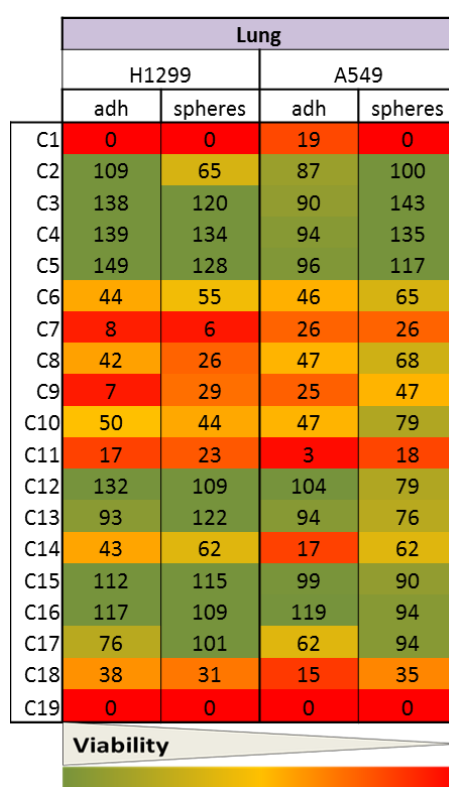
**Figure 9:** A scatterplot showing the results of screening experiments in breast cancer cell lines. Adherent cells are shown in black, tumorspheres in red. Only C2 selectively decreased viability of tumorspheres. C1, C7 and C19 significantly decreased viability in all breast cancer cell lines and in both culture conditions.

Figure 9 shows a scatterplot of the results from the screening experiment in all breast cancer cell lines. From this graph it can be seen that only compound 2 is able to selectively inhibit viability of tumorspheres (red dots) whereas the other lead compounds showed a similar effect on both cells grown as monolayer (black dots) and tumorspheres.

The same screening experiments were also performed with two lung adenocarcinoma cell lines, H1299 and A549. Again the effect of the compounds was examined on adherently growing cells and cells growing as tumorspheres (see Figure 10). Similar to the results obtained in breast cancer cell lines, numerous compounds (C1, C7, C9, C11, C18 and C19) reduced viability by greater than 50%. Viability of H1299 cells was significantly affected by C7 with a reduction of viability by almost 100%. A549 cells on the other hand showed a decreased viability of 30% with C7. Also, treatment with C11 resulted in relatively low levels of viability in both H1299 and A549 cell lines and under both culture conditions by reducing the viability to 3-23%.



Interestingly the same compounds C1 and C19 that completely inhibited viability in breast cancer cell lines also effectively inhibited viability in both lung adenocarcinoma cell lines and in both culture conditions. Hence C1 and C19 were chosen as lead compounds not only in breast but also in lung cancer cell lines. In contrast to breast cancer cell lines, spheres of the lung cancer cell lines remained (almost) unaffected by treatment with compound 2. Therefore, follow-up experiments using lung cancer cell lines were only performed with C1 and C19. Finally, the scatterplot in Figure 11 illustrates that no compound acted selectively on viability of lung cancer tumorspheres.



**Figure 10:** Results of the primary screening experiments in lung adenocarcinoma cell lines represented as heat map with green values representing high and red boxes showing low viability. Values are given in percent normalized to the vehicle control. Besides compounds 6, 7, 8, 9, 10, 11 and 18, which showed decreased viability by about 50 to 70% only C1 and C19 completely inhibited viability in all lung adenocarcinoma cell lines used.

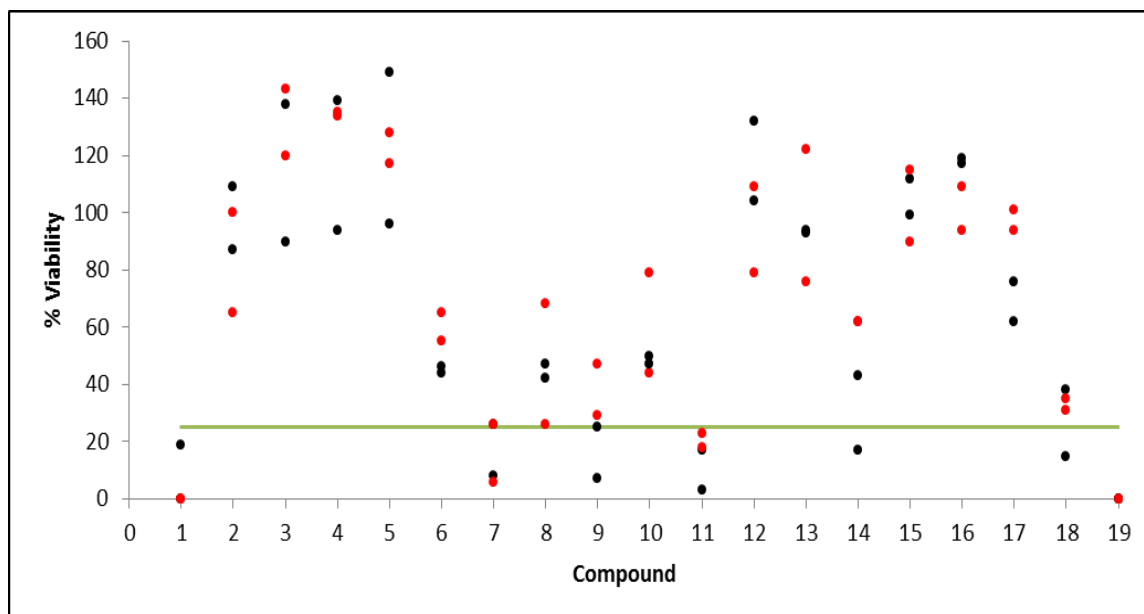


**Figure 11:** A scatterplot showing the results of screening experiments in lung adenocarcinoma cell lines. Adherent cells are shown in black, tumorspheres in red. No compound was identified that selectively decreased the viability in tumorspheres. Treatment with C1, 7, 11 and 19 showed the strongest decrease of viability in lung cancer cell lines.

The scatterplot in Figure 12 summarizes and represents the results from screening experiments in both breast and lung cancer cell lines. Three compounds significantly affected viability of all cancer cell lines, namely C1, C7 and C19. Additionally C2 showed a selective decrease of viability only in breast cancer tumorspheres (black dots). Compound 11 decreased viability below 25% only in lung cancer cell lines (red dots) under both, adherent and suspension culture conditions.

Based on these results C1 and C19 were chosen as lead compounds for follow-up experiments. Further experiments with breast cancer cell lines were also conducted with C2 as this compound selectively decreased viability of breast cancer tumorspheres.

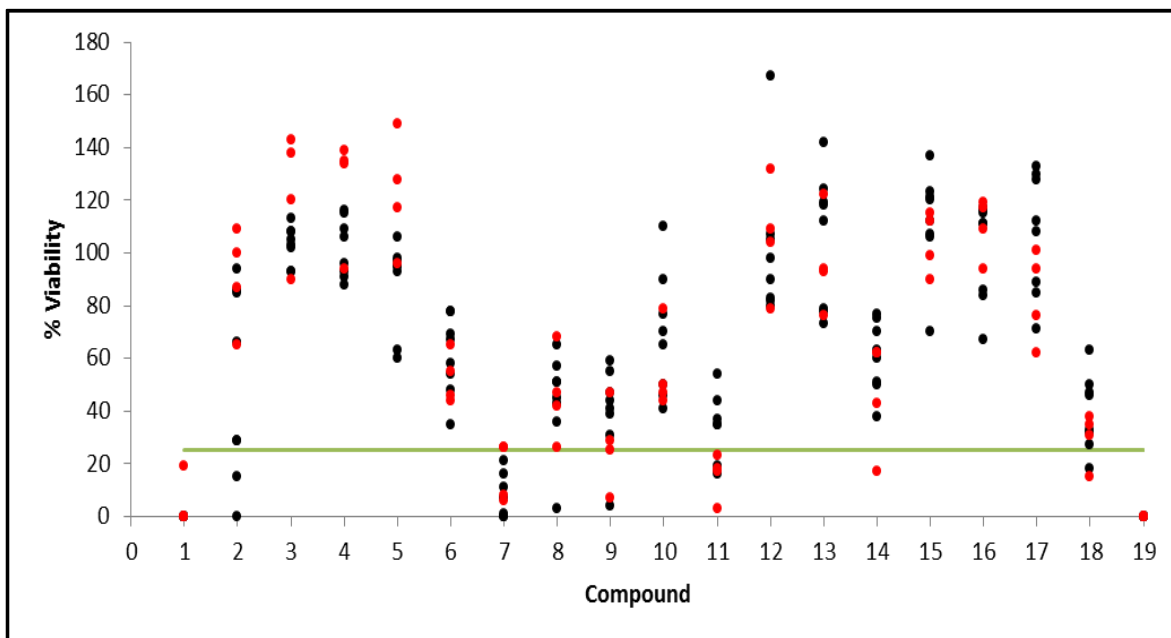


**Figure 12:** A scatterplot showing the results of screening experiments in breast cancer cell lines (black) and lung adenocarcinoma cell lines (red). The only compound that acted selectively on breast cancer spheres was C2. In contrast, no compound specifically affecting lung adenocarcinoma cells was identified.

### 4.3 Dose Response Experiments with lead compounds

To assess the potency of lead compounds and to determine IC<sub>50</sub> values, dose response experiments were performed as described in chapter 3.4.

#### 4.3.1 *Compound 1*

Compound 1 most effectively decreased viability of MCF7 cells with an IC<sub>50</sub> value of 8.5  $\mu\text{M}$  for adherently growing cells, and 5.7  $\mu\text{M}$  for cells cultured under suspension culture conditions. Importantly, MCF7 tumorspheres were more sensitive to C1 compared to adherently grown cells (Figure 13A and table 7). Besides MCF7, only tumorspheres of MDA-MB231 showed lower IC<sub>50</sub> values than adherently grown cells. Treatment with C1 in these cells lead to an IC<sub>50</sub> of 10.4  $\mu\text{M}$  in adherently growing cells and 8.2  $\mu\text{M}$  in tumorspheres respectively (table 7). However, this difference between IC<sub>50</sub> values was not significant as

In contrast to MCF7 and MDA-MB231 cells, treatment of adherently growing BT474 with C1 resulted in lower IC<sub>50</sub> values (10.5  $\mu\text{M}$ ) than treatment of the corresponding tumorspheres (13.5  $\mu\text{M}$ ) (Figure 13B and table 7). Finally, SUM159 showed similar IC<sub>50</sub> values for both culture conditions when treated with compound 1 (table 7, Figure 13C).

To sum this up, treatment of breast cancer cell lines with compound 1 resulted in IC<sub>50</sub> values around 10  $\mu\text{M}$  for adherently growing cells. Treatment of BT474 and SUM159 tumorspheres lead to IC<sub>50</sub> values similar to those found in adherently growing cells, whereas tumorspheres from MCF7 and MDA-MB231 cell lines showed a slightly lower IC<sub>50</sub> value than their corresponding monolayer cells.

In order to test the effect of C1 on viability of non-malignant mammary epithelial cells, dose-response experiments were also performed with normal human non-transformed mammary epithelial cells MCF10A and MCF12A. Since these cells did not grow as spheres, IC<sub>50</sub> values were only determined for monolayer conditions. IC<sub>50</sub> values of C1 ranged from 9.8 to 12.7  $\mu\text{M}$  in MCF10A and MCF12A cells and were similar to values of adherently grown breast cancer cells (supplementary Figure 1).

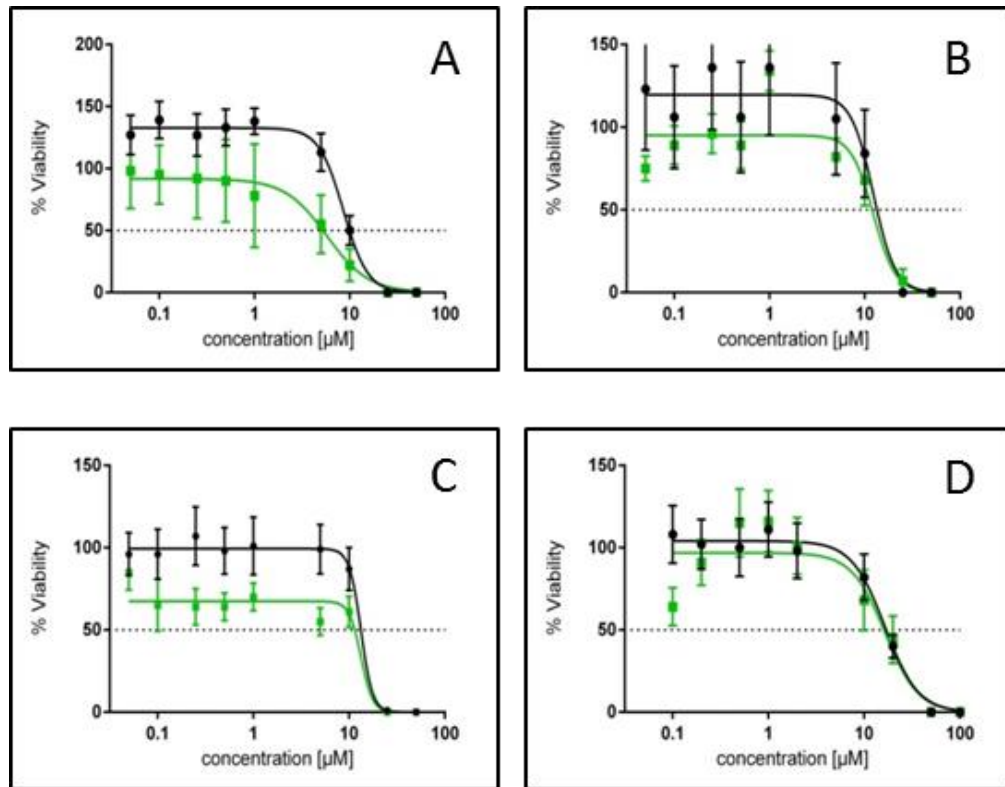


**Figure 13:** Dose-response curves of compound 1 in breast cancer cell lines grown as spheres (green) and monolayers (black). **A)** MCF7 tumorspheres exhibited a significantly lower  $\text{IC}_{50}$  as adherently growing cells. BT474 cells **B)** and SUM159 cells **C)** showed similar  $\text{IC}_{50}$  values for both tumorspheres and monolayer derived cells. **D)** Treatment of MDA-MB231 tumorspheres with C1 resulted in a slightly lower  $\text{IC}_{50}$  than treatment of adherently growing cells .

Compared to breast cancer cells, lung adenocarcinoma cells H1299 and A549 were significantly less sensitive to compound 1 with overall higher IC<sub>50</sub> values. IC<sub>50</sub> of H1299 monolayer cells was 20  $\mu$ M and of A549 cells 22.8  $\mu$ M. Compared to adherently growing cells, tumorspheres had significantly lower IC<sub>50</sub> values with 10.5  $\mu$ M for H1299 and 12.8  $\mu$ M for A549 indicating that lung tumorspheres were more sensitive to compound 1 (table 7 and Figure 14).

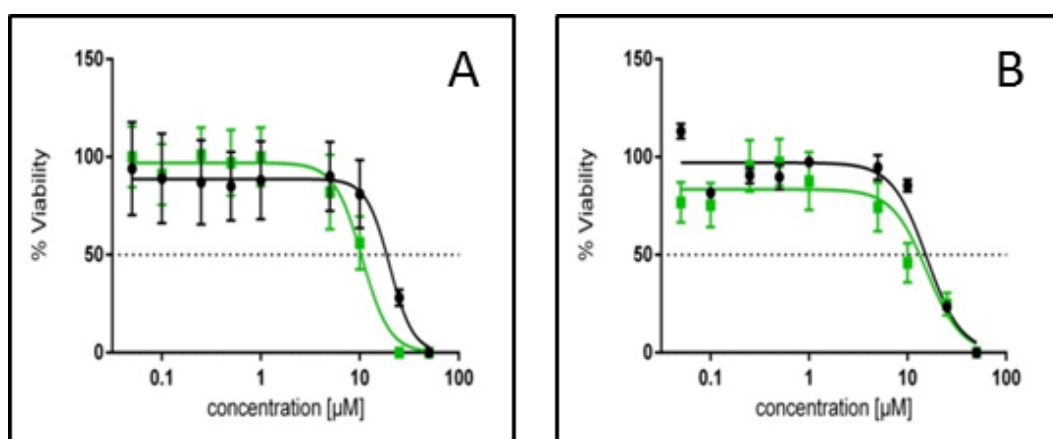


**Figure 14:** Dose-response curves of compound 1 in lung cancer cell lines grown as spheres (green) and monolayers (black). **A)** H1299 tumorspheres exhibited a significantly lower IC<sub>50</sub> as adherently growing cells. **B)** In A549 cells, IC<sub>50</sub> values of tumorspheres and monolayer derived cells also differed significantly.

**Table 7:** Overview of the calculated IC<sub>50</sub> values after treatment with C1

Cell line	IC <sub>50</sub> monolayer	IC <sub>50</sub> spheres
MCF7	8.5	5.7
BT474	10.5	13.5
SUM159	12.0	12.7
MDA-MB231	10.4	8.2
MCF10A	9.8	ND <sup>5</sup>
MCF12A	12.7	ND <sup>5</sup>
NCI-H1299	20	10.5
A549	22.8	12

### 4.3.2 Compound 19

Among all breast cancer cell lines tested, SUM159 tumorspheres were most sensitive to treatment with compound 19 with the lowest IC<sub>50</sub> value of 2.9  $\mu$ M. In contrast, adherently grown SUM159 showed an IC<sub>50</sub> value of 12.8  $\mu$ M, which was comparable to the other adherently grown breast cancer cells. This selective effect on viability is shown in Figure 15C.

Similar to treatment with C1, C19 moderately reduced viability of MCF7 and MDA-MB231 cells with lower IC<sub>50</sub> values in tumorsphere culture compared to adherently growing cells (Figure 15A and D, table 8). Similar to treatment with compound 1, in BT474 cells, C19 showed a higher IC<sub>50</sub> for tumorspheres (13.5  $\mu$ M) compared to IC<sub>50</sub> values of monolayer cells (10.5  $\mu$ M) which is summarized in table 8. BT474 cells are hence, the only breast cancer cell line tested, in which tumorspheres were more insensitive to treatment with the lead compounds than monolayer cells.

To summarize dose-response experiments with C19 in breast cancer cell lines IC<sub>50</sub> values are shown in table 8. In contrast to C1, experiments with C19 resulted in lower IC<sub>50</sub> values in tumorspheres compared to adherently growing cells in all breast cancer cell lines except for BT474. In general, IC<sub>50</sub> values of C19 were similar in all adherently grown breast cancer cell lines with values around 12  $\mu$ M, whereas IC<sub>50</sub> values of the corresponding tumorspheres ranged from 2.9  $\mu$ M in SUM159 tumorspheres to 13.5  $\mu$ M in BT474 tumorspheres.

Again, dose-response experiments were also carried out with MCF10A and MCF12A as normal mammary epithelial cells, showing slightly lower IC<sub>50</sub> values compared to breast cancer cells (Table 8 and supplementary Figure 2).

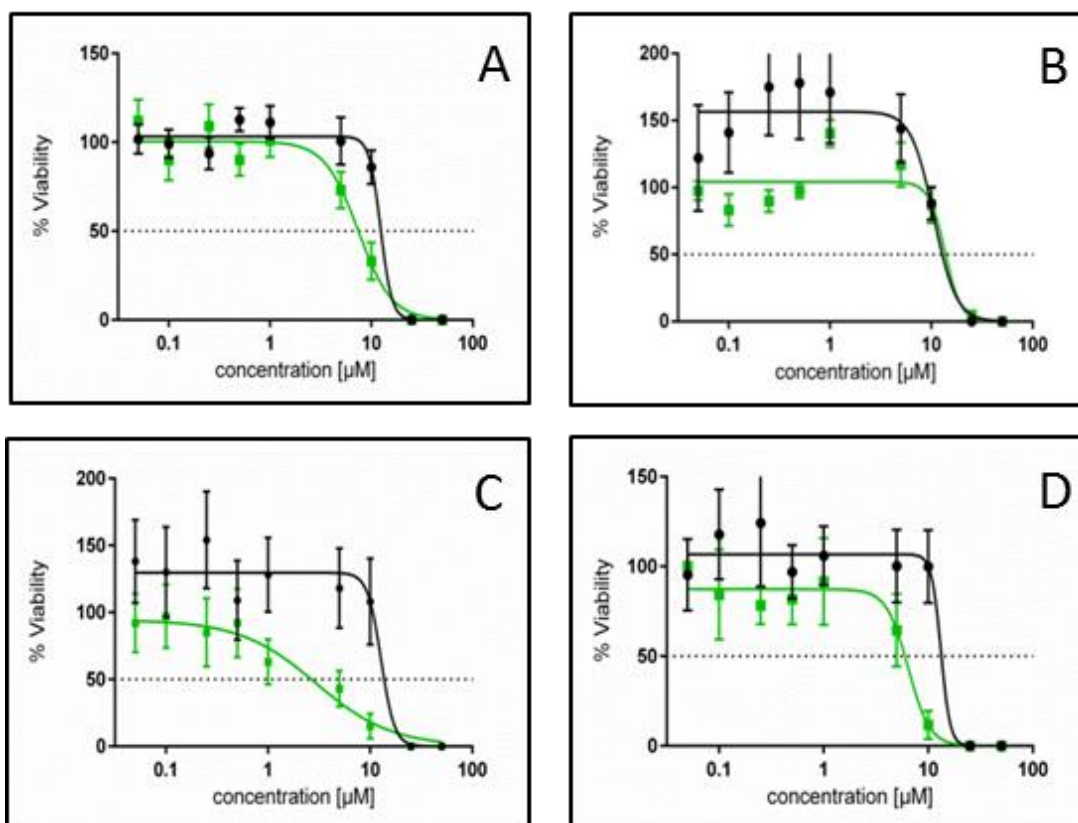


**Figure 15:** Dose-response curves of compound 19 in breast cancer cell lines grown as spheres (green) and monolayers (black). **A)** MCF7 tumorspheres exhibited a significantly lower  $\text{IC}_{50}$  as adherently growing cells. **B)** In BT474 cells,  $\text{IC}_{50}$  of tumorspheres and monolayer derived cells were comparable. **C)** Treatment of SUM159 tumorspheres resulted in a very low  $\text{IC}_{50}$  whereas  $\text{IC}_{50}$  of monolayer derived cells was comparable to  $\text{IC}_{50}$  of other adherently growing breast cancer cell lines. **D)** Treatment of MDA-MB231 tumorspheres with C19 also resulted in a lower  $\text{IC}_{50}$  than treatment of adherently growing cells.

Treatment with C19 of lung adenocarcinoma cell lines showed that tumorspheres reacted moderately more sensitive to C19 with lower  $\text{IC}_{50}$  values of tumorspheres compared to adherently growing lung adenocarcinoma cells (Figure 16). Overall, treatment of lung adenocarcinoma cell lines, H1299 and A549, with compound 19 resulted in lower  $\text{IC}_{50}$  values in adherently growing cells as compared to treatment with C1 (Table 7 and 8). However,  $\text{IC}_{50}$  values of lung adenocarcinoma tumorspheres were similar between C19 and C1.



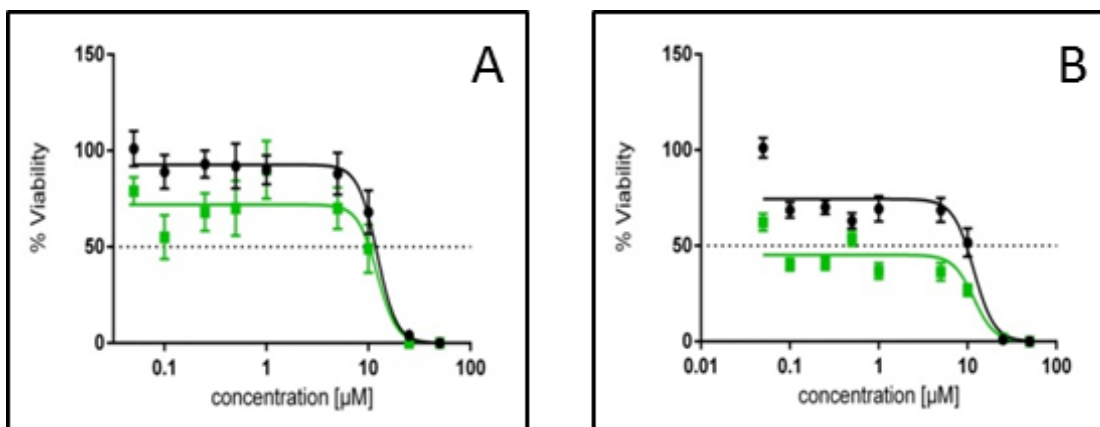


**Figure 16:** Dose-response curves of compound 19 in lung cancer cell lines grown as spheres (green) and monolayers (black). **A)** H1299 tumorspheres exhibited only a slightly lower C50 compared to adherently growing cells. **B)** In A549 cells treatment with C19 resulted in a lower IC50 of tumorspheres compared to monolayer derived cells.

Comparing the results of the dose-response experiments with C19 on lung and breast cancer cell lines, IC50 values for both types of cancer were comparable and within the same dimension, as summarized in table 8.

**Table 8:** Overview of the calculated IC50 values after treatment with C19

Cell line	IC50 adherently grown cells	IC50 spheres
MCF7	12.3	7.5
BT474	10.5	13.5
SUM159	12.8	2.9
MDA-MB231	12.6	7.2
MCF10A	7.0	ND <sup>5</sup>
MCF12A	9.2	ND <sup>5</sup>
NCI-H1299	13.2	11.4
A549	14.2	10.2

### 4.3.3 *Compound 2*

As primary screening experiments showed a selective decrease of viability after treatment with compound 2 in breast cancer tumorspheres (see Figures 8 and 9), dose-response experiments were also performed with this compound. Interestingly, compound 2 most effectively reduced viability only in MDA-MB231 tumorspheres (Figure 17D). Although there was a difference in viability and IC<sub>50</sub> between tumorspheres and adherently growing cells after treatment of MCF7, BT74 and SUM159 tumorspheres, the concentrations at which viability was reduced to 50% was still relatively high (table 9). Especially treatment of SUM159 tumorspheres showed no effect on viability at the highest compound concentration (50  $\mu$ M). Similar to MDA-MB231 tumorspheres, BT474 tumorspheres were the only breast cancer cells, where viability was diminished to almost 0% at the highest compound concentration.

Again MCF10A and MCF12A human non-transformed mammary epithelial cells were used for dose-response experiments with compound 2. Treatment of the control cells with this compound resulted in comparable IC<sub>50</sub> as seen in breast cancer cell lines growing under adherent culture conditions (supplementary Figure 3).

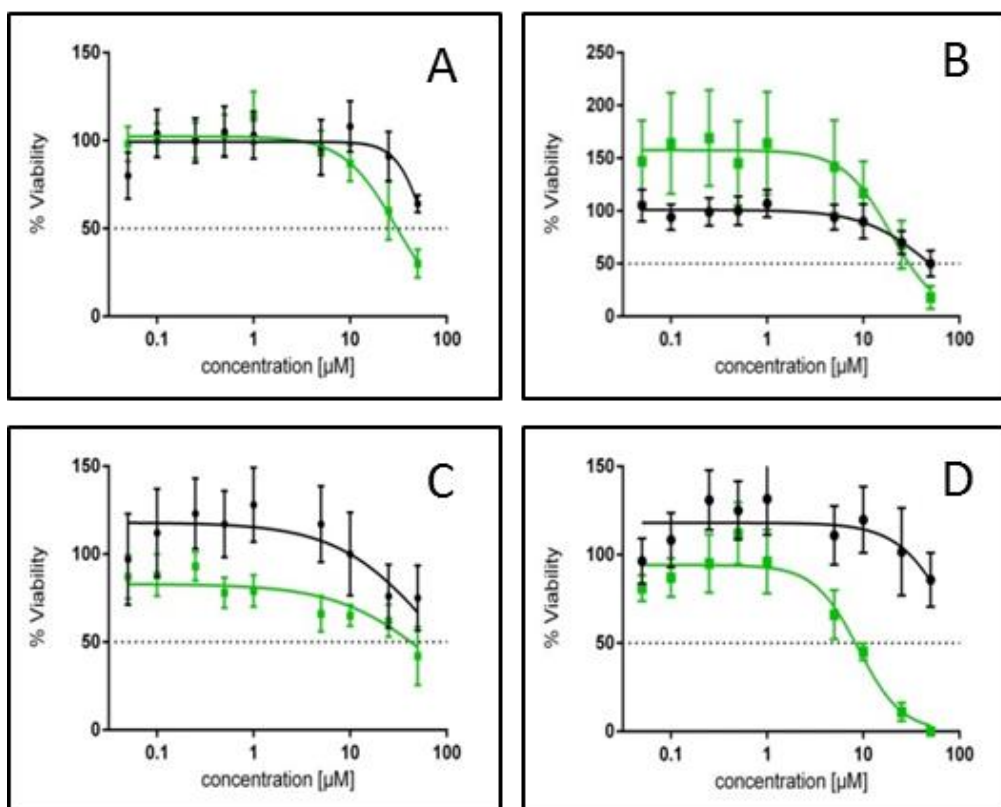


**Figure 17:** Dose-response curves of compound 2 in breast cancer cell lines grown as spheres (green) and monolayers (black). **A)** MCF7 tumorspheres exhibited a significantly lower IC<sub>50</sub> as adherently growing cells. **B)** In BT474 cells, IC<sub>50</sub> of tumorspheres was significantly lower compared to cells grown as monolayer. **C)** Treatment of SUM159 tumorspheres resulted in a very moderate reduction of IC<sub>50</sub> compared to cells grown as monolayer. **D)** MDA-MB231 tumorspheres treated with C2 were the only cells that showed almost complete reduction of viability, showing a significant selectivity for tumorspheres.

**Table 9:** Overview of the calculated IC<sub>50</sub> values after treatment with C2

Cell line	IC <sub>50</sub> adherently grown cells	IC <sub>50</sub> spheres
MCF7	61.0	29.8
BT474	48.6	19.3
SUM159	71.2	55.4
MDA-MB231	92.5	8.8
MCF10A	50.4	ND <sup>5</sup>
MCF12A	39.1	ND <sup>5</sup>

#### 4.3.4 *Primary breast and lung cancer cells*

Dose response-curves with the lead compounds C1, C19 and C2 for breast cancer cell lines and C1 and C19 for lung adenocarcinoma cell lines were also performed with primary patient-derived breast and lung cancer cells.

Overall, the results achieved from experiments with the established breast and lung cancer cell lines were confirmed in primary cancer cells. IC<sub>50</sub> of PL24 cells after treatment with C1 was 10.4  $\mu$ M which matches the average IC<sub>50</sub> of breast cancer tumorspheres after treatment with C1. Also treatment with C19 of PL24 resulted in an IC<sub>50</sub> of 7.4  $\mu$ M, comparable to that obtained by dose-response experiments in breast cancer tumorspheres. Interestingly, PL24 spheres were insensitive to treatment with C2 with a high IC<sub>50</sub> of 74.5  $\mu$ M (Figure 18C and table 10). This is in contrast to MDA-MB231, a breast cancer cell line belonging to the same molecular subtype (ER and PR negative, HER2 positive), which were sensitive to C2 treatment with an IC<sub>50</sub> value of 8.8  $\mu$ M. SUM159, representing the triple negative subtype of breast cancer, however, showed a similar high IC<sub>50</sub> value of 55.4  $\mu$ M. These results suggest, that current molecular subtypes may not sufficiently classify tumors, in order to improve treatment effectiveness.

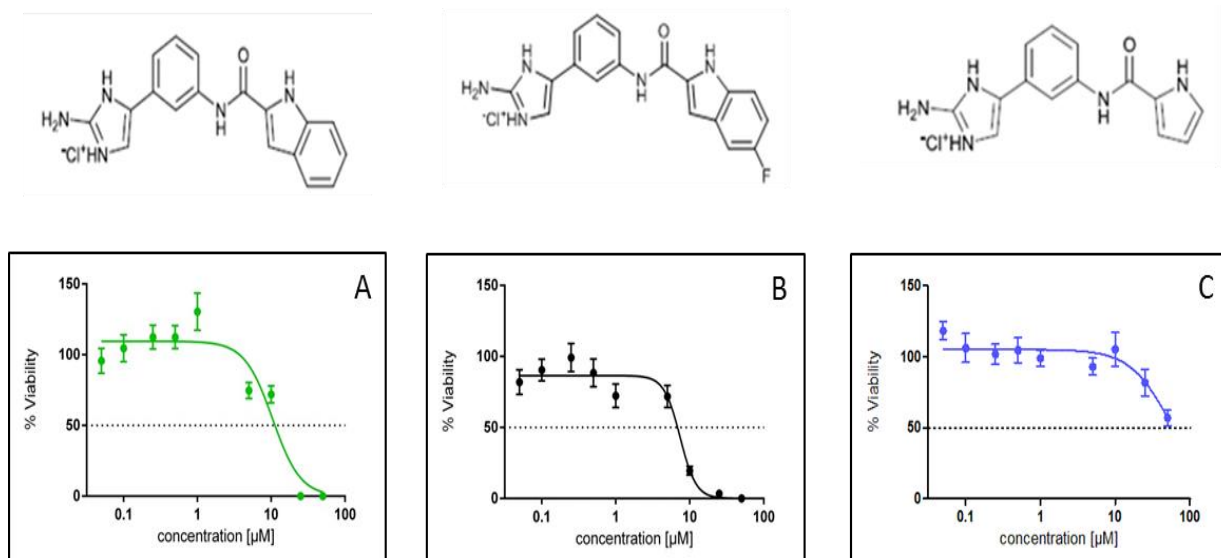


**Figure 18:** Treatment of primary breast cancer PL24 tumorspheres with C1 (A) decreased viability in a dose-dependent manner with an IC<sub>50</sub> of 10.4 μM. Treatment with compound 19 (B) also decreased the viability with a slightly lower IC<sub>50</sub> of 7.4 μM. In contrast, treatment of PL24 with C2 (C) showed merely no effect on viability with a high IC<sub>50</sub> of 74.5 μM.

Dose-response experiments with primary patient derived lung adenocarcinoma cells LT22 confirmed the results generated from lung adenocarcinoma cell lines (Figure 19). Treatment with lead compounds yielded an IC<sub>50</sub> value of 8.6 for C1 and 8.1 μM for C19 which were slightly lower than C<sub>50</sub> values obtained from established lung cancer cell lines.

The fact that the results of the primary patient derived cancer cells confirmed findings of established breast and lung cancer cell lines indicate that the compounds do not interfere with cellular pathways altered during long term cell culture. Numerous studies suggest, that there are differences concerning cellular response to extrinsic stress factors, DNA damaging agents and signalling pathways in cells from low and high passages.<sup>130,131,132,133</sup> Since the primary cancer cells PL24 and LT22 have not been cultured such a long time, these cells may better reflect the heterogeneity of primary tumors.

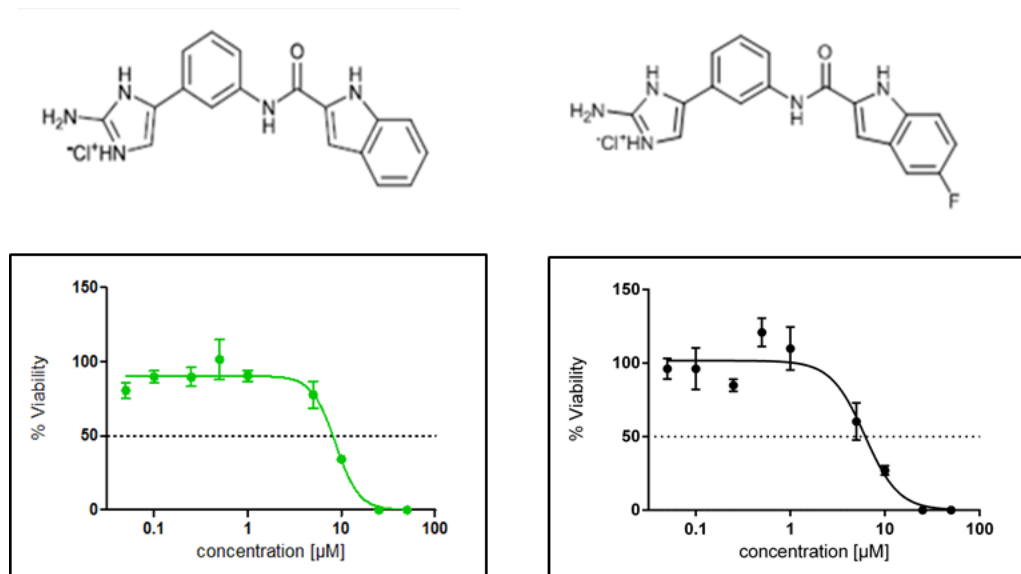


**Figure 19:** Dose-response curves of compound 1 (left panel) and compound 19 (right panel) in primary lung adenocarcinoma cells LT22 grown as tumorspheres. Both compounds showed a dose-dependent effect on cell viability with similar IC<sub>50</sub> of about 8 µM.

**Table 10:** Overview of the calculated IC<sub>50</sub> values for primary cancer cells

Cells	IC <sub>50</sub> Compound 1	IC <sub>50</sub> Compound 19	IC <sub>50</sub> Compound 2
PL24	10.4	7.4	74.5
LT22	8.6	8.1	ND <sup>5</sup>

In summary, all IC<sub>50</sub> values for all cell lines and all culture conditions are listed in table 11. The most significant and selective effect on viability of tumorspheres was observed in SUM159 cells after treatment with C19. Additionally, MDA-MB231 tumorspheres were also more sensitive to treatment with compound 2. All other cell lines tested, showed similar IC<sub>50</sub> values in tumorspheres and cells grown as monolayers.

Generally, breast cancer cells were more sensitive to treatment with the lead compounds compared to lung cancer cell lines. This is also mirrored by lower IC50 values (table 11). Therefore, further experiments were continued with breast cancer cell lines only and included the lead compounds C1, C19 and C2.

**Table 11:** Overview of IC50 values all cell lines and all compounds

Cell type	Cell line	C1 Adh	C1 Spheres	C19 Adh	C19 Spheres	C2 Adh	C2 Spheres
Breast cancer cell lines	MCF7	8.5	5.7	12.3	7.5	61	29.8
	BT474	12	12.7	10.5	13.5	48.6	19.3
	SUM159	13.1	13.4	12.8	2.9	71.2	55.4
	MDA-MB231	10.4	8.2	12.6	7.2	92.5	8.8
Primary breast cancer cells	PL24	ND <sup>5</sup>	10.4	ND <sup>5</sup>	7.4	ND <sup>5</sup>	74.5
Lung cancer cell lines	A549	22.8	12	14.2	10.2	ND <sup>5</sup>	ND <sup>5</sup>
	H1299	20	10.5	13.2	11.4	ND <sup>5</sup>	ND <sup>5</sup>
Primary lung cancer cells	LT22	ND <sup>5</sup>	8.6	ND <sup>5</sup>	8.1	ND <sup>5</sup>	ND <sup>5</sup>

#### 4.4 Sphere Formation Assay

To investigate the effect of lead compounds C1, C2 and C19 on the ability to self-renew, sphere formation assays were performed with all breast cancer cell lines.

In MCF7, C1 and C19 reduced sphere formation at a concentration of 10  $\mu\text{M}$  to a similar extent. Treatment with C1 and C19 at 25  $\mu\text{M}$  completely inhibited sphere formation (Figures 20A and B). In contrast, treatment with C2, which selectivity decreased viability of breast cancer tumorspheres, did not affect sphere formation in MCF7 tumorspheres (Figure 20C) .

Treatment of BT474 cells with Compound 1 reduced sphere formation starting at a concentration of 10  $\mu\text{M}$  (Figure 21A). In contrast, C19 almost abolished sphere formation at 10  $\mu\text{M}$  (Figure 21B). Both lead compounds, C1 and C19, completely abolished sphere formation at 25  $\mu\text{M}$  (Figure 21C). Similar to MCF7 cells, BT474 sphere formation was not significantly reduced after treatment with various concentration of C2.

When SUM159 cells were treated with C1, sphere formation decreased dose-dependently starting at a concentration of 1  $\mu\text{M}$ . A similar dose-dependent effect was seen with C19 with decreased sphere formation starting at 5  $\mu\text{M}$ . Both compounds completely abolished sphere formation at 25  $\mu\text{M}$  (Figures 22A and B). This finding is rather unexpected, as in dose-response experiments treatment with C19 resulted in significantly lower IC<sub>50</sub> of tumorspheres compared to treatment with C1 (see table 11).

Similar to BT474 and MCF7, treatment with C2 did not result in a decreased sphere formation at any concentrations tested. Again, this result was expected, as IC<sub>50</sub> of SUM159 tumorspheres after treatment with C2 was high (table 11) and viability was only decreased by about 40% at the highest compound concentration (Figure 17C).



When MDA-MB231 cells were treated with C1, sphere formation decreased dose-dependently, similar to SUM159 cells (Figure 22), starting at a concentration of 1  $\mu$ M. C19 treatment showed reduced sphere formation only at 10  $\mu$ M compound concentration. Again, similar to MCF7, BT474 and SUM159 cells, treatment with 25  $\mu$ M C1 or C19, completely abolished sphere formation (Figure 23). MDA-MB231 cells were the only cells that showed decreased sphere formation after treatment with C2. This result, however, is in line with the fact that compound 2 most effectively reduced viability only in MDA-MB231 tumorspheres (Figure 17D and Table 11). However, sphere formation was not completely abolished at the highest concentration of 25  $\mu$ M (Figure 23C).

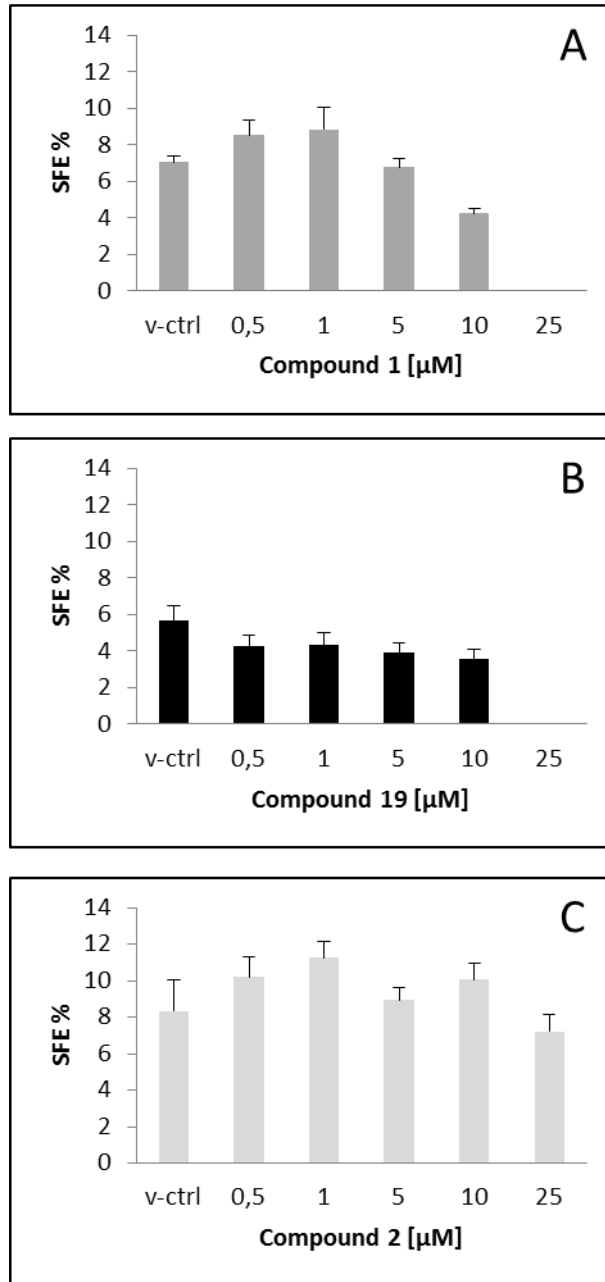


**Figure 20:** Effect of various concentrations of lead compounds C1, C19 and C2 on sphere formation efficiency of MCF7 cells (mean  $\pm$  SD of three replicates). C1 (A) and C19 (B) both reduced sphere formation at 10  $\mu$ M and completely abolished sphere formation at 25  $\mu$ M. In contrast, C2 (C) did not significantly reduce sphere formation at any tested concentration.

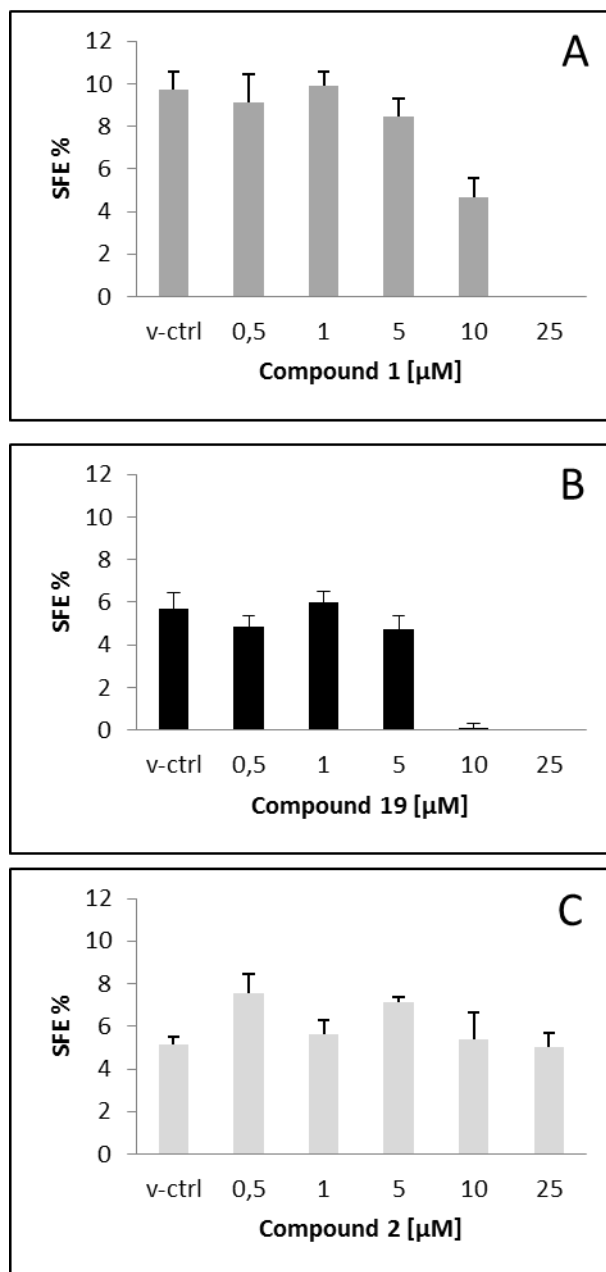


**Figure 21:** Effect of various concentrations of lead compounds C1, C19 and C2 on sphere formation efficiency of BT474 cells (mean  $\pm$  SD of three replicates). C1 treatment (A) reduced sphere formation at 10  $\mu$ M. C19 almost abolished sphere formation at 10  $\mu$ M (B). Similar to MCF7 cells, C2 (C) did not significantly inhibit sphere formation at any tested concentration.

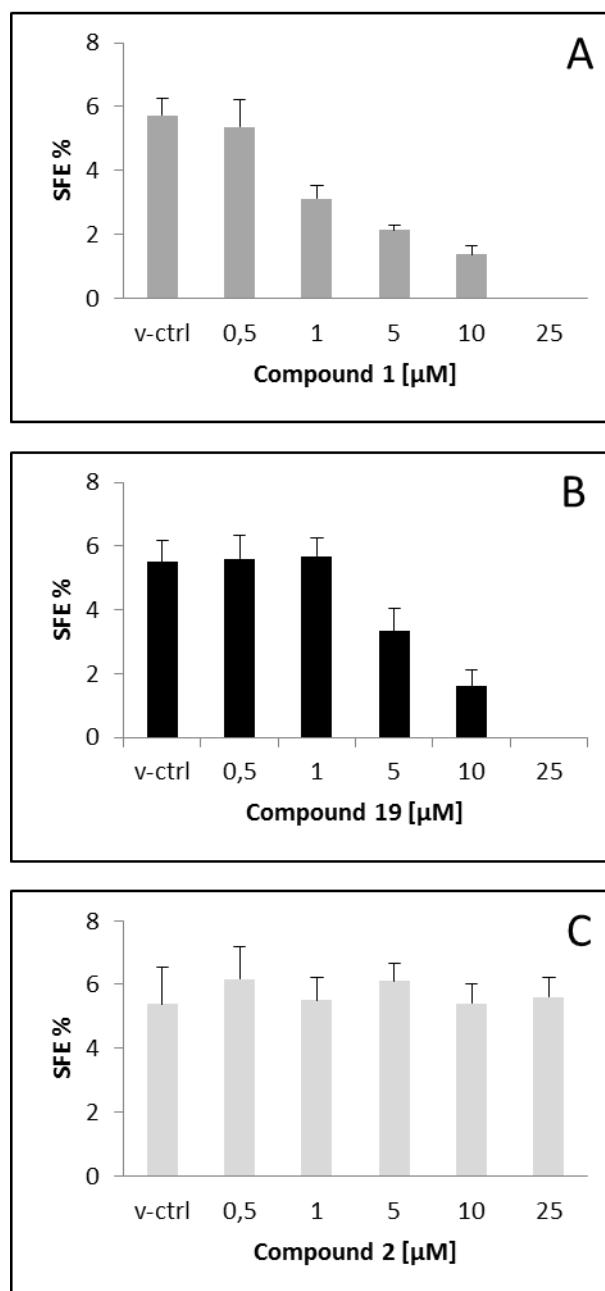


**Figure 22:** Effect of various concentrations of lead compounds C1, C19 and C2 on sphere formation efficiency of SUM159 cells (mean  $\pm$  SD of three replicates). C1 (A) slightly inhibited sphere formation at as little as 1  $\mu\text{M}$ , whereas C19 (B) reduced sphere formation at 5  $\mu\text{M}$ . Both compounds completely abolished sphere formation at 25  $\mu\text{M}$ . Similar to MCF7 and BT474, C2 (C) did not significantly reduce sphere formation at any tested concentration.

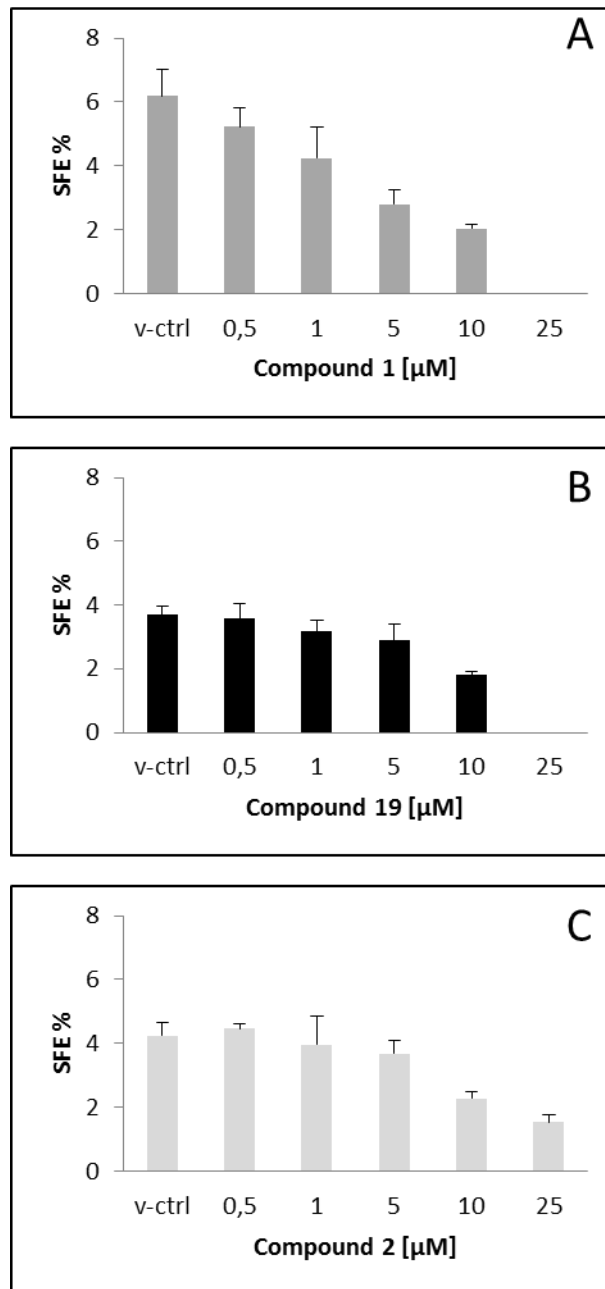


**Figure 23:** Effect of various concentrations of lead compounds C1, C19 and C2 on sphere formation efficiency of MDA-MB231 cells (mean  $\pm$  SD of three replicates). Treatment with C1 (A) reduced sphere formation at 5  $\mu\text{M}$ . C19 (B) reduced sphere formation at 10  $\mu\text{M}$ . Interestingly C2 (C) significantly reduced sphere formation at 10 and 25  $\mu\text{M}$  compound concentration. However, sphere formation was not completely abolished by C2 at 25  $\mu\text{M}$ .

## 4.5 q-PCR

Our next object was to identify differences in relative expression of CSC associated genes after treatment with the lead compound 19. Gene expression was normalized to the housekeeping genes LDHA, GAPDH and TBP and expressed as fold change compared to the vehicle control cells (0.7% DMSO).

Fibronectin (FN) expression, a gene associated with EMT, was significantly reduced after treatment with C19 (Figure 24). Similarly, expression of Twist, an EMT associated transcription factor (TF), was also downregulated upon treatment of tumorspheres. E-Cadherin (E-Cad) expression, which is associated with an epithelial phenotype, was also moderately decreased. Expression of other TF or EMT associated genes, including Oct4, Snail, and Sox2, was not altered after treatment with C19. CD44, Nanog and Slug were slightly overexpressed compared to the vehicle control treated tumorspheres. Vimentin (Vim), Aldehyde dehydrogenase 1 (ALDH1) and N-Cadherin (N-Cad) were not expressed in MCF7 tumorspheres (data not shown).

Overall, treatment of MCF7 tumorspheres with C19 did not clearly reduce the expression of the majority of CSC associated genes, suggesting that C19 had no effect on cancer stem cells. This result is in line with the observation that SFE was not effectively reduced at the same concentrations (5 and 10  $\mu\text{M}$ ) (Figure 20B).

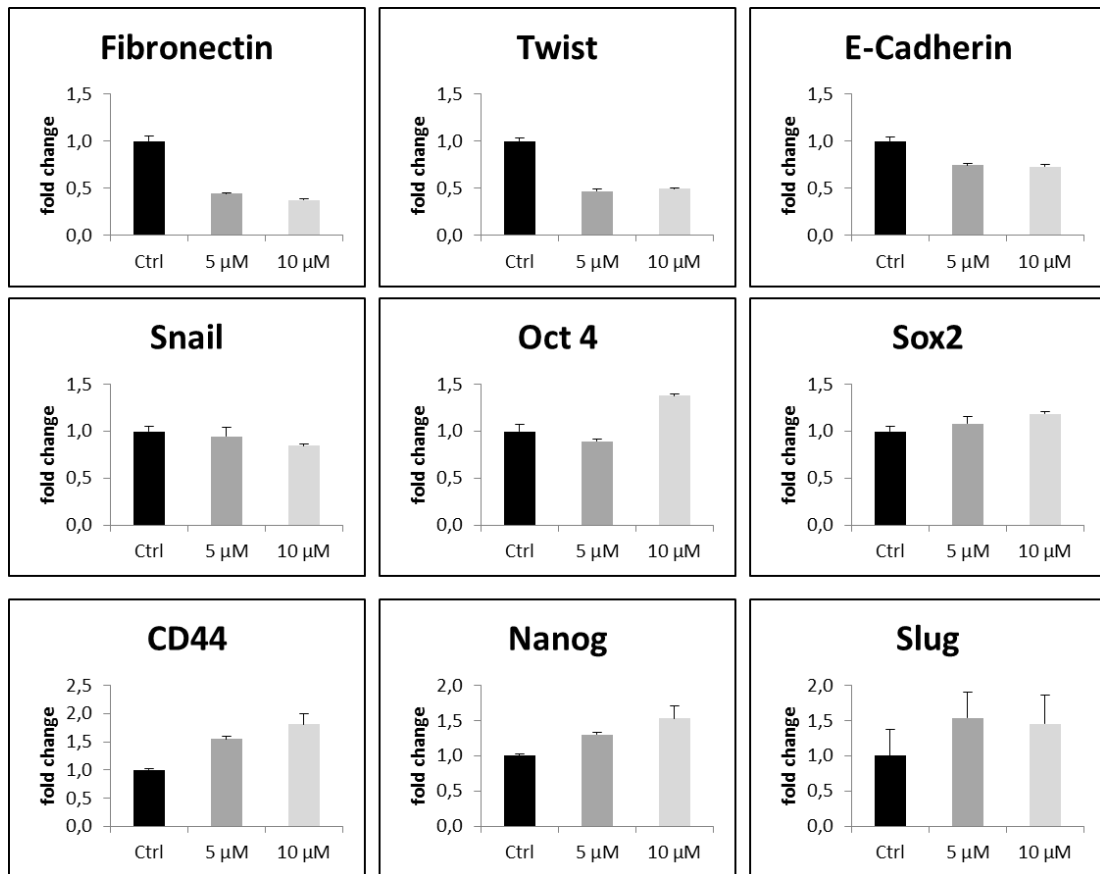


**Figure 24:** Effect of C19 on expression of CSC associated genes in MCF7 spheres. Spheres were treated for 24 hours. Expression is represented as a fold change of DMSO vehicle control. Data are represented as the mean  $\pm$  SEM ( $n=2$ ). Only Fibronectin and Twist decreased significantly by about 50%. E-Cad, Snail, Oct4 and Sox2 expression did not change significantly upon treatment with the compound. Expression levels of CD44, Nanog and Slug were moderately increased.

Similar to MCF7, treatment of BT474 tumorspheres with C19 did not reduce gene expression of CSC associated genes. Vim, N-Cad and ALDH1 expression were slightly decreased at a concentration of 5  $\mu$ M, while a slight increase of their expression was observed at 10  $\mu$ M. Expression of Oct4 remained unchanged at 10  $\mu$ M concentration. Increased expression levels of Sox2, Nanog, Slug, Twist, E-Cad, CD44 and Snail were observed in response to treatment with C19. While Sox2 expression was slightly increased after treatment, Nanog expression was almost 3-fold higher than the vehicle control at 10  $\mu$ M. Also, Slug, Twist, E-Cad and CD44 expression levels were 2- to 3-fold increased. Moreover, treatment with C19 at 10  $\mu$ M induced a 6-fold increase in expression of Snail (Figure 25). Fibronectin was not expressed in this cell line (data not shown).

The finding that most of the CSC associated gene levels were increased instead of decreased, was rather unexpected since treatment of BT474 spheres with C19 lead to a significant decrease of SFE, at least when incubated with 10  $\mu$ M. One would suggest that if sphere formation is no longer possible upon treatment with the compound, expression of genes involved in pathways associated with CSCs is also diminished.



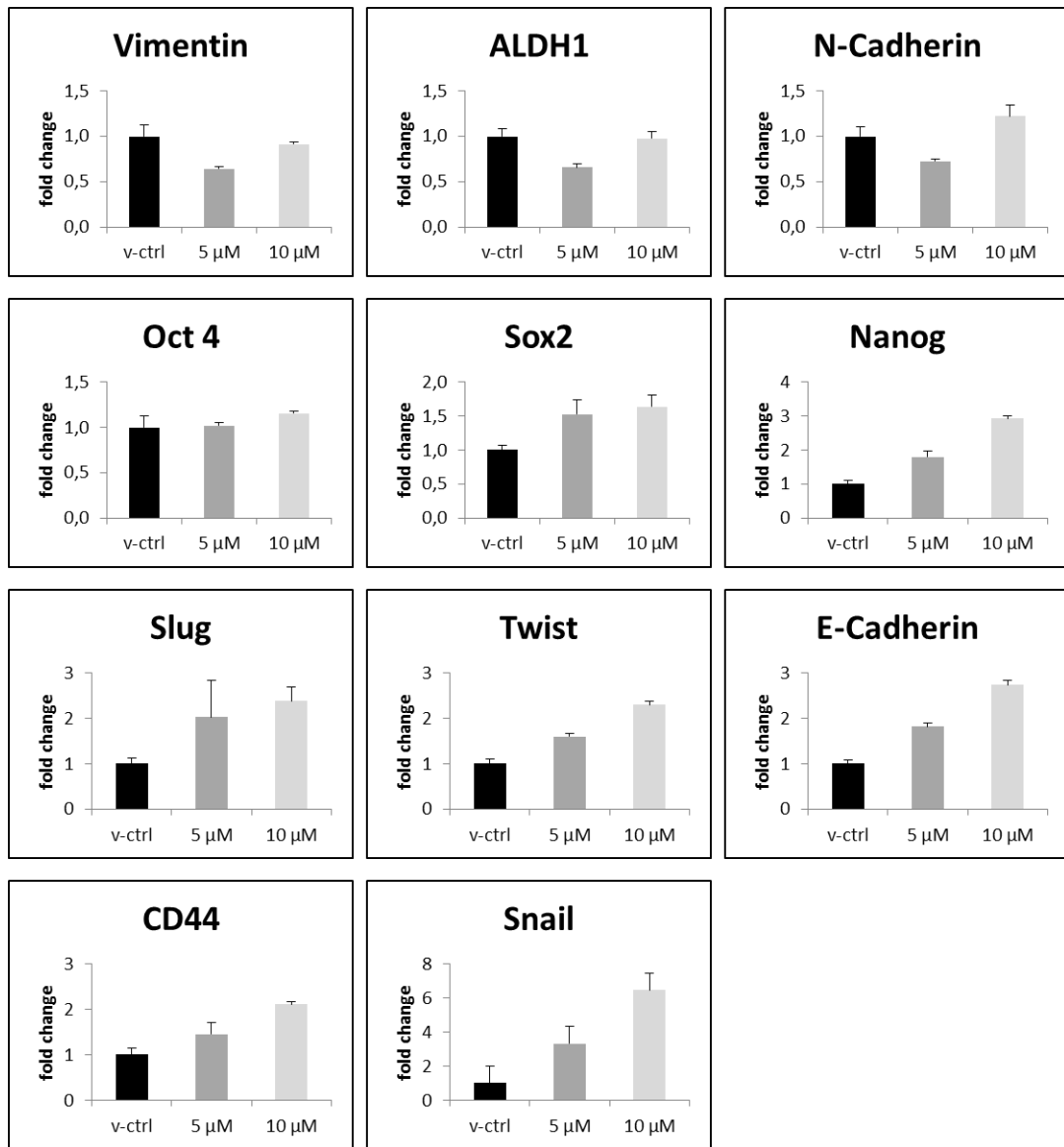


**Figure 25:** Effect of C19 on expression of CSC associated genes in BT474 spheres. Spheres were treated for 24h. Expression is represented as a fold change of DMSO vehicle control. Data are represented as the mean  $\pm$  SEM (n=2). Vimentin, ALDH1 and N-Cad showed a decrease in expression levels only at 5  $\mu$ M compound concentration. Oct4 expression was not significantly altered after treatment with C19. Relative expression levels of Sox2, Nanog, Slug, Twist, E-Cad, CD44 and Snail on the other hand were increased up to 3-fold (Nanog) and even 6-fold (Snail).

Incubation of SUM159 tumorspheres with C19 did not result in major changes of CSC associated gene expression levels. Sox2 expression was 2-fold lower at both concentrations tested. Nanog expression was 2-fold reduced at 5  $\mu$ M, but almost unaffected at 10  $\mu$ M compound concentration. Vim and ALDH1 expression levels were decreased at 5  $\mu$ M, whereas at 10  $\mu$ M C19 showed no detectable change in expression levels. Oct4, N-Cad and CD44 expression also remained unchanged upon treatment with the C19. Some genes, including FN, Twist, Snail and Slug, however, showed an increase in expression levels after treatment with C19 (Figure 26). E-Cadherin was not expressed in this cell line (data not shown).

Overall, treatment of SUM159 spheres at 5  $\mu$ M concentration resulted in a decreased expression of genes including Vim, ALDH1 and N-Cad. In contrast, treatment at 10  $\mu$ M did not show any considerable changes in expression of CSC associated genes. Considering the results of dose-response experiments, where SUM159 tumorspheres were most sensitive to C19 treatment with a very low IC<sub>50</sub> (2.9  $\mu$ M) it was surprising that treatment with compound concentrations above the IC<sub>50</sub> did not significantly change gene expression levels of CSC associated genes.

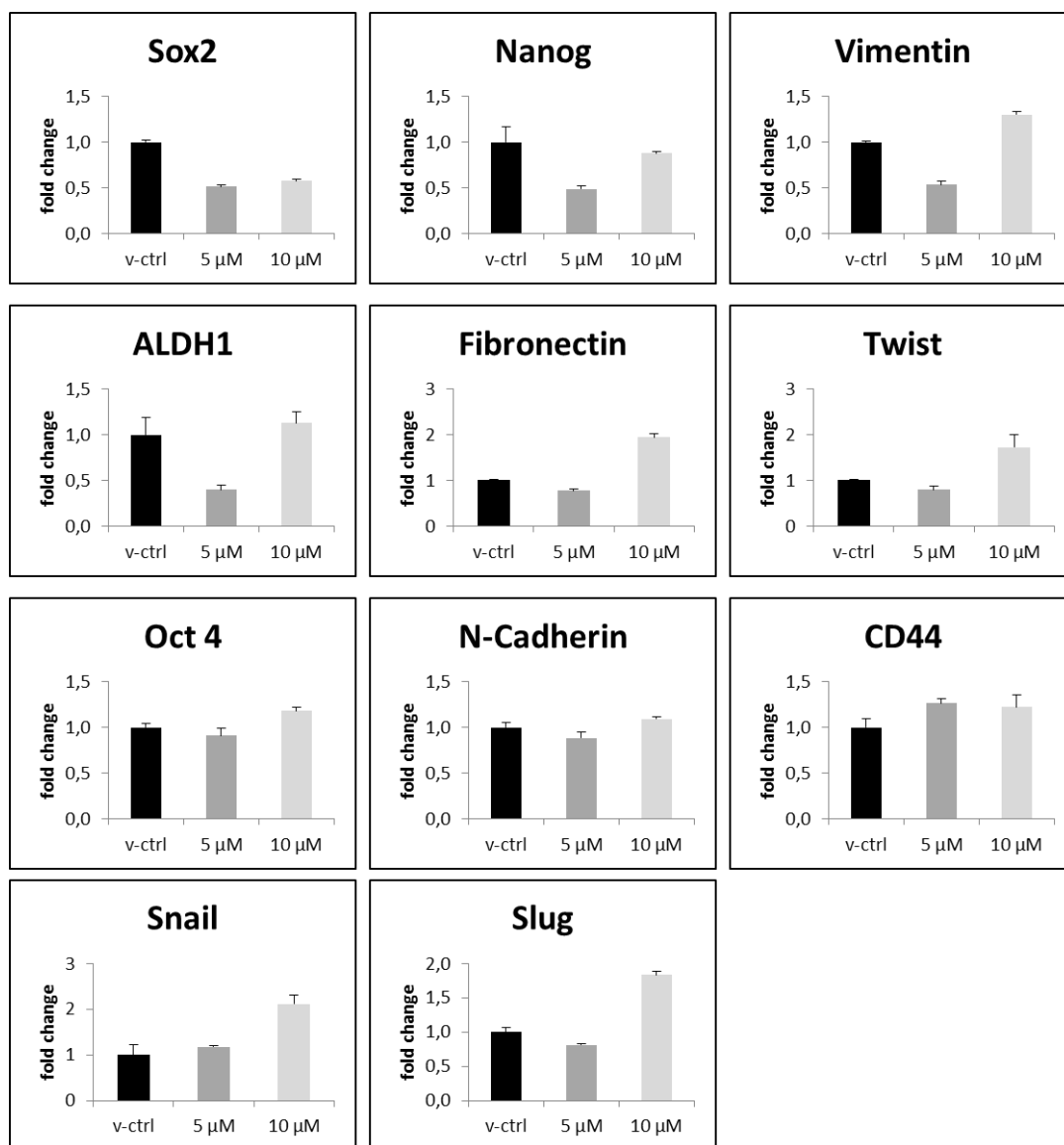


**Figure 26:** Effect of C19 on expression of CSC associated genes in SUM159 spheres. Spheres were treated for 24 hours. Expression is represented as a fold change of DMSO vehicle control. Data are represented as the mean  $\pm$  SEM (N=2). Sox2 expression was reduced by about 50% upon treatment. Nanog, Vimentin and ALDH1 expression did also decrease, although only at 5  $\mu$ M compound concentration. Relative expression levels of Fibronectin, Twist, Oct4, N-Cad and CD44 did not significantly change upon treatment with C19 and Snail and Slug expression slightly increased.

Overall, treatment of MDA-MB231 with C19 resulted in most substantial difference in expression a variety of CSC associated genes. Sox2 expression decreased to about 3-fold in response to the treatment at both concentrations. Expression levels of Snail, Slug and Vim were also diminished about 2-fold in response to C19 treatment at 5  $\mu$ M. However, expression of these genes was not further decreased at 10  $\mu$ M compound concentration. CD44 expression was also decreased but to a lesser extent. The expression level of FN did slightly increase after treatment with 10  $\mu$ M C19 (Figure 27). Nanog, Twist, ALDH1, E-Cad and N-Cad expression was also investigated but could not be detected in MDA-MB231 tumorspheres (data not shown).

Overall, gene expression results of MDA-MB231 tumorspheres treated with C19 confirmed results from sphere formation assays, where treatment significantly reduced sphere formation efficiency.

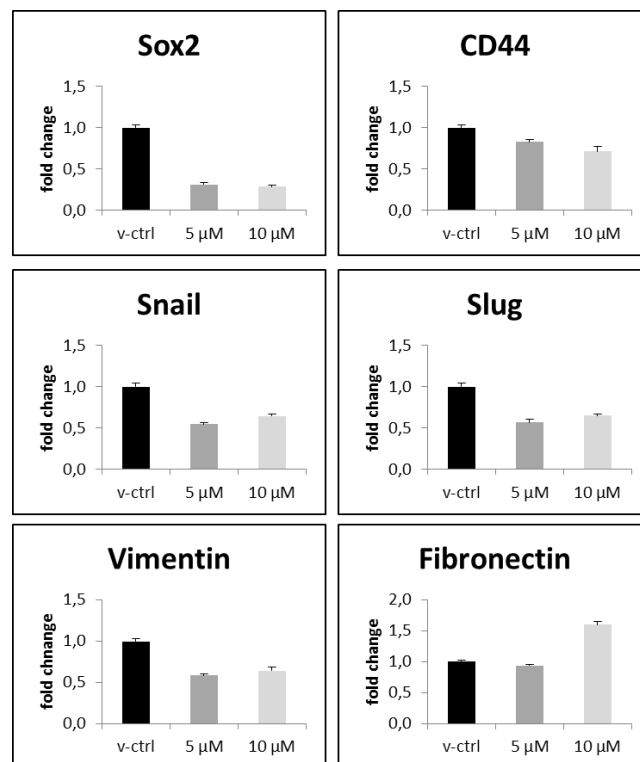


**Figure 27:** Effect of C19 on expression of CSC associated genes in MDA-MB231 spheres. Spheres were treated for 24 hours. Expression is represented as a fold change of DMSO vehicle control. Data are represented as the mean  $\pm$  SEM (N=2). Sox2 expression showed a 3-fold reduction. Expression of CD44, Snail, Slug and Vimentin was also about 2-fold decreased. In contrast, relative expression levels of Fibronectin increased about 2-fold at 10  $\mu$ M compound concentration.

Due to the fact, that treatment of MDA-MB231 cells with C2 resulted in reduced sphere formation efficiency, expression levels of CSC associated genes were also assessed with this compound. Overall the reduced expression of the CSC associated genes was not as clearly as after treatment with C19. CD44 and Sox2 expression was slightly decreased at only 10  $\mu$ M compound concentration. Expression levels of genes including Slug, Vim, FN and Snail remained unchanged (Figure 28).

This finding is in concordance with the results from the dose-response curves and sphere formation assays as viability and IC<sub>50</sub> of MDA-MB231 tumorspheres was only slightly decreased after treatment with C2 (table 11 and Figure 17D) and also sphere formation was moderately inhibited (Figure 23).

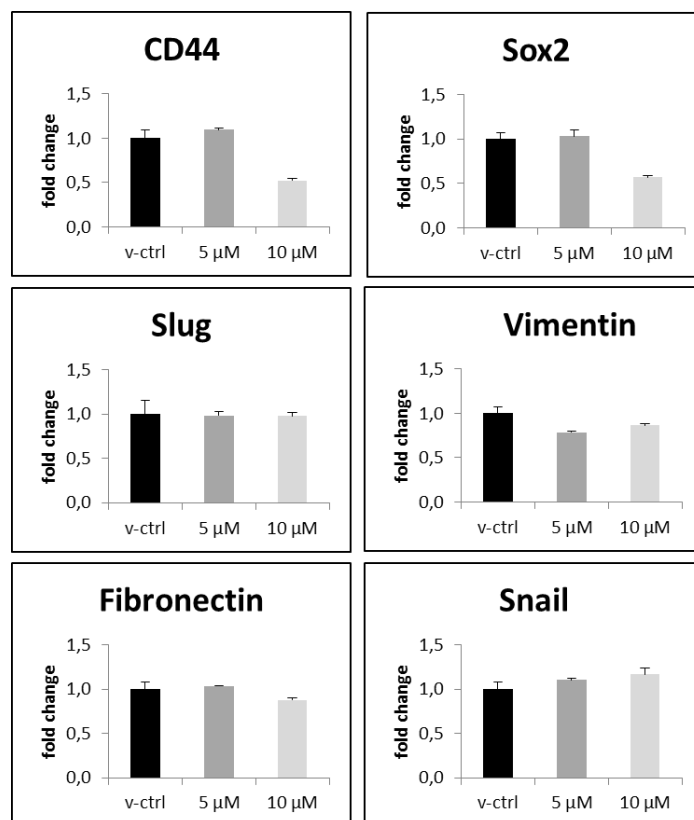


**Figure 28:** Effect of C2 on expression of CSC associated genes in MDA-MB231 spheres. Spheres were treated for 24 hours. Expression is represented as a fold change of DMSO vehicle control. Data are represented as the mean  $\pm$  SEM ( $n=2$ ). Expression of CD44 and Sox2 was slightly decreased only at 10  $\mu$ M compound concentration. Slug, Vim, FN and Snail expression levels were not altered significantly.

## 5. Discussion

### 5.1 Generation of spheres

The generation of spheres under non-adherent culture conditions at clonal density has been widely and successfully used in order to study cancer stem cells. Many groups have cultured tumor cells from solid tumors including breast,<sup>134</sup> lung,<sup>59</sup> brain,<sup>135</sup> prostate<sup>95</sup> or colon cancer<sup>56</sup> under these conditions. FACS analyses and qRT-PCR experiments have confirmed that CSC associated marker genes are upregulated in tumorspheres.<sup>91,92,59</sup> Soft agar assay experiments with CSCs resulted in increased tumorigenic potential *in vitro*<sup>136</sup> and experiments with mouse models have shown that cells derived from sphere culture conditions possess increased tumor initiating potential *in vivo*.<sup>72,56</sup> Sphere formation assays have been used to confirm that cells cultured as spheres possess the ability to self-renew.<sup>96</sup> Also these cells have been shown to grow more invasively.<sup>94</sup>

The decision to culture breast and lung cancer cell lines under these culture conditions is hence based on broad evidence that this method is sufficient and adequate to enrich for cells that possess CSC potential. Supplements added to the growth media vary slightly between different research groups but all share basic ingredients.

In this study, we used the same basal medium DMEM/F12 for all breast cancer cell lines studied, in order to minimize variations resulting from different media composition. Adherently growing breast cancer cells were also grown with DMEM/F12 media supplemented with 10% FBS. In contrast, lung cancer cell line monolayers were cultured with RPMI1640 media supplemented with 10% FBS.

All cancer cell lines used showed the ability to generate tumorspheres under these non-adherent growth conditions and could be passaged at least 10 times. We also observed morphological differences in generated tumorspheres. BT474, for example, generated perfectly round shaped and tightly packed spheres, whereas MDA-MB231 generated more grape-like structures (Figure 5). In these clusters, cells were also more loosely connected to each other and

were easily disrupted by harsh pipetting. Such morphological differences between phenotypically different breast cancer cell lines have been previously reported by Smart et al 2013. They also experienced differences between the sphere packaging density and stability when comparing tumorspheres from luminal with basal breast cancer cell lines.<sup>91</sup> This heterogeneity may be due to the differential expression of cell adhesion and cytoskeleton molecules, which was not only observed in monolayer grown cells but also in corresponding tumorspheres.

## 5.2 Screening and dose response experiments

To identify lead compounds, we performed preliminary screening experiments with all 19 candidate alkaloid derivatives. These experiments showed that many compounds reduced cell viability to less than 50%. Lead compounds were identified that completely inhibited cell viability at this relative high concentration of 50  $\mu\text{M}$  and were chosen for follow-up experiments. These compounds included C1 and C19 which only differ in their structure by one fluorine atom (see table 1). Interestingly both compounds completely inhibited viability in all cancer cell lines of both origin breast and lung cancer. Compound 7 also efficiently reduced viability in breast cancer cell lines, but only moderately affected viability of lung cancer cells.

The probably most interesting result of these screenings was that compound 2 selectively inhibited viability of breast cancer tumorspheres. Adherently growing breast cancer cells were left (almost) unaffected by this compound and lung cancer cells were also unaffected by this treatment independent of culture conditions.

The effect of the chosen lead compounds – C1, C19 (and C2 for breast cancer cells only) – on the viability were then investigated in more detail with dose response experiments. Treatment with compound concentrations ranging from 0.05 to 50  $\mu\text{M}$  showed that compounds reduced viability in a dose dependent manner. Dose response curves showed that C19 decreased viability at lower concentrations compared to C1 (Figures 13 to 16). Consequently, calculated IC<sub>50</sub> values were lower for compound 19 compared to C1 (table 6 and 7).

Unfortunately, treatment with compound 2, which looked promising in the screening experiments, did not reduce viability to a similar extent as C1 or C19. As expected, adherently growing cells remained unaffected after treatment with C2. In contrast, tumorspheres treated with C2 showed decreased viability only at high compound concentrations resulting in high IC<sub>50</sub> values (Figure 17). The only exceptions to this were tumorspheres from MDA-MB231 cells, which showed a significant decrease of viability at 10  $\mu\text{M}$  compound concentration. Also BT474 tumorspheres treated with C2 resulted in a significantly lower IC<sub>50</sub> value.



To further validate the results generated from breast and lung cancer cell lines, the same dose response assays were performed with primary breast and lung adenocarcinoma cells, which were established in our working group. These experiments, which were only performed with tumorspheres, showed that IC50 values were comparable to those generated from established cancer cell lines. Also the compound concentration at which the viability was significantly reduced was similarly low as in cancer cell lines.

Patient-derived cancer cells at low passage are believed to better retain the characteristics and heterogeneity of the original tumor.<sup>137</sup> The finding that dose-response measurements with primary patient-derived tumorspheres resulted in similar IC50 values compared to tumorspheres from established breast and lung cancer cell lines suggests that the effect of these compounds is also relevant for patient derived tumor samples.

The results generated from dose response experiments suggest that the chosen lead compounds efficiently target the subpopulation of CSCs as there was the tendency that IC50 values of tumorspheres were significantly lower than corresponding IC50 of monolayer cells. It is generally considered an important factor for future anti-cancer drug development that not only the bulk tumor is erased but also CSCs. Therefore, the finding that the examined compounds target both, monolayer cells and tumorspheres, may provide an interesting outlook for future anti-cancer drug development.

The ability to target cancer stem cells is of utmost importance as this population of cancer cells is held responsible for chemoresistance, metastasis and tumor recurrence. Previous studies showed that compounds that inhibited viability of tumorspheres *in vitro* also reduced tumor propagation *in vivo* leading to an improved survival.<sup>138</sup> Another study by Kim and Alexander (2014) showed that the tumorsphere model provides a promising way to assess and predict *in vivo* response to chemotherapeutics.<sup>129</sup> They also showed that tumorspheres exhibit a slow proliferation rate compared to monolayer cells, which might be one reason why they are frequently resistant to conventional chemotherapeutics targeting rapidly dividing cancer cells. Additionally, their findings demonstrated that tumorspheres are more applicable models to predict the response of anti-cancer drugs *in vivo*.

### 5.3 Sphere formation experiments

Sphere formation assays have been previously used by various groups working with stem and cancer stem cells<sup>139,135,140</sup>. This assay serves as *in vitro* method to investigate the capability of the cells to self-renew and grow clonally.<sup>96</sup> Using this assay, it is important to seed the cells at very low densities into multi-well plates that tumorspheres can form from single clones. In addition, the plates should not be moved and media must not be changed during at least the first 5 days of growth in order to minimize formation of aggregates rather than tumorspheres.<sup>124</sup> This assay has also been used in previous studies as a model for the identification of CSC-like targeting drugs.<sup>127</sup>

In this project, treatment with C19 and C1 decreased sphere formation efficiency in all breast cancer tumorspheres. However, the lowest concentration at which sphere formation capacity was decreased varied between cell lines and compounds. In most cases, tumorsphere formation was inhibited at 10  $\mu\text{M}$  or higher compound concentrations (C1: MCF7, BT474 and C19: MCF7, BT474, MDA-MB231; Figures 20A/B, 21A/B, 23B). Only SUM159 tumorspheres were more sensitive to the treatment which lead to a decrease in sphere formation efficiency at 1  $\mu\text{M}$  for C19 and 5  $\mu\text{M}$  for C19 (Figure 22A/B). Additionally, treatment with 1  $\mu\text{M}$  C1 of MDA-MB231 cells also resulted in impaired tumorspheres formation efficiency (Figure 23A). The only cell line which showed decreased tumorsphere formation capacity upon treatment with C2 was the MDA-MB231 cell line with a reduction of sphere formation efficiency at concentrations of 10  $\mu\text{M}$  and higher (Figure 23C). Overall, treatment with C1 or C19 reduced sphere formation at 10 $\mu\text{M}$  concentration or lower, while at the same concentration viability was not affected suggesting that these compounds affect self-renewal capacity.

The results of sphere formation experiments mostly correspond to findings from dose response experiments with similar IC50 values. Exception to this were SUM159 tumorspheres, which showed impaired tumorsphere formation capacity at as little as 1  $\mu\text{M}$  C1, whereas IC50 of C1 in tumorspheres was 13.4  $\mu\text{M}$  (Figure 22A and table 11). Similarly, treatment of MDA-MB231 tumorspheres with C1 leads to an IC50 of 8.2  $\mu\text{M}$  whereas sphere formation efficiency was already reduced at 1  $\mu\text{M}$ .

We also observed that the passage number of cells used for experiments influenced the sphere formation capacity. In BT474 cells, for example, the SFE of the cells treated with the vehicle control was approximately 5 % for experiments with C19 and C2, but almost 10 % for C2 treatment which was seeded two weeks later. Similarly, MCF7 cells treated with C19, which was done with cells from an earlier passage, lead to a SFE in cells treated with vehicle control of 5 %, whereas SFE in C1 was 7 % and 8 % in the experiment with C2. The effect of passage number on cell phenotype and experimental outcome has also been observed in previous studies.<sup>141</sup>

A previous study by Larzabal et al showed that anti-cancer drugs can have very diverse effects on monolayer cells compared to tumorspheres cultured cells. They also showed that the results obtained from sphere formation assays upon treatment with a chemotherapeutic agent could predict the outcome *in vivo* experiments.<sup>142</sup> Other studies have also successfully used tumorspheres formation assays to show that results from these *in vitro* experiments can predict the outcome of various *in vivo* studies.<sup>138,143</sup>

#### 5.4 Reverse transcription quantitative real-time PCR

Overall C19 treatment of breast cancer cell lines resulted in lower IC50 values and a decrease of sphere formation efficiency at lower compound concentrations compared to C1 treatment. Therefore, the expression of CSC associated genes was analysed with qPCR after 24h treatment with 5 and 10  $\mu$ M C19. Single cells were allowed to generate spheres for 72h prior to the treatment.

Since Al-Hajj et al described 2003 a subpopulation of breast cancer cells with a CD44<sup>high</sup>/CD24<sup>low</sup> phenotype. CD44 has been used as surface marker for the identification of breast-CSC. They found that this phenotypic population within breast cancer cells was highly tumorigenic, could be serially passaged and gave rise to phenotypically diverse mixture of tumor cells present in the initial tumor.<sup>51</sup> In our experiments, CD44 expression was moderately (less than 2-fold) increased in MCF7, BT474 and SUM159 tumorspheres after treatment with C19. Only MDA-MB231 tumorspheres showed a decrease of CD44 expression. These data indicate that treatment with compound 19 did not significantly reduce CD44 expression, a gene associated with CSCs.

Regarding ALDH1 expression, a marker which has widely been used for CSC in multiple cancer types including breast,<sup>144,145</sup> brain,<sup>146</sup> colon<sup>147</sup> and lung<sup>148</sup> cancer, we observed that ALDH1 expression was decreased in BT474 and SUM159 tumorspheres. This finding supports the results from previous experiments, where IC50 values were lower in tumorspheres compared to monolayer cells and sphere formation was inhibited upon treatment with C19. Interestingly, in both cell lines this effect could only be seen after treatment with 5  $\mu$ M but not 10  $\mu$ M compound concentration.

E-Cadherin (E-Cad), also known as Cadherin1 (CDH1), is a cell adhesion molecule typically expressed in epithelial cells. Loss of E-Cadherin is associated with cancer progression and metastasis<sup>149,150</sup> because cell-cell connections are loosened and cells become more motile. Recently, E-Cadherin has also been found to play a role in mammospheres formation in breast cancer cell lines.<sup>151</sup> In our qPCR experiments E-Cad expression was affected differentially in MCF7 and BT474 tumorspheres. Expression of E-Cad in MCF7 spheres was slightly reduced dose dependently, indicating a shift to a more mesenchymal like phe-

notype. On the other hand there was a significant increase of E-Cad expression in BT474 tumorspheres. Regarding the results from dose-response experiments, this is not a complete surprise as BT474 tumorspheres showed higher IC50 levels than corresponding monolayer cells. In contrast, sphere formation efficiency of BT474 cells was almost completely inhibited upon treatment with 10  $\mu$ M C19.

N-Cadherin (N-Cad) or Cadherin2 (CDH2) is associated with cells showing a mesenchymal phenotype. In contrast to E-Cad, increased expression levels of N-Cad have been found to play a role in cancer metastasis and progression.<sup>152</sup> Similarly to N-Cadherin, Fibronectin (FN)<sup>153</sup> and Vimentin (Vim)<sup>145</sup> have also been found to be involved in EMT. EMT has been described as dedifferentiation program in cancer that facilitates and is involved in tissue invasion and metastasis.<sup>110</sup> Several studies also describe an association of CSCs and the EMT phenotype.<sup>154</sup> In our study, BT474 tumorspheres showed decreased N-Cad and Vim expression when treated with 5  $\mu$ M C19. Similarly, SUM159 tumorspheres also expressed lower levels of Vim at 5  $\mu$ M concentration. In contrast, at 10  $\mu$ M concentration, N-Cad expression of SUM159 tumorspheres was not changed and FN expression was even increased at 10  $\mu$ M C19 treatment. Similarly to SUM159 tumorspheres, MDA-MB231 spheres also showed contradictory results. Whereas Vim expression was decreased, FN expression was elevated in MDA-MB231 tumorspheres after C19 treatment.

Overall no clear picture of how C19 treatment influences expression of N-Cad, Vim and FN could be drawn from the generated results. If the subpopulation of CSC was targeted by the treatment, expression of these three mesenchymal associated marker genes should decrease. However, this was not consistently the case for the cell lines used and at the concentrations and incubation time chosen. Further studies with different concentrations and incubation times are needed to better understand the effect of C19 treatment on gene expression.

Transcription factors including Slug, Snail or Twist are also associated with EMT, a process often associated with CSC. These transcription factors are frequently expressed in cancers and can lead to the generation of cells with CSC properties. Transduction of Snail1 or Twist for example has been described as being able to generate mammary stem cells with CD44<sup>high</sup>/CD24<sup>low</sup> phenotype

and tumorsphere formation properties in HMEC cells.<sup>108</sup> Snail and Slug have also been shown to activate the TGF- $\beta$  signalling pathway in breast cancer,<sup>155</sup> a pathway which if overexpressed, is frequently associated with many cancer types. Hence, selective targeting of CSCs should also decrease expression of these genes. In MCF7 tumorspheres, Slug levels were slightly increased, Snail was unaltered and Twist expression was decreased. A consistent tendency could be seen in BT474 spheres treated with C19, where all three EMT associated transcription factors were significantly overexpressed. These results suggest that treatment with C19 of these luminal B type breast cancer cells induces a more CSC like phenotype, at least at the transcriptional level. Similarly, SUM159 tumorspheres showed an elevation of Slug and Snail expression upon C19 treatment, whereas Twist expression remained unaffected. MDA-MB-231 was the only cell line showing a clear reduction in the expression of Snail and Twist upon treatment with C19, indicating a selective effect of C19 on the CSC subpopulation.

Oct4, Sox2 and Nanog are common markers for pluripotency. Oct4 has been used as putative stem cell marker and been found involved in pathways associated with self-renewal.<sup>156,157</sup> Similarly to Sox2, Oct4 is also a transcription factor knowingly involved in self-renewal, pluripotency and maintaining an undifferentiated phenotype in embryonic stem cells and overexpression of this gene has been found in lung,<sup>158</sup> prostate<sup>159</sup> and breast cancer.<sup>160</sup> Nanog together with Sox2 has also been found to be involved in EMT in breast cancer and they seem to be a marker for worse prognosis in breast cancer patients.<sup>161</sup> Decreased levels of these genes would hence again indicate a selective effect of C19 on the CSC subpopulation. In our experimental setting, Oct4 expression was unaffected upon treatment with compound 19 in all cell lines investigated. Similarly, in MCF7 tumorspheres Sox2 expression was not altered upon treatment. In contrast, Nanog expression level was slightly increased in MCF7 tumorspheres. BT474 tumorspheres on the other hand showed increased levels of Sox2 and Nanog. SUM159 spheres showed a slight reduction of Sox2 and Nanog expression. The most significant response to C19 treatment was observed in MDA-MB231 tumorspheres, where expression of Sox2 was reduced by 80%.

Overall, the hypothesis, that treatment with C19 affects transcription of CSC associated marker genes could not be consistently verified in our study, as no clear overall tendency towards reduced expression of CSC marker genes could be seen.

In fact, BT474 tumorspheres showed significantly increased expression of markers for EMT and pluripotency (Slug, Snail, Twist, Oct4, Sox2, Nanog) suggesting an expansion of the CSC phenotype. In contrast, treatment of BT474 spheres resulted in increased E-Cad expression and decreased Vim and N-Cad expression. Also CD44 expression was inhibited by the treatment. Also SUM159 tumorspheres showed overall an increase in CSC associated marker genes than a decrease. MCF7 tumorspheres were mostly unaffected by the treatment and only minor changes in gene expression levels could be observed.

The only cell line that showed a clear trend in a decrease of CSC associated marker gene expression was MDA-MB231. These tumorspheres showed reduced expression of CD44, Vim, Snail, Twist and an almost complete loss of Sox2 expression. These data suggest that the CSC subpopulation of MDA-MB231 tumorspheres is selectively targeted by the treatment.

Overall, treatment with C19 did not clearly decrease CSC associated gene expression. One reason for these results could be the differential setting of the experiments. While for sphere formation experiments tumorspheres were treated for 5 days with the compound, tumorspheres for qPCR experiments were allowed to grow for three days and then treated for 24h. On the other side, for dose-response experiments, cells were incubated for 72h with the compound. Also, the seeding densities were different, with cells for sphere formation assays being seeded at low density whereas cells for qPCR were seeded at relatively high density. Finally, compound concentrations could have been too low in order to induce a significant reduction of CSC associated gene expression.

As only MDA-MB231 tumorspheres showed a slight decrease in sphere formation efficiency upon treatment with compound 2, qPCR experiments were also performed after treatment with C2. As expected, changes observed upon treatment with this compound were not as substantial compared to treatment with C19. However, CD44 expression was significantly downregulated at 10  $\mu$ M

C19. Also, Sox2 expression was reduced by 50% upon the treatment. The expression of the other examined genes remained unaffected after treatment. These findings correspond to previous results from dose-response experiments and sphere formation assays, where viability and sphere formation of MDA-MB231 tumorspheres was decreased but to a lesser extent than it was seen upon treatment with C1 or C19.



## 6. Conclusion and Outlook

To sum up the results of my work, C19 and C1 clearly inhibited the viability of breast and lung cancer cells. Moreover, viability of breast and lung tumorspheres after 72h treatment was significantly reduced at lower concentrations when compared to cells grown as monolayer. These findings could also be verified in primary patient derived breast and lung cancer cells grown as tumorspheres. Furthermore, C19 and C1 inhibited sphere formation which can be used as indicator for the ability to self-renew. Finally, we could show that some genes associated with CSCs were downregulated after treatment with C19 for 24h, especially in MDA-MB231 cells, which belong to the very aggressive type of claudin-low breast cancer.

Overall, this work showed that alkaloid derivatives make up a very useful class of compounds that can be used in the fight against cancer. Especially derivatives of the alkaloid clathroidin, which can be naturally found in marine sponges, may be modified to specifically target the subpopulation of CSCs.

Further research is still needed to uncover the mechanism of action of these compounds. Chemical modification of these compounds could improve their effectiveness against CSCs in order to improve future cancer treatment.

## Appendix

### Abbreviations

ABAM	.....Antibiotics Antimycotics
ABC	.....ATP Binding Cassette Transporter
ALDH1	..... Aldehyde dehydrogenase 1
bFGF	.....basic Fibroblast Growth Factor
BRCA1/2	.....Breast Cancer 1/2
CD133	.....Cluster of Differentiation 133
CD24	.....Cluster of Differentiation 24
CD44	.....Cluster of Differentiation 44
CSC	.....Cancer Stem Cell
DMEM/F12	.....Dulbecoo's modified eagle media/Ham's F12
DMSO	.....Dimethylsulfoxid
DNA	.....Desoxyribonucleic acid
E-Cad	.....E-Cadherin
EGF	.....Epidermal growth factor
EGFR	.....Epidermal growth factor receptor
EML4	.....Echinoderm microtubule associated protein like 4
EMT	.....Epithelial mesenchymal transition
ER	.....Estrogen receptor
FACS	.....Fluorescence assisted/activated cell sorting

FBS	.....Foetal bovine serum
FDA	.....Food and Drug Administration
FN	.....Fibronectin
GAPDH	.....Glyceraldehyde-3-phosphate dehydrogenase
HER2	.....Human epidermal growth factor receptor 2
IDC	.....Invasive ductal carcinoma
K-ras	.....Kirsten rat sarcoma viral oncogene homologue
LDHA	.....Lactate dehydrogenase
MEBM	.....Mammary epithelial basal media
MET	.....Mesenchymal epithelial transition
mRNA	.....Messenger RNA
N-Cad	.....N-Cadherin
Nod/Scid	.....Non-obese diabetic, severe combined immunodeficiency
NSCLC	.....NonSmall cell lung cancer
Oct4	.....Octamer binding transcription factor 4
PBS	.....Phosphor buffered saline
PR	.....Progesteron receptor
qPCR	.....quantitative Real-Time Polymerase Chain Reaction
RNA	.....Ribonucleic acid
RPMI 1640	.....Roswell park memorial institute 1640 media
SCLC	.....Small cell lung cancer
SFE	.....Sphere formation efficiency

SP	.....Side population
TBP	.....TATA-box binding protein
TGF $\beta$	.....Tumor growth factor $\beta$
TME	.....Tumor microenvironment
Vim	.....Vimentin
ULA	.....Ultra Low Attachment
WHO	.....World Health Organisation

## List of Tables

<b>Table 1:</b> List of compounds received from the University of Ljubljana. ....	20
<b>Table 2:</b> List of cell lines used for experiments .....	23
<b>Table 3:</b> List of cell culture media and supplements .....	26
<b>Table 4:</b> Seeding densities of cell lines used for viability assays .....	28
<b>Table 5:</b> Light Cycler Conditions .....	32
<b>Table 6:</b> Primer sequences used for qRT-PCR.....	33
<b>Table 7:</b> Overview of the calculated IC50 values after treatment with C1 .....	46
<b>Table 8:</b> Overview of the calculated IC50 values after treatment with C19.....	49
<b>Table 9:</b> Overview of the calculated IC50 values after treatment with C2.....	51
<b>Table 10:</b> Overview of the calculated IC50 values for primary cancer cells .....	54
<b>Table 11:</b> Overview of IC50 values all cell lines and all compounds.....	55

## List of Figures

- Figure 1:** Stochastic model of cancer evolution<sup>47</sup> hypothesizing that any tumor cell within a tumor is capable to form a new tumor..... 7
- Figure 2:** Hierarchical organisation of tumors.<sup>47</sup>The CSC model posits that only a subset of cells (shown in yellow) are able to generate a new tumor. .... 8
- Figure 3:** Cancer stem cells and tumor recurrence after therapy. In a) CSCs with intrinsic therapy resistance survive chemo- or radiotherapy and lead to a relapse and a de-novo re-initiation of tumor growth. In b) CSCs acquire mutations that lead to therapy resistance. All cells of the recurring tumor are thus resistant to therapy as they arose through clonal expansion of the mutated CSC-clone..... 14
- Figure 4:** Structure of Clathrocin ..... 20
- Figure 5:** Morphology of breast cancer cells grown under adherent (left panel) and suspension (right panel) culture conditions. Tumorspheres were generated after 4-7 days of culture in serum-free suspension culture conditions. **A) MCF7 B) BT474 C) SUM159 D) MDA-MB231.** Scale bars represent 50  $\mu$ m. .... 35
- Figure 6:** Morphology of lung adenocarcinoma cells grown under adherent (left panel) and suspension (right panel) culture conditions. Tumorspheres were generated after 5 -7 days of culture in serum-free suspension culture conditions. **A) A549 B) NCI-H1299.** .... 36
- Figure 7:** Morphology of in-house patient-derived cancer cell lines grown under suspension culture conditions. PL24 originated from a pleural effusion of a breast cancer patient (left side) and LT22 originated from a lung adenocarcinoma patient (right side). .... 37
- Figure 8:** Results of the primary screening experiments in breast cancer cell lines depicted as a heat map with green representing high and red low viability. Values are given in percent normalized to the vehicle control. Only C1 and C19 completely inhibited viability in all breast cancer cell lines and both culture conditions analysed. Interestingly, C2 decreases viability selectively in breast cancer cells cultured as tumorspheres. .... 39

**Figure 9:** A scatterplot showing the results of screening experiments in breast cancer cell lines. Adherent cells are shown in black, tumorspheres in red. Only C2 selectively decreased viability of tumorspheres. C1, C7 and C19 significantly decreased viability in all breast cancer cell lines and in both culture conditions.

..... 40

**Figure 10:** Results of the primary screening experiments in lung adenocarcinoma cell lines represented as heat map with green values representing high and red boxes showing low viability. Values are given in percent normalized to the vehicle control. Besides compounds 6, 7, 8, 9, 10, 11 and 18, which showed decreased viability by about 50 to 70% only C1 and C19 completely inhibited viability in all lung adenocarcinoma cell lines used..... 41

**Figure 11:** A scatterplot showing the results of screening experiments in lung adenocarcinoma cell lines. Adherent cells are shown in black, tumorspheres in red. No compound was identified that selectively decreased the viability in tumorspheres. Treatment with C1, 7, 11 and 19 showed the strongest decrease of viability in lung cancer cell lines. .... 42

**Figure 12:** A scatterplot showing the results of screening experiments in breast cancer cell lines (black) and lung adenocarcinoma cell lines (red). The only compound that acted selectively on breast cancer spheres was C2. In contrast, no compound specifically affecting lung adenocarcinoma cells was identified. 43

**Figure 13:** Dose-response curves of compound 1 in breast cancer cell lines grown as spheres (green) and monolayers (black). **A)** MCF7 tumorspheres exhibited a significantly lower IC50 as adherently growing cells. BT474 cells **B)** and SUM159 cells **C)** showed similar IC50 values for both tumorspheres and monolayer derived cells. **D)** Treatment of MDA-MB231 tumorspheres with C1 resulted in a slightly lower IC50 than treatment of adherently growing cells . . . 45

**Figure 14:** Dose-response curves of compound 1 in lung cancer cell lines grown as spheres (green) and monolayers (black). **A)** H1299 tumorspheres exhibited a significantly lower IC50 as adherently growing cells. **B)** In A549 cells, IC50 values of tumorspheres and monolayer derived cells also differed significantly..... 46

**Figure 15:** Dose-response curves of compound 19 in breast cancer cell lines grown as spheres (green) and monolayers (black). **A)** MCF7 tumorspheres exhibited a significantly lower IC50 as adherently growing cells. **B)** In BT474 cells, IC50 of tumorspheres and monolayer derived cells were comparable. **C)** Treatment of SUM159 tumorspheres resulted in a very low IC50 whereas IC50 of monolayer derived cells was comparable to IC50 of other adherently growing breast cancer cell lines. **D)** Treatment of MDA-MB231 tumorspheres with C19 also resulted in a lower IC50 than treatment of adherently growing cells..... 48

**Figure 16:** Dose-response curves of compound 19 in lung cancer cell lines grown as spheres (green) and monolayers (black). **A)** H1299 tumorspheres exhibited only a slightly lower IC50 compared to adherently growing cells. **B)** In A549 cells treatment with C19 resulted in a lower IC50 of tumorspheres compared to monolayer derived cells..... 49

**Figure 17:** Dose-response curves of compound 2 in breast cancer cell lines grown as spheres (green) and monolayers (black). **A)** MCF7 tumorspheres exhibited a significantly lower IC50 as adherently growing cells. **B)** In BT474 cells, IC50 of tumorspheres was significantly lower compared to cells grown as monolayer. **C)** Treatment of SUM159 tumorspheres resulted in a very moderate reduction of IC50 compared to cells grown as monolayer. **D)** MDA-MB231 tumorspheres treated with C2 were the only cells that showed almost complete reduction of viability, showing a significant selectivity for tumorspheres. .... 51

**Figure 18:** Treatment of primary breast cancer PL24 tumorspheres with C1 (A) decreased viability in a dose-dependent manner with an IC50 of 10.4  $\mu\text{M}$ . Treatment with compound 19 (B) also decreased the viability with a slightly lower IC50 of 7.4  $\mu\text{M}$ . In contrast, treatment of PL24 with C2 (C) showed merely no effect on viability with a high IC50 of 74.5  $\mu\text{M}$ . .... 53

**Figure 19:** Dose-response curves of compound 1 (left panel) and compound 19 (right panel) in primary lung adenocarcinoma cells LT22 grown as tumorspheres. Both compounds showed a dose-dependent effect on cell viability with similar IC50 of about 8  $\mu\text{M}$ . .... 54



**Figure 20:** Effect of various concentrations of lead compounds C1, C19 and C2 on sphere formation efficiency of MCF7 cells (mean  $\pm$  SD of three replicates). C1 (A) and C19 (B) both reduced sphere formation at 10  $\mu$ M and completely abolished sphere formation at 25  $\mu$ M. In contrast, C2 (C) did not significantly reduce sphere formation at any tested concentration. .... 58

**Figure 21:** Effect of various concentrations of lead compounds C1, C19 and C2 on sphere formation efficiency of BT474 cells (mean  $\pm$  SD of three replicates). C1 treatment (A) reduced sphere formation at 10  $\mu$ M. C19 almost abolished sphere formation at 10  $\mu$ M (B). Similar to MCF7 cells, C2 (C) did not significantly inhibit sphere formation at any tested concentration..... 59

**Figure 22:** Effect of various concentrations of lead compounds C1, C19 and C2 on sphere formation efficiency of SUM159 cells (mean  $\pm$  SD of three replicates). C1 (A) slightly inhibited sphere formation at as little as 1  $\mu$ M, whereas C19 (B) reduced sphere formation at 5  $\mu$ M. Both compounds completely abolished sphere formation at 25  $\mu$ M. Similar to MCF7 and BT474, C2 (C) did not significantly reduce sphere formation at any tested concentration..... 60

**Figure 23:** Effect of various concentrations of lead compounds C1, C19 and C2 on sphere formation efficiency of MDA-MB231 cells (mean  $\pm$  SD of three replicates). Treatment with C1 (A) reduced sphere formation at 5  $\mu$ M. C19 (B) reduced sphere formation at 10  $\mu$ M. Interestingly C2 (C) significantly reduced sphere formation at 10 and 25  $\mu$ M compound concentration. However, sphere formation was not completely abolished by C2 at 25  $\mu$ M. .... 61

**Figure 24:** Effect of C19 on expression of CSC associated genes in MCF7 spheres. Spheres were treated for 24 hours. Expression is represented as a fold change of DMSO vehicle control. Data are represented as the mean  $\pm$  SEM (n=2). Only Fibronectin and Twist decreased significantly by about 50%. E-Cad, Snail, Oct4 and Sox2 expression did not change significantly upon treatment with the compound. Expression levels of CD44, Nanog and Slug were moderately increased..... 63

**Figure 25:** Effect of C19 on expression of CSC associated genes in BT474 spheres. Spheres were treated for 24h. Expression is represented as a fold change of DMSO vehicle control. Data are represented as the mean  $\pm$  SEM (n=2). Vimentin, ALDH1 and N-Cad showed a decrease in expression levels only at 5  $\mu$ M compound concentration. Oct4 expression was not significantly altered after treatment with C19. Relative expression levels of Sox2, Nanog, Slug, Twist, E-Cad, CD44 and Snail on the other hand were increased up to 3-fold (Nanog) and even 6-fold (Snail). ..... 65

**Figure 26:** Effect of C19 on expression of CSC associated genes in SUM159 spheres. Spheres were treated for 24 hours. Expression is represented as a fold change of DMSO vehicle control. Data are represented as the mean  $\pm$  SEM (N=2). Sox2 expression was reduced by about 50% upon treatment. Nanog, Vimentin and ALDH1 expression did also decrease, although only at 5  $\mu$ M compound concentration. Relative expression levels of Fibronectin, Twist, Oct4, N-Cad and CD44 did not significantly change upon treatment with C19 and Snail and Slug expression slightly increased. .... 67

**Figure 27:** Effect of C19 on expression of CSC associated genes in MDA-MB231 spheres. Spheres were treated for 24 hours. Expression is represented as a fold change of DMSO vehicle control. Data are represented as the mean  $\pm$  SEM (N=2). Sox2 expression showed a 3-fold reduction. Expression of CD44, Snail, Slug and Vimentin was also about 2-fold decreased. In contrast, relative expression levels of Fibronectin increased about 2-fold at 10  $\mu$ M compound concentration..... 68

**Figure 28:** Effect of C2 on expression of CSC associated genes in MDA-MB231 spheres. Spheres were treated for 24 hours. Expression is represented as a fold change of DMSO vehicle control. Data are represented as the mean  $\pm$  SEM (n=2). Expression of CD44 and Sox2 was slightly decreased only at 10  $\mu$ M compound concentration. Slug, Vim, FN and Snail expression levels were not altered significantly..... 69

## Bibliography

1. Ferlay, J. *et al.* Cancer incidence and mortality worldwide : Sources , methods and major patterns in GLOBOCAN 2012. **386**, (2015).
2. Torre, L. A. *et al.* Global Cancer Statistics, 2012. *CA a cancer J. Clin.* **65**, 87–108 (2015).
3. Jemal, A. *et al.* Cancer Statistics, 2008. *CA. Cancer J. Clin.* **58**, 71–96 (2008).
4. Austria, S. Lungenkrebs Statistik. at <[https://www.statistik.at/web\\_de/statistiken/menschen\\_und\\_gesellschaft/gesundheit/krebserkrankungen/luftroehre\\_bronchien\\_lunge/index.html](https://www.statistik.at/web_de/statistiken/menschen_und_gesellschaft/gesundheit/krebserkrankungen/luftroehre_bronchien_lunge/index.html)>
5. Collins, L. G., Haines, C., Perkel, R. & Enck, R. E. Lung cancer: Diagnosis and management. *Am. Fam. Physician* **75**, 56–63 (2007).
6. Thun, M. J. *et al.* Lung cancer occurrence in never-smokers: An analysis of 13 cohorts and 22 cancer registry studies. *PLoS Med.* **5**, 1357–1371 (2008).
7. Yang, I. a, Holloway, J. W. & Fong, K. M. Genetic susceptibility to lung cancer and co-morbidities. *J. Thorac. Dis.* **5 Suppl 5**, S454–62 (2013).
8. Kenfield, S. A., Wei, E. K., Stampfer, M. J., Rosner, A. & Colditz, G. A. Comparison of Aspects of Smoking Among Four Histologic Types of Lung Cancer. *Tob. Control* **17**, 198–204 (2008).
9. Hong, W. K. & Hait, W. N. in *Holland-Frei Cancer Med.* 2021 (2010).
10. Travis, W., Brambilla, E., Noguchi, M. & Nicholson, A. IASLC/ATS/ERS interantional multidisciplinary classification of lung adenocarcinoma. *J. Thorac. Oncol.* **6**, 244–84 (2011).
11. Pao, W. & Girard, N. New driver mutations in non-small-cell lung cancer. *Lancet Oncol.* **12**, 175–80 (2011).
12. Herbst, R. S., Heymach, J. V. & Lippman, S. M. Lung Cancer. *N. Engl. J. Med.* **359**, 1367–1380 (2008).
13. Thomas, A., Liu, S. V., Subramaniam, D. S. & Giaccone, G. Refining the treatment of NSCLC according to histological and molecular subtypes. *Nat. Rev. Clin. Oncol.* **12**, 511–526 (2015).
14. Meerbeeck, van J. P., Fennell, D. A. & Ruyscher, D. D. K. Small-cell lung cancer. *Lancet* **378**, 1741–1755 (2011).
15. Oze, I. *et al.* Twenty-Seven Years of Phase III Trials for Patients with Extensive Disease Small-Cell Lung Cancer: Disappointing Results. *PLoS One* **4**, (2009).
16. UK, C. R. World Wide Cancer Incidence Statistics. at <<http://www.cancerresearchuk.org/health-professional/cancer-statistics/worldwide-cancer/incidence#heading-Zero>>
17. Austria, S. Brustkrebs Statistik. at <[https://www.statistik.at/web\\_de/statistiken/menschen\\_und\\_gesellschaft/gesundheit/krebserkrankungen/brust/index.html](https://www.statistik.at/web_de/statistiken/menschen_und_gesellschaft/gesundheit/krebserkrankungen/brust/index.html)>
18. WHO. *World Cancer Report 2014.* (2014).
19. Gage, M., Wattendorf, D. & Henry, L. Translational advances regarding hereditary breast cancer syndromes. *J. Surg. Oncol.* **105**, 444–451 (2012).
20. Viale, G. The current state of breast cancer classification. *Ann. Oncol.* **23 Suppl 1**, x207–10 (2012).
21. Perou, C. *et al.* Molecular portraits of human breast tumours. *Nature* **406**, 747–752 (2000).
22. Hu, Z. *et al.* The molecular portraits of breast tumors are conserved across microarray platforms. *BMC Genomics* (2006).
23. T, S. *et al.* Gene expression patterns of breast carcinomas distinguish tumor subclasses with clinical implications. *Proc. Natl. Acad. Sci. United States Am.* **98**, 10869–74 (2001).
24. Perou, C. & Borresen, A. Systems Biology and Genomics of Breast Cancer. *Cold spring Harb Perspect. Biol.* 1–18 (2011). doi:10.1101/cshperspect.a003293
25. Carey, L., Winer, E., Viale, G., Cameron, D. & Gianni, L. Triple-negative breast cancer: disease entity or title of convenience? *Nat Rev Clin Oncol.* **7**, 683–92 (2010).

26. Sabatier, R. *et al.* Claudin-low breast cancers: clinical, pathological, molecular and prognostic characterization. *Mol. Cancer* **13**, 228 (2014).
27. Prat, A. *et al.* Phenotypic and molecular characterization of the claudin-low intrinsic subtype of breast cancer. **12**, R68 (2010).
28. Anders, C. & Carey, L. Biology, metastatic patterns, and treatment of patients with triple-negative breast cancer. *Clin. Breast Cancer* (2009).
29. Carey, L. *et al.* The triple negative paradox: primary tumor chemosensitivity of breast cancer subtypes. *Clin. Cancer Res.* **13**, 2329–34 (2007).
30. Sorlie, T. *et al.* Repeated observation of breast tumor subtypes in independent gene expression data sets. *Proc. Natl. Acad. Sci. U. S. A.* **100**, 8418–23 (2003).
31. Phipps, A. *et al.* Association between molecular subtypes of colorectal cancer and patient survival. *Gastroenterology* **148**, 77–87 (2015).
32. Lei, Z. *et al.* Identification of molecular subtypes of gastric cancer with different responses to PI3-kinase inhibitors and 5-fluorouracil. *Gastroenterology* **3**, 554–565 (2013).
33. Travis, W., Brambilla, E. & Riely, G. New pathologic classification of lung cancer: relevance for clinical practice and clinical trials. *J. Clin. Oncol.* **31**, 992–1001 (2013).
34. Quackenbush, J. Microarray Analysis and Tumor Classification. *N. Engl. J. Med.* **354**, 2463–2472 (2006).
35. Perez-Diez, A., Morgun, A. & Shulzhenko, N. Microarrays for Cancer Diagnosis and Classification. *Madame Curie Biosci. Database* at <<http://www.ncbi.nlm.nih.gov/books/NBK6624/>>
36. Knowles, M. & Hurst, C. Molecular biology of bladder cancer: new insights into pathogenesis and clinical diversity. *Nat. Rev. Cancer* **15**, 25–41 (2015).
37. Imadome, K. *et al.* Subtypes of cervical adenosquamous carcinomas classified by EpCAM expression related to radiosensitivity. *Cancer Biol. Ther.* **10**, 1019–1026 (2010).
38. Kendal, W. & Mai, K. Histological subtypes of prostatic cancer: a comparative survival study. *Cancer J. Urol.* **17**, 5355–9 (2010).
39. National Cancer Institute (National Institutes of Health, U. S. Department of Human Health and Services, June 18th, 2015). What is Cancer? at <<http://www.cancer.gov/about-cancer/what-is-cancer>>
40. Burrell, R. a, McGranahan, N., Bartek, J. & Swanton, C. The causes and consequences of genetic heterogeneity in cancer evolution. *Nature* **501**, 338–45 (2013).
41. Marusyk, A. & Polyak, K. Tumor heterogeneity: causes and consequences. *Biochim Biophys Acta* **1805**, 1–28 (2011).
42. Marusyk, A., Almendro, V. & Polyak, K. Intra-tumour heterogeneity: a looking glass for cancer? *Nat. Rev. Cancer* **12**, 323–334 (2012).
43. Jamal-Hanjani, M., Quezada, S., Larkin, J. & Swanton, C. Translational implications of tumor heterogeneity. *Clin. Cancer Res* **21**, 1258–66 (2015).
44. Engelman, J. & Settleman, J. Acquired resistance to tyrosine kinase inhibitors during cancer therapy. *Curr Opin Genet Dev* **18**, 73–9 (2008).
45. Misale, S. *et al.* Emergence of KRAS mutations and acquired resistance to anti-EGFR therapy in colorectal cancer. *Nature* **486**, 532–6 (2012).
46. Kreso, A. & Dick, J. E. Evolution of the cancer stem cell model. *Cell Stem Cell* **14**, 275–291 (2014).
47. Reya, T., Morrison, S. J., Clarke, M. F. & Weissman, I. L. Stem cells, cancer, and cancer stem cells. *Nature* **414**, 105–111 (2001).
48. Meacham, C. E. & Morrison, S. J. Tumour heterogeneity and cancer cell plasticity. *Nature* **501**, 328–337 (2013).
49. Medema, J. P. Cancer stem cells: the challenges ahead. *Nat. Cell Biol.* **15**, 338–44 (2013).
50. Bonnet, D. & Dick, J. E. Human acute myeloid leukemia is organized as a hierarchy that originates from a primitive hematopoietic cell. *Nat. Med.* **3**, 730–737 (1997).

51. Al-Hajj, M., Wicha, M. S., Benito-Hernandez, A., Morrison, S. J. & Clarke, M. F. Prospective identification of tumorigenic breast cancer cells. *Proc. Natl. Acad. Sci. U. S. A.* **100**, 3983–3988 (2003).
52. Singh, S. K. *et al.* Identification of a Cancer Stem Cell in Human Brain Tumors. *Pathobiology* 5821–5828 (2003).
53. Collins, A., Berry, P., Hyde, C., Stower, M. & Maitland, N. Prospective identification of tumorigenic prostate cancer stem cells. *Cancer Res.* **65**, 10946–51 (2005).
54. Bapat, S., Mali, A., Koppikar, C. & Kurrey, N. Stem and progenitor-like cells contribute to the aggressive behavior of human epithelial ovarian cancer. *Cancer Res.* **65**, 3025–9 (2005).
55. Dalerba, P. *et al.* Phenotypic characterization of human colorectal cancer stem cells. *Proc. Natl. Acad. Sci. U. S. A.* **104**, 10158–63 (2007).
56. Ricci-Vitiani, L. *et al.* Identification and expansion of human colon-cancer-initiating cells. *Nature* **445**, 111–115 (2007).
57. O'Brien, C. A., Pollett, A., Gallinger, S. & Dick, J. E. A human colon cancer cell capable of initiating tumour growth in immunodeficient mice. *Nature* **445**, 106–110 (2007).
58. Yang, Z. *et al.* Significance of CD90+ cancer stem cells in human liver cancer. *Cancer Cell* **13**, 153–66 (2008).
59. Eramo, a *et al.* Identification and expansion of the tumorigenic lung cancer stem cell population. *Cell Death Differ.* **15**, 504–514 (2008).
60. Hermann, P. C. *et al.* Distinct Populations of Cancer Stem Cells Determine Tumor Growth and Metastatic Activity in Human Pancreatic Cancer. *Cell Stem Cell* **1**, 313–323 (2007).
61. Ghani, F. *et al.* Identification of cancer stem cell markers in human malignant mesothelioma cells. *Biochem Biophys Res Commun* **404**, 735–42 (20211).
62. Dou, J. *et al.* Isolation and identification of cancer stem-like cells from murine melanoma cell lines. *Cell. Mol. Immunol.* **4**, 467–72 (2007).
63. Zahng, C., Li, C., He, F., Cai, Y. & Yang, H. Identification of CD44+CD24+ gastric cancer stem cells. *J. Cancer Res. Clin. Oncol.* **137**, 1679–86 (2011).
64. Hermann, P. C., Hermann, P. C., Bhaskar, S., Cioffi, M. & Heeschen, C. Cancer stem cells in solid tumors. *Semin. Cancer Biol.* (2010). doi:10.1016/j.semcancer.2010.03.004
65. Marcato, P. *et al.* Aldehyde dehydrogenase activity of breast cancer stem cells is primarily due to isoform ALDH1A3 and its expression is predictive of metastasis. *Stem Cells* **29**, 32–45 (2011).
66. Velasco-Velázquez, M., Popov, V., Lisanti, M. & Pestell, R. The role of breast cancer stem cells in metastasis and therapeutic implications. *Am. J. Pathol.* **179**, 2–11 (2011).
67. Leung, E. *et al.* Non-small cell lung cancer cells expressing CD44 are enriched for stem cell-like properties. *PLoS One* **5**, (2010).
68. Tirino, V. *et al.* The role of CD133 in the identification and characterisation of tumour-initiating cells in non-small-cell lung cancer. *Eur. J. Cardiothorac. Surg.* **36**, 446–53 (2009).
69. Dean, M., Fojo, T. & Bates, S. Tumour stem cells and drug resistance. *Nat. Rev. Cancer* **5**, 275–284 (2005).
70. Huang, C. *et al.* ALDH-positive lung cancer stem cells confer resistance to epidermal growth factor receptor tyrosine kinase inhibitors. *Cancer Lett.* **328**, 144–51 (2013).
71. Bonnet, D. & Dick, J. E. Human acute myeloid leukemia is organized as a hierarchy that originate from a primitive haematopoietic cell. *Nat. Med.* **3**, 730–737 (1997).
72. Singh, S. K. *et al.* Identification of human brain tumour initiating cells. *Nature* **432**, 396–401 (2004).
73. Bender Kim, C. F. *et al.* Identification of bronchioalveolar stem cells in normal lung and lung cancer. *Cell* **121**, 823–835 (2005).
74. Li, C. *et al.* Identification of pancreatic cancer stem cells. *Cancer Res.* **67**, 1030–7 (2007).
75. Louderbough, J. & Shoreder, J. Understanding the dual nature of CD44 in breast cancer progression. *Mol. Cancer Res.* **9**, 1573–86 (2011).
76. Kitamura, H., Okudela, K., Yazawa, T., Sato, H. & Shimoyamada, H. Cancer stem cell: Implications in cancer biology and therapy with special reference to lung cancer. *Lung Cancer* **66**, 275–281 (2009).

77. Fang, X., Zheng, P., Tang, J. & Liu, Y. CD24: from A to Z. *Cell. Mol. Immunol.* **7**, 100–103 (2010).
78. Jaggupilli, A. & Elkord, E. Significance of CD44 and CD24 as Cancer Stem Cell Markers: An Enduring Ambiguity. *Clin. Dev. Immunol.* (2012).
79. Marchitti, S., Brocker, C., Stagos, D. & Vasiliou, V. Non-P450 aldehyde oxidizing enzymes: the aldehyde dehydrogenase superfamily. *Expert Opin Drug Metab Toxicol* **4**, 697–720 (2008).
80. Johanna. CD133 and ALDH1 as Prospective Markers for Cancer Stem Cells in Ileal Carcinoids. **1**, 1–12 (2013).
81. Goodell, M. A., Brose, K., Paradis, G., Conner, S. A. & Mulligan, R. C. Isolation and Functional Properties of Murine Hematopoietic Stem Cells that are Replicating In Vivo. *J. Exp. Med.* **184**, 1797–1806 (1996).
82. Szotek, P. P. *et al.* Ovarian cancer side population defines cells with stem cell-like characteristics and Mullerian Inhibiting Substance responsiveness. *Proc Natl Acad Sci U S A* **103**, 11154–9 (2006).
83. Misutake, N. *et al.* Characterization of side population in thyroid cancer cell lines: cancer stem-like cells are enriched partly but not exclusively. *Endocrinology* **148**, 1797–803 (2007).
84. Kondo, T., Setoguchi, T. & Taga, T. Persistence of a small subpopulation of cancer stem-like cells in the C6 glioma cell line. *Proc. Natl. Acad. Sci. U. S. A.* **101**, 781–6 (2004).
85. Haraguchi, N. *et al.* Cancer stem cells in human gastrointestinal cancers. *Hum. Cell* **19**, 24–9 (2006).
86. Brown, M. D., Grey, B., Oates, J. & Clarke, N. W. in *Cancer Stem Cells* (Guan, X.-Y.) (Transworld Research Network, 2010).
87. Ailles, L. E. & Weissman, I. L. Cancer stem cells in solid tumors. *Curr. Opin. Biotechnol.* **18**, 460–466 (2007).
88. Han, L., Shi, S., Gong, T., Zhang, Z. & Sun, X. Cancer stem cells: therapeutic implications and perspectives in cancer therapy. *Acta Pharm. Sin. B* **3**, 65–76 (2013).
89. Chen, Y. C. *et al.* Oct-4 expression maintained cancer stem-like properties in lung cancer-derived CD133-positive cells. *PLoS One* **3**, 1–14 (2008).
90. Kondo, T. Stem cell-like cancer cells in cancer cell lines. *Inflamm. Regen.* **27**, 506–511 (2007).
91. Smart, C. E. *et al.* In Vitro Analysis of Breast Cancer Cell Line Tumourspheres and Primary Human Breast Epithelia Mammospheres Demonstrates Inter- and Intrasphere Heterogeneity. *PLoS One* **8**, (2013).
92. Li, Y. F., Xiao, B., Tu, S. F., Wang, Y. Y. & Zhang, X. L. Cultivation and identification of colon cancer stem cell-derived spheres from the Colo205 cell line. *Brazilian J. Med. Biol. Res.* **45**, 197–204 (2012).
93. Zhang, S. *et al.* Identification and Characterization of Ovarian Cancer-Initiating Cells from Primary Human Tumors. *Cancer Res.* **68**, 4311–4320 (2009).
94. Grimshaw, M. J. *et al.* Mammosphere culture of metastatic breast cancer cells enriches for tumorigenic breast cancer cells. *Breast Cancer Res.* **10**, R52 (2008).
95. Rybak, A. P., He, L., Kapoor, A., Cutz, J. C. & Tang, D. Characterization of sphere-propagating cells with stem-like properties from DU145 prostate cancer cells. *Biochim. Biophys. Acta - Mol. Cell Res.* **1813**, 683–694 (2011).
96. Pastrana, E., Silva-Vargas, V. & Doetsch, F. Eyes wide open: A critical review of sphere-formation as an assay for stem cells. *Cell Stem Cell* **8**, 486–498 (2011).
97. Lo, P. *et al.* CD49f and CD61 identify Her2/neu-induced mammary tumor-initiating cells that are potentially derived from luminal progenitors and maintained by the integrin-TGFbeta signaling. *Oncogene* **31**, 2614–2626 (2012).
98. Liu, J., Deng, T., Lehal, R., Kim, J. & Zacksenhaus, E. Identification of tumorsphere- and tumor-initiating cells in HER2/Neu-induced mammary tumors. *Cancer Res.* **67**, 8671–8681 (2007).
99. Akunuru, S., Zhai, Q. J. & Zheng, Y. Non-small cell lung cancer stem/progenitor cells are enriched in multiple distinct phenotypic subpopulations and exhibit plasticity. *Cell Death Dis.* **3**, (2012).
100. Penchev, V. R., Rasheed, Z. A., Maitra, A. & Matsui, W. Heterogeneity and Targeting of Pancreatic Cancer Stem Cells. *Clin. Cancer Res.* **18**, 4277–4284 (2012).

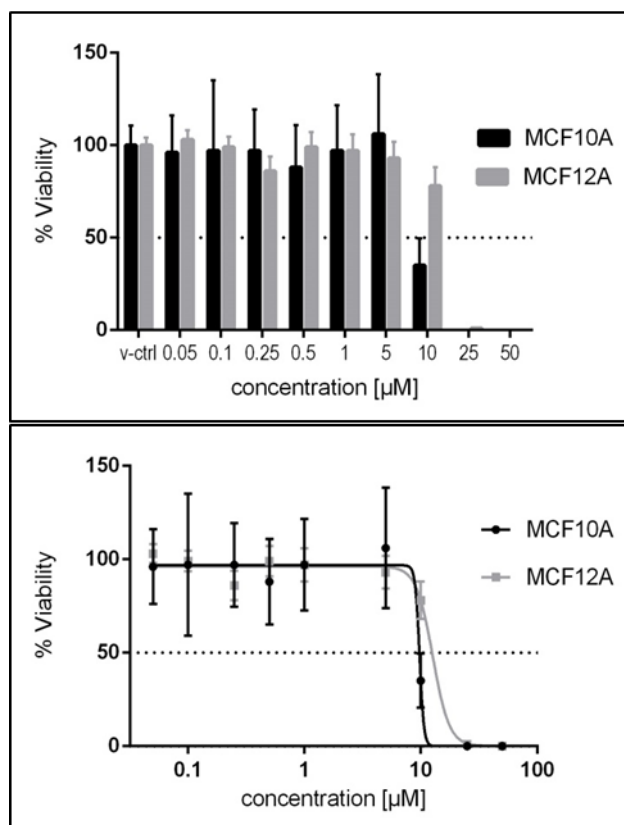
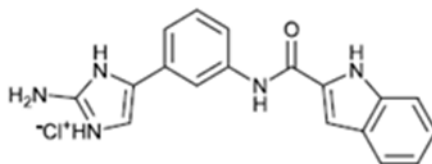
101. Piccirillo, S. *et al.* Distinct pools of cancer stem-like cells coexist within human glioblastomas and display different tumorigenicity and independent genomic evolution. *Oncogene* **28**, 1807–1811 (2009).
102. Sampieri, K. & Fodde, R. Cancer stem cells and metastasis. *Semin. Cancer Biol.* **22**, 187–193 (2012).
103. Gottesman, M. M., Fojo, T. & Bates, S. Multidrug resistance in cancer: role of ATP-dependant transporters. *Nat. Rev. Cancer* **2**, 48–54 (2002).
104. Dean, M., Hamon, Y. & Chimini, G. The human ATP-binding cassette (ABC) transporter superfamily. *J. Lipid Res.* **42**, 1007–17 (2001).
105. Frank, N. Y., Schatton, T. & Frank, M. H. The therapeutic promise of the cancer stem cell concept. *J. Clin. Invest.* **120**, 41–50 (2010).
106. Thiery, J., Aclogue, H., Huang, R. & Nieto, M. Epithelial-mesenchymal transitions in development and disease. *Cell* **139**, 871–890 (2009).
107. Yang, J. & Weinberg, R. A. Epithelial-Mesenchymal Transition: At the Crossroads of Development and Tumor Metastasis. *Cell* **13**, 818–829 (2008).
108. Mani, S. A. *et al.* The Epithelial-Mesenchymal Transition Generates Cells with Properties of Stem Cells. 704–715 (2008). doi:10.1016/j.cell.2008.03.027
109. Scheel, C. & Weinberg, R. a. Cancer stem cells and epithelial-mesenchymal transition: Concepts and molecular links. *Semin. Cancer Biol.* **22**, 396–403 (2012).
110. Ansieau, S. EMT in breast cancer stem cell generation. *Cancer Lett.* **338**, 63–68 (2013).
111. Pattabiraman, D. R. & Weinberg, R. a. Tackling the cancer stem cells - what challenges do they pose? *Nat. Rev. Drug Discov.* **13**, 497–512 (2014).
112. Hesse, M. *Alkaloids: Nature's Curse or Blessing?* (Wiley-VCH, 2002).
113. Aniszewski, T. *Alkaloids - Secrets of Life.* (Elsevier, 2007).
114. Grinkevich, N. & Safronich, L. *The chemical analysis of medicinal plants.* (1983).
115. Sinatra, R., Jahr, J. & Watkins-Pitchford, J. The Essence of Analgesia and Analgesics. *Cambridge Univ. Press* 82–90 (2010).
116. Cushnie, T. & Lamb, A. Antimicrobial activity of flavonoids. *Int. J. Antimicrob. Agents* **26**, 343–56 (2005).
117. Kittakoop, P., Mahidol, C. & Ruchirawat, S. Alkaloids as important scaffolds in therapeutic drugs for the treatments of cancer, tuberculosis, and smoking cessation. *Curr. Top. Medicinal Chem.* **14**, 239–52 (2014).
118. Begley, T. P. *Encyclopaedia of Chemical Biology.* (Wiley, 2009).
119. Lewis, R. *Lewis' Dictionary of Toxicology.* (Informa Healthcare, 1997).
120. *Modern Alkaloids: Structure, Isolation, Synthesis and Biology.* (Wiley, 2007).
121. Aniszewski, T. in *Alkaloids - Secrets Life* (Elsevier B.V., 2007).
122. Moudi, M., Go, R., Yong Seok Yien, C. & Nazre, M. Vinca Alkaloids. *Int. J. Prev. Med.* **4**, 1231–1235 (2013).
123. Takimoto, C. H. & Calvo, E. in *Cancer Manag. A Multidiscip. Approach* (Oncology, 2008).
124. Lombardo, Y., Giorgio, A. De, Coombes, C. R., Stebbing, J. & Castellano, L. Mammosphere Formation Assay from Human Breast Cancer Tissues and Cell Lines. 1–5 (2015). doi:10.3791/52671
125. Hellemans, J., Mortier, G., De Paepe, A., Speleman, F. & Vandesompele, J. qBase relative quantification framework and software for management and automated analysis of real-time quantitative PCR data. *Genome Biol.* **8**, R19 (2007).
126. Palafox, M. *et al.* RANK Induces Epithelial-Mesenchymal Transition and Stemness in Human Mammary Epithelial Cells and Promotes Tumorigenesis and Metastasis. *Cancer Res.* **72**, 2879–2888 (2012).
127. Cioce, M. *et al.* Mammosphere-forming cells from breast cancer cell lines as a tool for the identification of CSC-like- and early progenitor-targeting drugs. *Cell Cycle* **9**, 2878–2887 (2010).

128. Mancini, R. *et al.* Spheres derived from lung adenocarcinoma pleural effusions: molecular characterization and tumor engraftment. *PLoS One* **6**, (2011).
129. Kim, S. & Alexaner, C. Tumorsphere assay provides more accurate prediction of in vivo responses to chemotherapeutics. *Biotechnology* **36**, 481–488 (2014).
130. Esquenet, M., Swinnen, J. V, Heyns, W. & Verhoeven, G. LNCaP Prostatic Adenocarcinoma Cells Derived from Low and High Passage Numbers Display Divergent Responses not Only to Androgens but Also to Retinoids. **62**, 391–399 (1997).
131. Sambuy, Y. *et al.* The Caco-2 cell line as a model of the intestinal barrier : in Influence of cell and culture-related factors on Caco-2 cell functional characteristics. 1–26 (2005).
132. Chang-Liu, C. & Woloschak, G. Effect of passage number on cellular response to DNA-damaging agents: cell survival and gene expression. *Cancer Lett.* **26**, 77–86 (1997).
133. O’Driscoll, L. *et al.* Phenotypic and global gene expression changes in low and high passage MIN6 cells. *J. Endocrinol.* **191**, 665–676 (2006).
134. Fillmore, C. & Kuperwasser, C. Human breast cancer stem cell markers CD44 and CD24: enriching for cells with functional properties in mice or in man? *Breast Cancer Res.* **9**, 303 (2007).
135. Singh, S., Clarke, I., Terasaki, M. & Bonn, V. Identification of a cancer stem cell in human brain tumors. *Cancer Res.* 5821–5828 (2003).
136. Borowicz, S. *et al.* The Soft Agar Colony Formation Assay. *J. Vis. Exp.* (2014).
137. Weiswald, L., Richon, S., Massonnet, G. & Guinebretie, J. A short-term colorectal cancer sphere culture as a relevant tool for human cancer biology investigation. 1720–1731 (2013). doi:10.1038/bjc.2013.132
138. Nishi, M., Akutsu, H., Kudoh, A. & Kimura, H. Induced cancer stem-like cells as a model for biological screening and discovery of agents targeting phenotypic traits of cancer stem cell. **5**, (2014).
139. Reynolds, B. a & Weiss, S. Clonal and population analyses demonstrate that an EGF-responsive mammalian embryonic CNS precursor is a stem cell. *Dev. Biol.* **175**, 1–13 (1996).
140. Dontu, G. *et al.* In vitro propagation and transcriptional profiling of human mammary stem / progenitor cells. *Genes Dev.* **17**, 1253–1270 (2003).
141. Xie, G. *et al.* Mammosphere cells from high-passage MCF7 cell line show variable loss of tumorigenicity and radioresistance. *Cancer Lett.* **316**, 53–61 (2012).
142. Larzabal, L. *et al.* Differential Effects of Drugs Targeting Cancer Stem Cell (CSC) and Non-CSC Populations on Lung Primary Tumors and Metastasis. **8**, (2013).
143. Gupta, P. B. *et al.* Identification of Selective Inhibitors of Cancer Stem Cells by High-Throughput Screening. *Cell* **138**, 645–659 (2009).
144. Ginestier, C. *et al.* ALDH1 Is a Marker of Normal and Malignant Human Mammary Stem Cells and a Predictor of Poor Clinical Outcome. *Cell Stem Cell* **1**, 555–567 (2007).
145. Liu, S. *et al.* Breast cancer stem cells transition between epithelial and mesenchymal states reflective of their normal counterparts. *Stem Cell Reports* **2**, 78–91 (2014).
146. Bar, E. E. *et al.* Cyclopamine-Mediated Hedgehog Pathway Inhibition Depletes Stem-Like Cancer Cells in Glioblastoma. *Stem Cells* **25**, 2524–2533 (2007).
147. Huang, E. H. *et al.* Aldehyde Dehydrogenase 1 Is a Marker for Normal and Malignant Human Colonic Stem Cells (SC) and Track SC Overpopulation during Colon Tumorigenesis. *Cancer Res.* **69**, 3382–3389 (2010).
148. Patel, M. *et al.* ALDH1A1 and ALDH3A1 expression in lung cancers: Correlation with histologic type and potential precursors. *Lung Cancer* **59**, 340–349 (2008).
149. Weinber, R. A. *The Biology of Cancer.* (Garland Science, 2006).
150. Beavon, I. R. G. The E-cadherin-catenin complex in tumor metastasis. *Eur. J. Cancer* **36**, 1607–1620 (2000).
151. Manuel Iglesias, J. *et al.* Mammosphere Formation in Breast Carcinoma Cell Lines Depends upon Expression of E-cadherin. *PLoS One* **8**, 1–12 (2013).
152. Ramis-Conde, I., Chaplain, M. A., Anderson, A. R. & Drasdo, D. Multi scale modelling of cancer cell intravasation: the role of cadherins in metastasis. *Phys. Biol.* **6**, (2009).

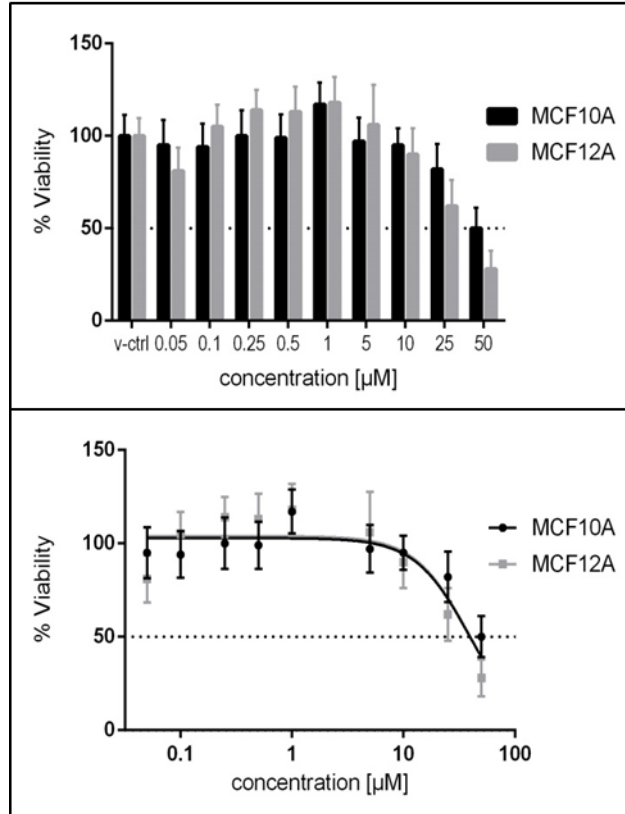
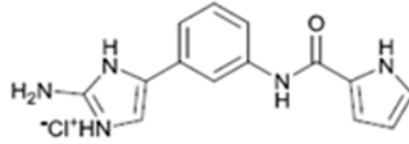


153. Mallini, P., Lennard, T., Kirby, J. & Meeson, A. Epithelial-to-mesenchymal transition: What is the impact on breast cancer stem cells and drug resistance. *Cancer Treat. Rev.* **40**, 341–348 (2014).
154. Liu, X. & Fan, D. The Epithelial-Mesenchymal Transition and Cancer Stem Cells: Functional and Mechanistic Links. *Curr. Pharm. Des.* **21**, 1279–1291 (2015).
155. Dhasarathy, A., Phadke, D., Mav, D., Shah, R. R. & Wade, P. A. The transcription factors Snail and Slug activate the transforming growth factor-beta signaling pathway in breast cancer. *PLoS One* **6**, e26514 (2011).
156. Ponti, D. *et al.* Isolation and In vitro Propagation of Tumorigenic Breast Cancer Cells with Stem/Progenitor Cell Properties. *Cancer Res.* **65**, 5506–5511 (2005).
157. Velasco-Velázquez, M. a., Homsí, N., De La Fuente, M. & Pestell, R. G. Breast cancer stem cells. *Int. J. Biochem. Cell Biol.* **44**, 573–577 (2012).
158. Lu, Y. *et al.* Evidence that SOX2 overexpression is oncogenic in the lung. *PLoS One* **5**, e11022 (2010).
159. Kregel, S. *et al.* Sox2 Is an Androgen Receptor-Repressed Gene That Promotes Castration-Resistant Prostate Cancer. *PLoS One* **8**, e53701 (2013).
160. Leis, O. *et al.* Sox2 expression in breast tumors and activation in breast cancer stem cells. *Oncogene* **31**, 1354–1365 (2012).
161. Wang, D. *et al.* Oct-4 and Nanog promote the epithelial-mesenchymal transition of breast cancer stem cells and are associated with poor prognosis in breast cancer patients. *Oncotarget* **5**, 10803–15 (2014).

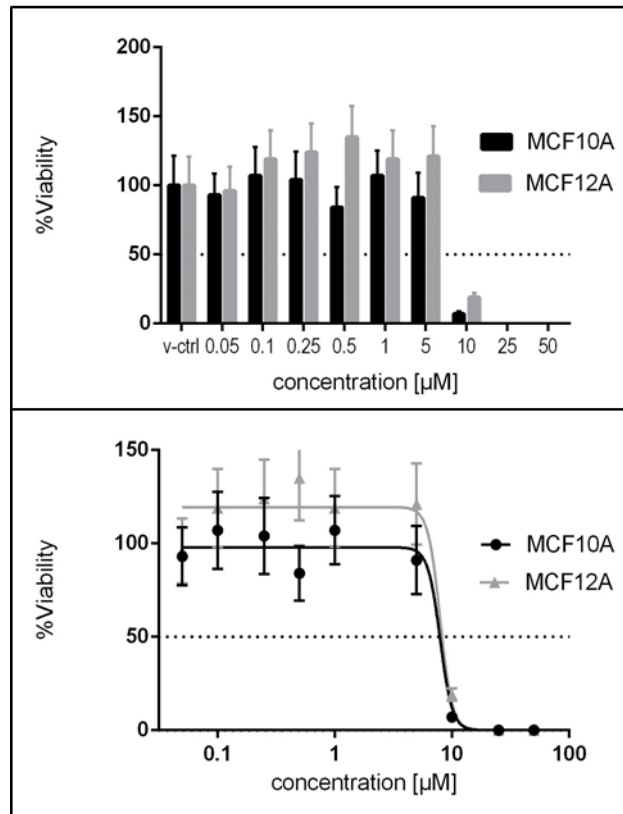
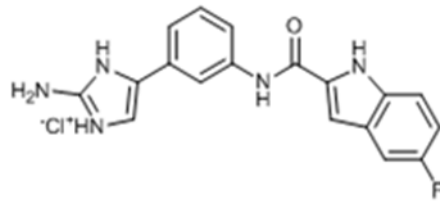
## Supplementary Data



**Supplementary Figure 1:** Effect of Compound 1 on MCF10A and MCF12A human non-transformed mammary cells growing under adherent culture conditions.



**Supplementary Figure 2:** Effect of Compound 2 on MCF10A and MCF12A human non-transformed mammary cells growing under adherent culture conditions.



**Supplementary Figure 3:** Effect of Compound 21 on MCF10A and MCF12A human non-transformed mammary cells growing under adherent culture conditions.